CONSTRAINTS ON PROTEROZOIC CRUSTAL EVOLUTION FROM AN ISOTOPIC AND GEOCHEMICAL STUDY OF CLASTIC SEDIMENTS OF THE GAWLER CRATON, SOUTH AUSTRALIA

Clayton A. Simpson   B.Sc.

Supervisor: J. Foden

This thesis is submitted as partial fulfilment for the
Honours Degree of Bachelor of Science.
November 1994

The University of Adelaide
The Department of Geology and Geophysics

MAP SHEETS:
Lincoln (SI 53-11)   1: 250 000
Tumby Bay (SI 53-6129)   1: 100 000

TABLE OF CONTENTS

List of Abbreviations.

Abstract.

Ch6: Proterozoic crustal growth in the Gawler Craton

Ch7: Discussion and conclusions

Acknowledgments.

References.

Appendices:

A: Sample locations and drill hole logs

B: Selected sample descriptions & Photographs

C: Analytical procedures

D: Isotope systematics

E: Compiled Isotopic data

F: Compiled XRF data

G: Mapping methodology & measurements

H: Tumby Bay structural & geological maps

List of Figures:

List of Tables:

KEY TO ABBREVIATIONS.

CHUR	= Chondritic Uniform Reservior
εNd, Eps. Nd	= Epsilon Neodymium
Ma	= Mega-anna; millions of years before present
Ga	= Giga-anna; billions of years before present
GRV	= Gawler Range Volcanics
KMZ	= Kalinjala mylonite zone
KD1	= Deformation event 1 of Kimban orogeny
KD2	= Deformation event 2 of Kimban orogeny

S0	= Sedimentary layering	REE	= Rare Earth Elements
S1	= Metamorphic layering	Nd	= Neodymium
S2	= Axial planar foliation	Sm	= Samarim
Au	= Gold	Rb	= Rubidium
Ag	= Silver	Sr	= Strontium
Cu	= Copper	U	= Uranium
^{143}Nd	= Isotope of particular element	Pb	= Lead

KEY TO STRATIGRAPHIC SYMBOLS

Pp, PMp	= Mesoproterozoic Pandurra Formation
Phi, PMhi	= Mesoproterozoic Hiltaba suite granitoids
Pa, PMa	= Mesoproterozoic Gawler Range Volcanics
Pcc, PMcc	= Mesoproterozoic Corunna Conglomerates
Pbr, PMbr	= Mesoproterozoic Blue Range Beds
Pv, PPv	= Palaeoproterozoic Nuyts Volcanics
Pt, PPt	= Palaeoproterozoic Tarcoola Formation
Pmw, PPmw	= Palaeoproterozoic Wandearah Metasiltstone
Pmg, PPmg	= Palaeoproterozoic McGregor Volcanics
Pmm, PPmm	= Palaeoproterozoic Moonabie Formation
Pd, PPd	= Palaeoproterozoic Myola Volcanics, & Broadview schist
Pl, PPl	= Palaeoproterozoic Lincoln Complex Granitoids
Plmy, PPlmy	= Palaeoproterozoic Lincoln Complex; Moody suite granitoids
Pld, PPld	= Palaeoproterozoic Lincoln Complex; Donington suite granitoids
Ph, PPh	= Palaeoproterozoic Hutchison Group Metasediments
Pbo, PPbo	= Palaeoproterozoic Bosanquet Formation
Phb, PPhb	= Palaeoproterozoic Hutchison Group; Amphibolites
Phy, PPhy	= Palaeoproterozoic Hutchison Group; Yadnarie schist
Phm, PPhm	= Palaeoproterozoic Hutchison Group; Middleback sub-group
Phc, PPhc	= Palaeoproterozoic Hutchison Group; Cookgap schist
Phk, PPhk	= Palaeoproterozoic Hutchison Group; Katunga dolomite
Phw, PPhw	= Palaeoproterozoic Hutchison Group; Warrow quartzite
Ap	= Archaean Sleaford, & Mulgathing complexes

ABSTRACT

The Gawler Craton comprises tocks varying in age from Archaean to more recent Phanerozoic sediments. The rocks of greatest interest in defining processes of early crustal formation and evolution in the Australian continent, are the basement material older than approximately 1400 Ma (pre-cratonisation), comprising deformed and metamorphosed rocks suites of Archaean and Proterozoic metasediments and gneisses. These suites span an immense period of intense geological history, and as such are a topic of much past and present study.

Detailed mapping in the Tumby Bay region of eastern Eyre Peninsula outlines stratigraphic and structural evolution of a sequence of Proterozoic rock suites, these are proposed to be related to other recognised deformation episodes elsewhere within the Gawler Craton, thus regional correlation is inferred. A new theory for development of two lineations within the map region is postulated by two movement directions along the Kalinjala Mylonite Zone.

Geochemically the Proterozoic sediments of the Gawler Craton are similar to upper crustal average values of Taylor & McClennan (1985). However, characteristic depletions in Nb and Sr are recognised. Consistency in trace element compositions for Archaean and Proterozoic samples would suggest recycling of older Archaean crust into Proterozoic sediments and granitoids. Analysis of representative trace element ratios and indices of alteration and weathering suggest some change in geochemistry throughout the Proterozoic period.

Selected Proterozoic clastic sedimentary suites were geochemicaly and isotopically (Sm-Nd) analysed, with the data being presented within this thesis. The most interesting of these being the Pandurra Formation, red-bed sediments deposited within the north-eastern Stuart Shelf region of the Gawler Craton. These sediments exhibit a change in measured isotopic values, with younger epsilon neodymium (ϵNd), and higher Sm/Nd ratios observed (ϵNd(0) = -14.67, Sm/Nd = 0.2441), than typical older Gawler Craton rocks (average Proterozoic sediments ϵNd(0) = -21.85, Sm/Nd = 0.1847). This isotopic shift is also recognised within the Adelaide Fold Belt to the east of the Gawler Craton (average shales ϵNd(0) = -16.20, Sm/Nd = 0.1942). A source for these younger signatures is not recognised within the Gawler Craton, and therefore more distal province sources, OR isotopic alteration in the originally considered 'robust' Sm-Nd isotopic system, are proposed.

CHAPTER 1.   INTRODUCTION

1.1   Introduction

The Gawler Craton, Eyre Peninsula (Fig 1.1), is the oldest stable crystalline basement province in South Australia. Rocks which comprise this basement are of Archaean and Proterozoic age, with younger Phanerozoic sediments covering some extents of the Craton.

The oldest rocks (Archaean) are basement granites, gneisses, and metasediments which were formed, deformed, and metamorphosed before approximately 2000 million years (Ma), after which sedimentation during the Proterozoic was initiated. The Proterozoic period 2000 - 1400 Ma was a period of combined sedimentation, intrusive and extrusive magmatism, and orogenesis, ceasing by approximately 1400 Ma when the Gawler province became cratonised, (ie. no further orogenic activity). Post-cratonic Neoproterozoic sedimentation occured on the Stuart Shelf to the north-east of the craton, with contemporaneous extensive sedimentation also deposited within the Adelaide Geosyncline to the east of the craton (Fig 1.1). These later sediments are not considered part of the cratonic suites as they unconformably overly older cratonic rocks. Isotopic and geochemical analysis of these latter sediments combined with Gawler Craton data is addressed in section B.

The older Archaean crust is suggested to have been recycled extensively throughout the Proterozoic, both by direct erosion into sedimentary basins, and by granitic magmatism (ie. older crust as source rocks for melts). There are many sedimentary basins of differing ages, and lateral extents, covering large proportions of the craton, with periods of orogenic and anorogenic magmatism during the Proterozoic era also observed. These magmatics could have components of possibly 'new' crustal material (mantle sources), and if so would have an influence in changing the geochemical and isotopic composition of the upper Gawler Craton continental crust (ie. younger average crustal ages). Thus the geochronological method of samarium - neodymium (Sm-Nd) isotopic systematics is applied to attempt to unravel the process of upper crustal evolution acting upon the Gawler Craton. Results of this study will also be applied to problems already addressed by Turner *et. al.* . (1992), incorporating the change in isotopic signature from the older Archaean crust of the Gawler Craton, to the younger Neoproterozoic sediments analysed within the Adelaide Geosyncline to the east.

This thesis is sub-divided into two sections. Section A. deals with regional geology, structure and stratigraphy of the Gawler Craton, with field evidence given from detailed mapping within the Cleve tectonic sub-domain. Section B. deals with geochemistry and isotopic compositions of Gawler Craton clastic sedimentary rocks, with changing signatures giving implications towards models of upper crustal evolution.

1.2   Aims and Methods

In section A, all suites of the Gawler Craton are addressed, giving relative stratigraphic correlations and possible source origins for both sediments and magmatics, as determined from the compiled literature. A detailed analysis of the Hutchison Group Metasediments, and Lincoln Complex Granitoids was achieved via detailed mapping of an inland area of outcrop

within the Tumby Bay region, eastern Eyre Peninsula. (Fig 1.1 & 3.1 location maps), which involved these two rock suites intercalated within a highly deformed orogenic belt.

In section B, shale units from within the following suites;- Hutchison Group, Moonabie Formation, Wandearah Metasiltstone, Tarcoola Formation, Blue Range Beds, Corunna Conglomerate, and Pandurra Formation were geochemically and isotopically analysed. These suites range in age from Palaeoproterozoic to Mesoproterozoic (Fig 1.2), and represent a great proportion of the sedimentary suites that were deposited on the Gawler platform before cratonisation. Fresh samples were collected both from rock-grab samples taken from outcrops upon Eyre Peninsula, and also from diamond drill core stored in the Mines and Energy department of South Australia (MESA) core library, Glenside, Adelaide (see Appendix A - Sample locations). Selected samples were then viewed in thin section processed, and analysed by X-Ray Fluorescence (XRF) and Thermal Ionisation Mass Spectrometery (TIMS), at resources within Adelaide University. The data obtained from these analyses will enable a comparison of the differing lithologies being studied, and also help determine isotopic and secular evolutionary trends for Proterozoic rocks of the Gawler Craton.

Fig. 1.1 - South Australian geology & location map

Legend:

PHANEROZOIC
- Basin sediments
- Adelaidean sediments

PROTEROZOIC
- Pandurra Fm
- Hiltaba Suite
- Lincoln Complex

YORKE PENINSULA
- Wandearah Metasiltstone / Willamulka Volcanics
- Moonta Porphyry / Doora Schist

EYRE PENINSULA/ NORTHWEST CRATON
- Gawler Range Volcanics
- Blue Range Beds
- Tarcoola Fm / Corunna Conglomerates
- Moonabie Fm / McGregor Volcanics
- Myola Volcanics / Broadview Schist
- Hutchison Group
- Miltalie Gneiss

ARCHAEAN
- Mulgathing Complex / Sleaford Complex
- Fault

Adapted From Parker (1990)

Map labels: Coober Pedy, Mt Woods Inlier, inferred edge of Craton, Olympic Dam, STUART SHELF, Tarcoola, Woomera, ADELAIDE GEOSYNCLINE, TORRENS HINGE ZONE, Carriewerloo Basin, GAWLER RANGES PROVINCE, Port Augusta, GREAT AUSTRALIAN BIGHT, N, Middleback Ranges, Moonabie Ranges, Whyalla, Itiledoo Basin (Polda trough), EYRE PENINSULA, Pt. Neil, Moonta, KALINJALA MYLONITE ZONE, SPENCER GULF, Port Lincoln, YORKE PENINSULA

0   200
KILOMETRES

Fig 1.2   GAWLER CRATON

RELATIVE STRATIGRAPHIC DIAGRAM

AGES Ma	METHOD	Reference		
1424	Rb-Sr	[1]	Pp	Pandurra Formation
1514	U-Pb	[2]	P hi	Hiltaba Suite
~1592	U-Pb	[3]	Pa	Gawler Range Volcanics
~1522	Rb-Sr	[4]	Par	Roopena Volcanics
1740 - 1585	Rel. Strat.	[5]	Pcc	Corunna Conglomerate
As above		[5]	Pbr	Blue Range Beds
1631	U-Pb	[2]	Pv	Nuyts Volcanics
1656	U-Pb	[6]	Pt	Tarcoola Formation
			Pmw	Wandearah Metasiststone
				Moonta Porphryr, Doora Schist
~1740	U-Pb	[3]	Pmg	McGregor Volcanics
			Pmm	Moonabie Formation
1791	U-Pb	[3]	Pd	Myola Volcanics, Broadview Schist
			Pl	Lincoln Complex
			Plyy	Yunta Well
1677	Rb-Sr	[4]	Plmy	Moody Suite
1843	U-Pb	[7]	Pld	Donington Suite
			Ph	Hutchison Group
1845	U-Pb	[8]	Phbo	Bosanquet Formation
			Phb	Amphibolites
			Phy	Yadnarie schist
			Phm	Middleback subgroup
			Phc	Cook-gap schist
			Phk	Katunga dolomite
			Phw	Warrow quartzite
2014	U-Pb	[3]		Miltalie gneiss
> 2300	U-Pb	[5]	AP	Sleaford Complex, Mulgathing Complex

MESOPROTEROZOIC (spans from Pp through Pbr)

PALAEOPROTEROZOIC (spans from Pv through AP)

References: [1]-Fanning et.al. 1983, [2]-Cooper et.al. 1985, [3]-Fanning et.al. 1988a, [4]-Webb et. al. 1986, [5]-Drexel et. al. 1993, [6]-Fanning 1990, [7]-Mortimer et. al. 1988, [8]-Rankin et. al. 1988.

SECTION A:

CHAPTER 2.   REGIONAL GEOLOGY

2.1 Gawler Craton;   Regional Geology

The Gawler Craton is the largest exposed stable crystalline basement region in South Australia (Fanning *et.al.*, 1988). The area spans over 400 000 square kms, with boundaries being loosely defined along aeromagnetic / gravity lineaments, or structural features, ie. the Torrens hinge zone to the east. (Fig 1.1).

The Gawler Craton shows much resemblance to Northern and Western Australian Proterozoic provinces (Pine Creek inlier, Mt Isa inlier, McArthur basin, etc.), many of which contain substantial economic deposits (Parker, 1990). Thus the Gawler Craton with as yet few working large mines, could be an important site for economical mineralisation.

Three tectonic megacycles are recognised within the Gawler Craton, pertaining to evolution of sedimentation, magmatism, metamorphism and orogenesis (Parker *et. al.*, 1988). The earliest of these is Archaean sedimentation and igneous activity followed by early Palaeoproterozoic magmatism and granulite metamorphism (>700 °C, >4 Kbar) occurring during the Sleaford Orogeny (2500 - 2300 Ma, Webb *et. al.*, 1986). Following this is a phase of initial basin and platformal sedimentation (Hutchison Group) commencing at approximately 2000 Ma, followed by a second orogenic event, the Kimban orogeny (1820 - 1580 Ma, Webb *et. al.*, 1986). Continued sedimentation, magmatism, and amphibolite (500 - 700°C, 4 - 7 Kbar) to granulite metamorphism occurred with deformation throughout this orogenic period. The third, and final megacycle groups the remaining anorogenic magmatism and sedimentation observed upon the Gawler platform before it was cratonised at approximately 1400 Ma. Local folding and faulting of the Wartakan event (Parker *et. al.*, 1988) is seen through this period (1600 - 1500 Ma), see Fig. 3.3 - structural evolution of the Gawler Craton.

Cratons are defined as old regions of the Earths crust characterised by low heat flow, and absence of volcanic or seismic activity (Brown *et.al.*, 1992). Cratons are determined to have larger lithospheric thicknesses than other parts of continental crust (150 km compared to 100 km average, Brown *et. al.*, 1992), thus accounting for low heat flow and tectonic stability of the region. Processes for overthickening of the continental lithosphere in these regions are poorly understood, methods may include large scale orogenesis of provinces prior to cratonisation, or underplating of lower density mantle into the continental lithosphere.

Tectonically the Gawler Craton can be subdivided into several subdomains, on the basis of distinct structural, metamorphic, and stratigraphic character. These divisions are named the Christie, Coulta, Cleve, Moonta, Wilgena, Nuyts, and Nawa subdomains (Fig 2.1), with boundaries defined by convention along major linear aeromagnetic features (possible extensive shear zones) (Parker, 1990).

The Stuart Shelf abuts west of the Torrens Hinge zone which defines the eastern boundary of the Gawler Craton (Fig 1.1). However it is not considered a domain of the craton as it contains younger (Neoproterozoic, and Cambrian) sediments overlying older cratonic

basement. Originally the Stuart Shelf was considered to contain Pandurra Formation sediments, but these were later defined to be older (Mesoproterozoic, Fanning *et. al.* 1983) than other rocks within the basin, and thus were assigned to the Cariewerloo Basin (Fig. 1.1) of Cowley (1991), an elongate depression marking the last sedimentary basin developed prior to cratonisation.
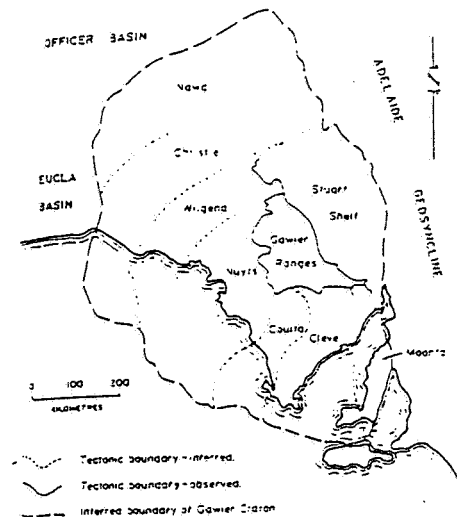
Fig 2.1 - Tectonic sub-divisions of the Gawler Craton, from Fanning *et. al.* (1988).

2.2 Gawler Craton Stratigraphy and Geochronology

The study area comprises rock suites of Archaean to Mesoproterozoic in age, spanning two eras of immense geological development and Earth history. The lithologies deposited within the craton were originally igneous, volcanic and sedimentary, but have been subsequently variably metamorphosed, and deformed by several tectonic events that occurred throughout this period of continental development. Gneisses, metasediments and granitoids are a result.

Archaean:

The oldest rocks are of Archaean age, involving the Sleaford and Mulgathing complexes, as well as some unnamed lithologies. Rock types are both igneous and metasedimentary, and include units within the Sleaford Complex, of the Carnot gneiss (ortho- and paragneisses), Dutton suite (Whidbey and Kiana granites, Coulta granodiorite), Wangary gneiss, and an unnamed gneiss. Units of the Mulgathing complex include the Glenloth granite, Christie gneiss (paragneiss), and other variable lithologies (Drexel *et. al.*, 1993). Isotopic ages vary from 2300 - 2650 Ma (Fanning *et. al.*, 1986a). Both complexes exhibit similar lithological behaviour, with older layered gneisses (Carnot, and Christie) being intruded by younger Archaean granitoids (Dutton, and Glenloth) (Parker, 1990). These Archaean complexes show much similarity to the Yilgarn gneiss terrain of Western Australia (Parker, 1990). However greenstone belts which are source to much of the mineralisation of this terrain, are only just being discovered within the Gawler Craton, represented by komatiites (see Tesselar, 1994 - Lake Harris area).

Palaeoproterozoic:

The Palaeoproterozoic is an early subdivision of the Proterozoic era, approximately 2300 - 1600 Ma. During this time several igneous and sedimentary sequences were deposited and subsequently deformed. These sequences are widespread and diverse throughout the Gawler Craton, but dominantly outcrop within the Cleve, Moonta, and Wilgena tectonic subdomains (Fig 2.1). Other sequences of correlative ages occur throughout South Australia in other tectonic domains, and also as inliers within the Adelaide Geosyncline.

Perhaps the most thoroughly studied of these sequences is the early Palaeoproterozoic **Hutchison Group** metasediments and associated rocks, within the Cleve sub-domain, eastern Eyre Peninsula (more detailed description see Ch 3.). These rocks outcrop within an amphibolite facies fold belt through the Lincoln uplands, Cleve Hills, and other scattered localities. They comprise dominantly shallow marine clastic sediments, iron formations, carbonates, mafic and acid volcanics. Lithologies include the Warrow Quartzite, Katunga Dolomite, Middleback Iron Formations, and the Cook Gap, and Yadnarie Schists (Parker & Lemon, 1982).

In central-eastern Eyre Peninsula, near Carapee Hill, clastic sediments are seen to be overlain by a mixed acid volcanic and calcsilicate unit (see DDH Broadveiw 1 drill hole log - Appendix A) named the Bosanquet Formation. U-Pb dating (Rankin et.al., 1988) gives a zircon crystallisation age of 1845±9 Ma constraining a minimum deposition age for the underlying Hutchison Group sediments of ~1850 Ma. The Bosanquet Formation is proposed to be laterally equivalent with the Yadnarie Schist, which is found within the Cleve district of eastern Eyre Peninsula (Drexel *et. al.*, 1993). A maximum deposition age of ~2010 Ma for the Hutchison group is given by an unconformity observed within the Plug Range region (Parker *et. al*., 1988), between the basal Warrow quartzite of the Hutchison group, and the underlying Miltalie gneiss dated at 2014±28 Ma (Fanning *et. al.*, 1988).

Magmatic intrusions into these and other Palaeoproterozoic sediments, being of mafic and felsic granitoid compositions, are collectively known as the **Lincoln Complex** (Thomson, 1980). Orogenic magmatism is proposed to be driven from tectonism through the Kimban orogeny (approx. 1850 - 1700 Ma), mantle sources may have been accessed at this time due to large scale fracturing of the crust associated with orogenesis. Three subdivisions of this complex have been made on southern Eyre Peninsula, where outcrops in coastal exposures, offshore islands, and within the hilly uplands are quite good. These are the early tectonic (syn-KD1) Donington Granitoid Suite, mid tectonic (late-KD2 to pre-KD3) Colbert Suite, and the late tectonic (syn-KD3) Moody Suite granitoids (Mortimer *et. al.*, 1988) (see Ch 3. for explanation of Kimban structural terminology). Within the Cleve tectonic sub-domain of the Gawler Craton (eg. Ch 3; map area) these granitoids can be extensively mylonitised, and of variable grade metamorphism due to late stage tectonism during the Kimban orogeny (Parker *et. al.*, 1988).

Outcropping east of the Middleback Ranges, but of uncertain stratigraphic position, is a deformed sequence comprising acid volcanics, gneisses, schists, and quartzites, belonging to the **Myola Volcanics** and **Broadview Schist**. U-Pb zircon dating defines an age of

1791±4 Ma (Fanning *et. al.*, 1988), for a volcanic sampled from the Myola type locality ~6 km east of Iron Baron (Parker *et. al.*, 1988).

Major copper (minor gold and silver) deposits of the Moonta, and Wallaroo district, Yorke Peninsula, are hosted within units of the **Moonta Porphyry** and **Doora Schist**, contained within the Moonta tectonic sub-domain. U-Pb zircon dating in a rhyolite (Moonta Porphyry) gives an isotopic age of 1737±5 Ma (Fanning *et.al.*, 1988).

Of similar age is the **McGregor Volcanics** and **Moonabie Formation** volcanic grits, dated at ~1740 Ma by U-Pb zircon work (Fanning *et.al.*, 1988). These units are observed on north-western Eyre peninsula, also with good outcrops in the Moonabie Ranges and the Whyalla region, eastern Eyre Peninsula (Fig. 1.1). The volcanics are both acidic and basaltic in composition (bimodal), and the grits, seen intercalated with the volcanics in the Moonabie Ranges, vary from a sandstone to a pebble conglomerate with clasts of the former volcanic unit. McGregor Volcanics have typical within plate, A-type, geochemical characteristics, but they do contain components of possible mantle or subduction derivation (Drexel *et. al.*, 1993). Temperatures needed for melting of the crust at this time to form the magmatics, would be in excess of the regional post-orogenic geothermal gradient, and thus mantle diaparism is proposed as a source for supplying this heat (Giles *et. al.*, 1980). Mixing of mantle and crustal components (geochemically) would likely result. Deposition of the Moonabie Formation is believed to be of an epiclasitic character proximal to an active volcanic source (Drexel *et. al.*, 1993).

Overlying the Doora Schist, and Moonta Porphyry in the Wallaroo - Kadina region are rock units of the **Wandearah Metasiltstone** and Willamulka Volcanics, drill hole intersections within the Stuart Shelf region have also identified sedimentary rock units as possible Wandearah Metasiltstone. The metasiltstone commonly comprises weakly metamorphosed siliceous and haematitic siltstone, dolomite, and calcsilicate lithologies, with the Willamulka Volcanics observed as amygdaloidal basalts interbedded within the metasiltstones (Whitehead, 1978). Characteristically the Wandearah Metasiltstone shows irregularly shaped, mottled fawn, greenish fawn, and reddish-brown alteration zones. Graded bedding and cross laminations are occasionally preserved (Drexel *et. al.*, 1993). However, the deposition environment is not indicative as to a marine or fluvial nature. Age of the metasiltstone is determined to be substantially younger than the schist and porphyry, via a variation of high to low grade metamorphism across an inferred unconformity in the Kadina region (Drexel *et. al.*, 1993), but is currently a topic of some debate (Wurst, 1994).

Outcropping in the Kingoonya - Tarcoola region of the north-western Gawler Craton is the **Tarcoola Formation**, comprising fluvial to marginal marine, clastic sediments (shales, quartzites, and conglomerates). The Tarcoola Formation has been sub-divided into three members (Daly, 1985); these being basal Peela Conglomerate, overlying Fabian Quartzite, and upper Sullivan Shale. The shale member was sampled for isotope work for this project [Appendix A - Wilgena 1 drill hole log]. Interbedded tuffs within the shales give a U-Pb zircon age of 1656±7 Ma (Fanning *et. al.*, 1986a). These tuffs indicate contemporaneous volcanism (possibly an independent local event) at the time of deposition of the Tarcoola Formation

sediments. Other rock units within the region include the Hiltaba Suite Granitoids, which intrude sedimentary members of Tarcoola Formation. Major gold mineralisation occurs within quartz veins intersecting the shales around the Tarcoola region, (Daly, 1984a&b)

Rhyolites and Rhyodacites of the **Nuyts Volcanics** outcrop on islands of the Nuyts Archipelago. These are suggested to be an independent igneous event upon the Gawler Craton, due to U-Pb zircon ages of 1631±3 Ma (Cooper *et. al.*, 1985) and 1627±2 Ma (Rankin *et. al.*, 1990), contrasting to ages of any other Cratonic suites (Drexel *et. al.*, 1993).

A subdivision of the Proterozoic into the early Palaeoproterozoic and later Mesoproterozoic is made around 1600 Ma. Further anorogenic sedimentation and magmatism is then seen throughout the Gawler Craton.

Mesoproterozoic:

This era is host to a great diversity of anorogenic magmatism and sedimentation events that are widely distributed throughout the state.

At ~1592 Ma, huge volumes of bimodal, anorogenic volcanics were erupted mid-craton, this province extends over 250 000 km^2 and is described as the Gawler Range Volcanics (GRV). Rock types include felsic dacite, rhyodacite, and rhyolite, as well as basic andesites, and basalts in lower volcanic successions (Drexel *et. al.*, 1993). The GRV province is recognised world wide as a major Proterozoic volcanic event, a comparism to similar extrusive volume to the Deccan traps of India is made (Drexel *et. al.*, 1993). The extremely large volume and outpouring extent of extruded volcanics, could be accounted for by many vents sampling a large magma chamber, however calderas which would result from such activities have not as yet been accounted for at any location throughout the entire Gawler Range province. Thus other methods of extrusion are tenuously proposed, involving such processes as differential subsidence along fissure zones, or cauldron subsidence from crustal collapse (Drexel *et. al.*, 1993). The source for such a large volume of magmatism is also speculative. Giles (1980) proposes (with evidence from geochemical modelling), that a segregating rising deep mantle plume is source to much of the early basaltic magmatism associated with the GRV. Felsic magmatism would then be derived from melting of crustal sources (plume as a heat source), and mixing with mantle components to give resultant geochemical signatures.

Both U-Pb and Rb-Sr dates have been established for rocks of the GRV. The U-Pb dates average around 1592 Ma (Fanning *et. al.*, 1988), being sampled from a variety of areas, and different authors, throughout the province. Rb-Sr total rock studies show highly variable ages centred ~1450 Ma, this being around 100 Ma younger than the U-Pb dates thus should be considered disturbed due to remobilisation of Rb and Sr (Drexel *et. al.*, 1993).

Approximately synchronous with the GRV, intracratonic shallow marine or fluvial sedimentation took place, and is observed as the Corunna Conglomerates and Blue Range Beds.

The **Corunna Conglomerates** vary from boulder conglomerates (photo 1 - Appendix B), to carbonaceous siltstones and sandstones. Felsic volcanics are observed interlayered within the sediments in drillholes (eg. DDH Corunna CC1 - Appendix A), and are

proposed to be of GRV origin (Parker and Daly, 1982). Depositional textures are dominantly of fluvial nature, however carbonaceous siltstones and sandstones at the top of the sequence may be of marine origin (Drexel *et.al.*, 1993). The conglomerates are very clastic, with some clasts being defined to be sourced from specific basement rocks; these include examples of GRV and Hutchison Group metasediments. Timing of sedimentation is constrained solely by stratigraphy. An unconformable contact with underlying McGregor volcanics and Moonabie Formation (Parker *et. al.*, 1988) giving maximum deposition age (~1740), and minimum deposition age constrained by intrusion of the dated (Hiltaba suite) Charleston granite (1585±5 Ma, Drexel *et. al.*, 1993). This gives a large depositional age range of 1740 - 1585 Ma. The appearance of interlayered felsic volcanics may suggest a more constrained deposition age approximately synchronous with GRV extrusion (~1592 Ma). Depositional setting is inconclusive, but is likely to be represented by a continental restricted basin with multiple protolith sources, abundant clasts of proximal basement indicating active faulting during deposition (Drexel *et. al.*, 1993).

The **Blue Range Beds** are a sequence of shallow water, or non-marine grits and conglomerates. Nomenclature and stratigraphic correlation of these rocks is a subject of some debate (Flint and Parker, 1981). Names such as Talia Sandstone, Blue Range Sandstone, and Mt Wedge Grit, have previously been used. However, here the term Blue Range Beds (Flint & Parker, 1981) is applied as an encompassing label. Age correlation with the Corunna conglomerate (Flint and Parker, 1981) is also favoured, but evidence in exposed contacts to confirm this is tenuous, the only exposed contact being an unconformity with the Palaeoproterozoic Hutchison Group in the Cleve region (hence a poorly constrained maximum deposition age). Correlation with the Pandurra Formation (Flint and Rankin, 1991) is also suggested, based on the abundance of (proposed) GRV and Hiltaba suite clasts. Outcrops of these lithologies are seen to be distributed within a major east - west trending trough, defined as the Itiledoo basin (Fig 1.1), which is of essentially the same configuration as the Polda Trough (Thomson, 1980). However, a distinction of the two basins is made upon the age of the rocks contained within, the Itiledoo basin containing only Proterozoic sediments, whereas the Polda Trough contains also younger (post cratonic) Phanerozoic sediments which overly the Proterozoic sediments. Rock types within the Itiledoo basin vary from sandy conglomerates (Cleve region), to sandstone and siltstone / silty shale (Mt Wedge), [see also Appendix A - DDH Newland 1 Drill hole log]. A braided stream / alluvial fan environment of deposition is proposed for the sequence (Drexel *et. al.*, 1993), based on both upward coarsening and fining sequences, and clastic poorly sorted nature of the sediments.

Hiltaba Suite granitoids are late stage, anorogenic intrusions and are widesread across much of the Gawler Craton province. This is a bimodal suite but is dominantly composed of granitic members. Named units within the suite are; the Charleston Granite, Tickera Granite, Roxby Downs Granite, and Balta Granite, along with several other unnamed granites of widely distributed localities. Stratigraphically the maximum age of Hiltaba plutonism is constrained by intrusion into the GRV (Drexel *et. al.*, 1993) with an age of ~1592 Ma. U-Pb and Rb-Sr dates for Hiltaba granitoids have been established from a variety of

different source localities and authors, the U-Pb ages vary from 1600 - 1585 Ma (Fanning *et. al.*, 1988) and the Rb-Sr show a 100 Ma younger age similar to the GRV, thus can be concluded to be disturbed in a similar way. U-Pb ages are essentially syn-extrusion age of the GRV, and thus the source origin for the Hiltaba granites may be represented by the waning stages of anorogenic magmatism that occurred to form the GRV province (Drexel *et. al.*, 1993). The Hiltaba Suite (Roxby Downs) granite is also host to one of the worlds largest Cu-U-Au-Ag-REE mining operations, the Olympic Dam deposit, with an indicated resource of 450 Mega tonnes of mineable ore.

The **Pandurra Formation** (Crawford, 1964) is the youngest pre-cratonic sedimentary suite deposited upon the Gawler platform. These arenaceous redbed sediments are situated in the Cariewerloo Basin of the north-eastern Gawler Craton (Fig 1.1), adjacent to the Neoproterozoic Stuart shelf sediments. Lithologies vary from conglomerate to shale, but are dominantly found as a medium grained poorly sorted sandstone (Drexel *et. al.*, 1993), [see also CSR drill holes - Appendix A]. A non-marine depositional enviroment is proposed for the Pandurra Formation (Drexel *et. al.*, 1993), due to its high haematite content (oxidation during depostion and diagenesis), and generally coarse grain size and textural immaturity. An unconformable relation with underlying Hiltaba suite is observed, and thus the unit must be younger than ~1580 Ma. Stratigraphically the unit was initially thought to be of Cambrian or Adelaidean age, but more recent Rb-Sr geochronology determined a minimum age of 1424±51 Ma (Fanning *et. al.*, 1983) constraining it to the Mesoproterozoic (pre-cratonisation).

Neoproterozoic:

Later post-cratonic sedimentation and magmatism is observed within the Adelaide Geosyncline to the east of the Craton (Fig 1.1). The Gawler Craton province is basement to this younger intracratonic basin (Turner *et. al.*, 1993), which is believed to evolve in a classic steers head morphology (initial rift-phase subsidence, with following thermal sag-phase subsidence) causing an extensive basin to develop. Source protoliths for sediments within this basin are logically the surrounding rocks which are comprised of Archaean and Proterozoic Gawler Craton suites. However more distal sources such as from the Musgrave Block, and Willyama and Mt Painter inliers (Proterozoic provinces) of South Australia, or even from the Grenville province of eastern and south eastern North America, which was proposed to be adjacent to eastern Australia at Proterozoic times (Mores, 1991), must also be considered.

Phanerozoic:

Younger sediments are observed within shallow basins covering large extents of the Gawler Craton, and therefore mask much of the underlying basement rocks. Thus geological and mineral exploration, which can be of significant interest in these former very old, highly deformed, rocks is hampered by the younger cover sequences.

CHAPTER 3.   TUMBY BAY MAPPING AREA

3.1   Previous investigations

Mapping of a chosen area on the Lincoln 1:250 000, Tumby Bay 1:100 000 geology sheets (Fig 3.1 - location map) was performed in order to understand, on a detailed scale, the structure and lithological relationships affecting the Cleve sub-domain (Fig 2.1) of eastern Eyre Peninsula. Processes which act upon the Cleve sub-domain may be related to processes acting upon the whole of the Gawler Craton.

Previous workers include Coin 1976 (Tumby Bay), Parker 1978 (Cleve hills), Parker *et. al.* 1988 (Eyre Peninsula; Field guide), Fanning *et. al.* 1986b (Sleaford Complex), Parker & Lemon 1982 (regional), Davi 1993 (Tumby Bay), Oussa 1993 (Pt. Neil), Mortimer 1985 (Lincoln Complex), as well as recent unpublished MESA mapping by Lee Rankin, and ongoing work by Adelaide University students.

The rock suites contained within the map region belong to the Hutchison Group Metasediments, and Lincoln Complex Granitoids (Fig 1.2, stratigraphic diagram). Within the map region the sequence has been highly deformed, and metamorphosed to amphibolite or greater grade, via tectonic processes involved within the Kimban Orogeny (Parker *et. al.*, 1988). The area is also traversed by a major high grade shear-zone, the Kalinjala Mylonite Zone (Coin, 1976).

The selected area was chosen (based on availability of outcrop), within the hills west of Lipson; in the Tumby Bay district. Mapping was achieved on 'foot' and also via a 4WD Subaru wagon, generously supplied by the Mines and Energy department of South Australia (MESA). A total area of approximately 50 km^2 was traversed.

3.2   Geology

The map area was sub-divided into eight discrete mappable units, corresponding to geochemically / petrographically distinct lithologies. However adjacent to the defined mylonite zone (eastern edge of map - Appendix H) the lithologies are more highly sheared and deformed, thus making it much more difficult to define true lithologies in hand specimen. Selected samples are briefly described from field hand specimens, and thin sections in Appendix A & B, any samples used for analytical work having been ascribed an accession (analytical) number as well as its field sample number.

The Kalinjala Mylonite Zone (KMZ) is a major linear zone of intense ductile deformation extending north-south along the eastern coastal region of Eyre Peninsula (Fig 1.1). Mylonites are defined as rocks within which intense ductile deformation has caused fracturing and deformation of individual crystals (Parker, 1980), such that 'finer grained' rocks are produced. These mylonites of the Gawler Craton have been formed in response to intense ductile deformation related to shearing and folding of the Kimban orogeny (Parker, 1980). Within the Tumby Bay region the KMZ is observed juxtaposing Lincoln Complex Granitoids to the east, and Hutchison Group Metasediments, with associated intrusives, to the west [Appendix H - map area]. High grade mylonites are observed within Mine Creek (Fig 3.1) to

Fig 3.1

Tumby Bay location map

Lipson Cove

**Tumby Bay
Map Area
See Appendix G**

Township of
Lipson

Mine Creek

SPENCER GULF

To Cummins ~30 Km

N

KEY

— Lincoln Highway

— Other roads

Township of
Tumby Bay

To Pt Lincoln ~50 Km

Scale

0   Km   5

Tumby Island

Cape Euler
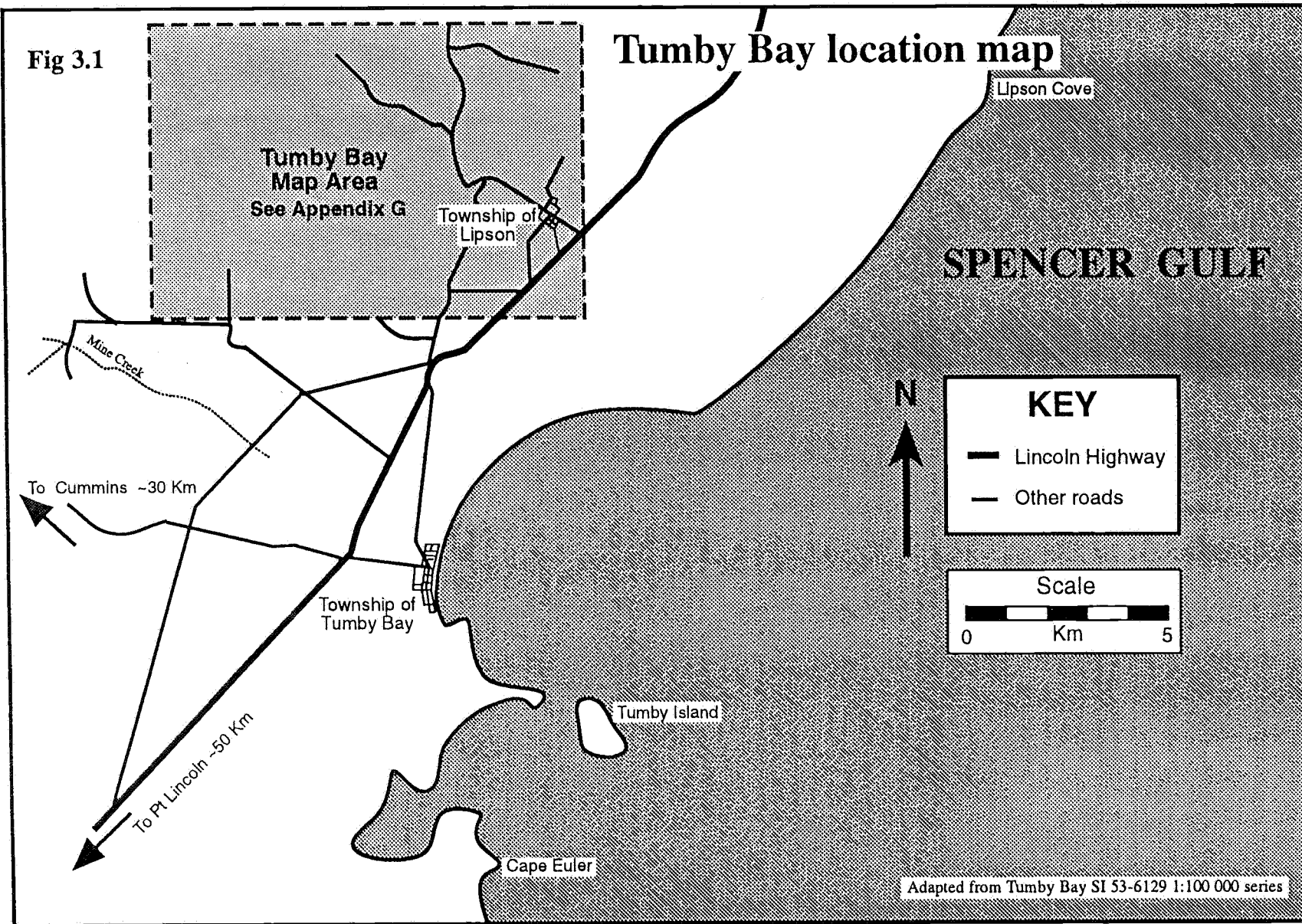
the south-west of the map region (Coin,1976), and also north at Pt Neil (Oussa, 1993) (Fig 1.1), both in similar rock types as found within the map area. Heterogeneous strain on all scales is observed accross and within the KMZ (Oussa, 1993), with high grade zones adjacent to zones of apparently low strain.

Sedimentary units described within the map area are similar to units described by Parker *et. al.* (1988) within the Cleve hills further north, thus a correlation of the map units to the Palaeoproterozoic Hutchison Group can be made. These units are the Warrow Quartzite, Cook Gap Schist, Katunga Dolomite, Middleback Iron Formations, and concordant amphibolites. Granitoids mapped within the area can similarly be correlated with descriptions of other workers; Black gneiss - Lincoln complex, Donington Granitoid (Mortimer, 1985), Leucogranite - Yunta Well Leucogranite (Drexel *et. al.,* 1993), and Muscovite granite - Carpa Granite (Drexel *et. al.,* 1993). These units are all interrelated in a complex, highly sheared amphibolite facies gneiss terrain with moderate to poor outcrop within the map region.

3.3   Sequence of events

Within the map area, the oldest lithologies belong to the Palaeoproterozoic Hutchison Group Metasediments. Granitoids of the Lincoln Complex are younger as defined by intrusive relations at some field localities (eg. xenoliths, location eS12 - photo 2 - Appendix B) and also via field evidence given from authors at other Gawler Craton localities. eg. Refuge rocks; Kimba - Quartzite xenoliths within granites, (Parker *et. al.* 1988).

In other parts of the Gawler Craton (Cleve hills, Parker 1978), a stratigraphic sequence has been defined for these Hutchison group metasediments. The sequence begins with deposition of a basal quartzite unit, followed by chemical sedimentation of dolomite and jaspilite units, which is subsequently followed by deposition of a schistose unit which may contain concordant amphibolites. Partial repetition of the upper part of this sequence is observed in the Cleve hills (Parker, 1978), but is not observed within the Tumby Bay area (Appendix H - Cross sections, & map). This total sequence is poorly represented within the map area, the sequence being obliterated due to the intense shearing caused by stresses exerted in and around the mylonite zone. However,some correlations may be made (Appendix H - cross sections).

Orogenesis occurred beginning approx. 1850 Ma and extending to around 1600 Ma (Webb *et. al.,* 1986). This orogenesis is termed the Kimban orogeny, and is proposed to contain at least three main tectonic events, of decreasing metamorphic grade, staggered throughout the time span of this event (Parker *et. al.,* 1988). Effects of this orogenesis are observed throughout the whole of the Craton, but are best observed in outcrop within the Cleve tectonic sub-domain (Fig 2.1).

The first event (KD1) is seen to form a layer parallel fabric, defined by metamorphic minerals (Appendix B - thin section photos B & F). The next event (KD2) is observed by very tight isoclinal folds, with an axial planar foliation (s_2), sub-parallel to s_0 sedimentary layering and s_1 foliation, being selectively preserved, lineations are also produced in lithologies of suitable competency eg. the quartzites of gneisses (Rock photos A & C -

Appendix B). The third deformation event (KD3) is seen by tight or open folding and local mylonitisation (Parker *et. al.*, 1988). This deformation is very heterogeneous with distinct 'mylonite zones', and other zones of relatively little observed deformation (readily seen within Tumby Bay map area - Appendix H). Tight antiformal and synformal folding is observed within the eastern region of the map, (Appendix H - structural map, & Fig 3.2a - stereoplots) with dips alternating from steep east to steep west. [See Fig 3.3 for outline of Kimban structural development]. Recognition of all these events is hard in the field, as KD3 mylonitisation has masked most of the earlier events in the more deformed zones, and other areas are highly weathered such as to deter the effort of making accurate measurements and conclusions.

It is proposed that during Kimban orogenesis many suites of synorogenic igneous and volcanic rocks were emplaced, grouped together they represent the Lincoln Complex. The Donington Suite Granitoids (Photos C & D - Appendix B), vary in composition from quartz gabbronorite, through to hypersphene granite and leucogranite (Parker *et. al.* 1988), these are seen east of the mylonite zone within the map area as highly deformed gneisses (Photo 3 - Appendix B). The Moody Suite Granites (Rock photo E - Appendix B), are seen as relatively undeformed (thus late tectonic) granites, and leucogranites in the west of the map area (Yunta Well and Carpa granites), tourmaline pegmatites intruding much of the map sequence may also belong to this suite. Evidence for these granites being intrusives can be seen at location eS12 (location - Appendix H, & photo 2 - Appendix B) where xenoliths of metasedimentary material are found within leucogranitic rocks. Other granitic and volcanic suites are seen over other parts of the Gawler Craton, but are not observed within the map area.

Contacts of the above intrusives to other rock types are often sheared (ie. Photo 4 - Appendix B), reflecting intrusions before last stages of deformation. However strain gradients often exist across contact boundaries between Hutchison Group Metasediments and Moody Suite Granitoids, with the granitoids exhibiting lower apparent strain fabric than the metasediments they are intruded into. Thus it is postulated these granitoids were emplaced after initial deformation was initiated but before final deformation, ie syn-KD3 (Drexel *et. al.*, 1993). The Donington suite granitoids (black gneisses) to the east of the KMZ show a much greater strain fabric than the Moody suite granitoids of the west. This may simply be due to relative proximity to the mylonite zone, which is believed to form much of the present observed fabric (s_3 sub-parallel to s_0 & s_1). However based on evidence elsewhere within the Gawler Craton, the Donington Suite Granitoids are believed to be the oldest (syn-KD1, Parker *et. al.* 1988) of the two granitoid suites represented within the map area.

A later deformation event is proposed to occur around 1600 to 1500 Ma, involving cross folding and faulting. This, the Wartakan event (Parker *et. al.*, 1988), may be represented within the map area by cross faulting (at few recognised localities- Appendix H), off-setting lithological trends.

Fig 3.2a

Tumby Bay - foliation plots
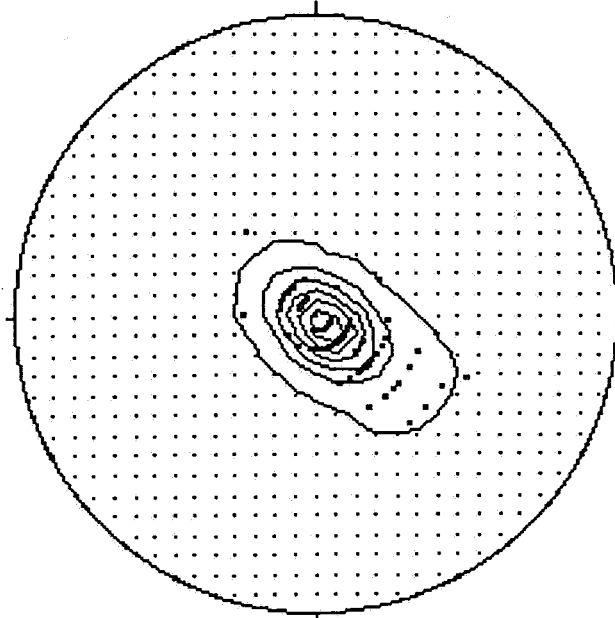
269 Data. Contoured at 1 9 ... 41 times uniform

Dips in foliation vary from predominantly steep east (80° to 130) to steep west
(80° to 310), thus antiformal and synformal folding is proposed. See Appendix G
Tumby Bay map.

Fig 3.2b

Tumby Bay - lineation plots
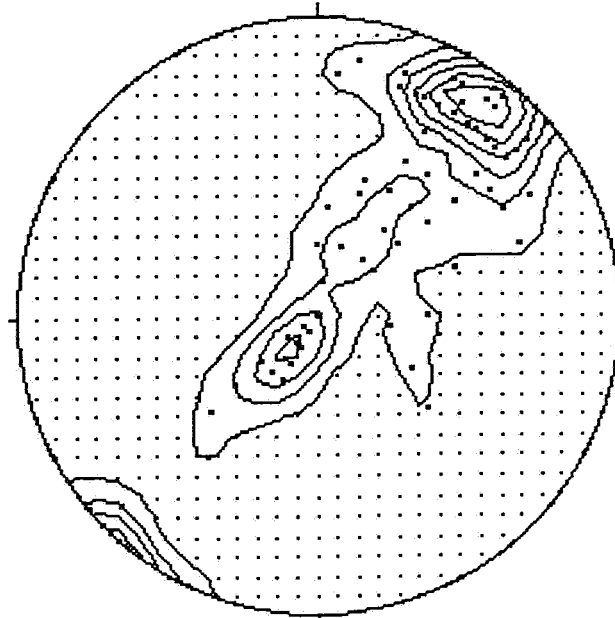
94 Data. Contoured at 1 3 ... 11 times uniform

2 groups of lineations are observed, predominantly shallow north (15° to 030), wtih a
grouping of steep south lineations (80° to 210) also observed.
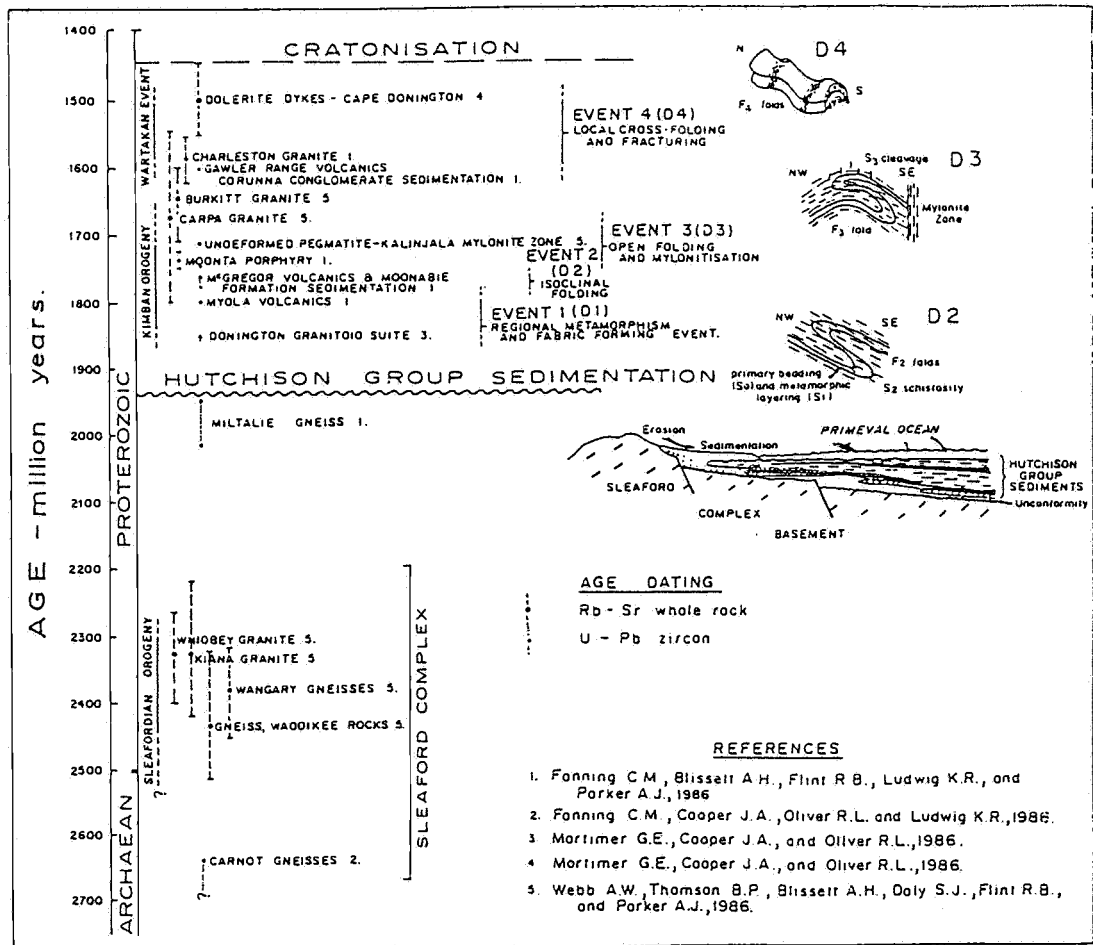
Fig 3.3 - Stratigraphy of the Galwer Craton, and Kimban structural development. From Parker *et. al.* (1988).

The large 'kink band' in the south-east of the map region may represent either cross folding of the Wartakan event; OR a large scale dilatational zone. The latter being formed during heterogeneous deformation around an inelastic 'point', which may cause an increase in bulk volume due to folding and fracturing within intensely deformed areas (Hobbs *et. al.*, 1976). The later structural development is favoured, based on recognition of local fracturing and folding within this deformed area (not able to be structurally resolved or shown on map scale), and that if cross-folding were the case, it would be represented also further west, but is not observed within the map region.

Lineations are highly varied within the map region, but two groupings of lineations are recognised based on stereographic plotting (Fig 3.2b). One grouping at approximately 80° towards 210° (steep south), in northern central region of map [section (a) - Appendix H], and another predominant direction at 15° towards 030° (shallow north), located within the eastern (mylonitised) region of map [section (b) - Appendix H]. Note that lineations could not be measured accurately in all portions of map region, as reliable outcrop with preserved structural indicators is dramatically lacking in the highly weathered areas. The proposed structural explanation for these two bearings, is that the lineations are recording two directions of

movement along the KMZ. One a period of near vertical movement (steep south lineations) which is preserved in the less deformed areas, but is overprinted and not recognisable in the highly deformed mylonitised areas, which record the dominant strike-slip shallow north movement of the KMZ (Oussa, 1993). [See Fig 3.4 - Block diagram of lineation development]. This development of two lineations is not unique to Tumby Bay area alone, but is observed more regionally elsewhere within the Cleve sub-domain, eg. shallow north at Pt. Neil (Oussa, 1993), and steep south within the Pt Lincoln district (Bendall, 1994) (Fig 1.1).

Fig 3.4 - Block diagram, lineation development
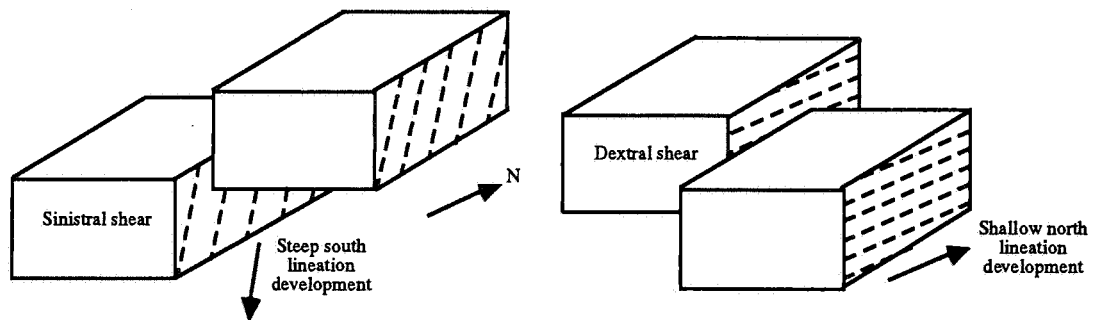
Strain markers are kinematic indicators developed due to accumulation of stresses (Oussa, 1993), directions of movement may be determined by select strain markers. eg. rotated porphyroblasts (Fig 3.5). Dextral (clockwise) and sinistral (anti-clockwise) indicators such as these were both observed within the map area. Outcrop being poor these were not recorded as were determined to not be continuously reliable. The two directional indicators could be developed via the two different directions of movement along the KMZ (Fig 3.4).

Fig 3.5 - Rotated porphyroblast, dextral shear

Matrix fabric

Shear sense

Porphyroblasts composed of more resistant mineral (to deformation) than matrix. eg. Feldspar.
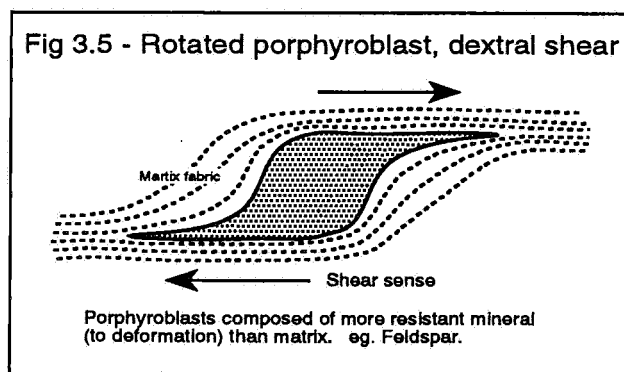
Cratonisation is defined as occurring at 1450 Ma, the age after which no further orogenesis is observed. Subsequent weathering and erosion processes since this time have caused the landscapes that we see today on Eyre Peninsula. Some Tertiary sediments are recognised within the map area, the remaining cover must be ascribed to quaternary weathering and erosion to form regolith. Human influence on the area is moderately high, with the major land use for the area being cereal crop farming. Mappable outcrop is greatly restricted to summits of hills, the topography flattening to the west, and thus restricting mappable outcrop in this direction.

SECTION B:

Introduction

The continental crust in comparison to the mass of the Earth as a whole, is minute (less than 1%) with the upper crust composing only 25% of this. However this upper continental crustal zone is the most directly accessible region to sample, and obtain information pertaining to processes of evolution of the Earth. The oldest recorded radiometric age is 4200 Ma, recorded from zircons in a quartzite from Mt. Narrayer (Western Australia) (Brown *et.al.*, 1992). Thus continental crustal rocks record a history of formation spanning from close to the age of formation of the Earth (4500 Ma) until the present. Models of crustal evolution have been postulated by many authors (eg. Armstrong 1991, McCulloch & Wasserburg 1978, Taylor & McClennan 1985) and some of these models are addressed herein.

The aim of this section is to propose processes of upper crustal evolution acting upon a portion of continental crust, that being the Gawler Craton, and Adelaide Fold Belt, South Australia. Data used to show evidence of evolution was obtained by myself, and also from other cited references.

Clastic sediments are products of mechanical weathering and erosion of the upper crust, with deposition into sites of low relief (basins). Thus analyses of sediments would give results reflecting weighted averages of the different source rocks which comprise their provenance regions. The principle of determining provenance of sediments from geochemical and isotopic techniques was first applied by McCulloch and Wasserburg (1978) upon rocks comprising the Canadian shield. The process involves measuring the compositional make-up of the sediment (eg. isotopically, geochemically) and knowing similar information for the suspected rocks which may comprise the provenance region, models of weighted averages for the source rocks can be deduced.

New isotopic and geochemical data for Proterozoic sediments of the Gawler Craton is presented within this thesis. This data was obtained in order to determine a better 'average' of the Gawler Craton Proterozoic upper crust, in proposing it as a possible provenance source for sediments within the Adelaide Fold Belt to the east. Previous investigations (Turner *et. al.*, 1992) have already adressed the problem in that Sm-Nd isotopic values for the Adelaide Fold Belt samples, show a younger signature than older rocks of the Gawler Craton. Thus younger source regions may have been accessed in order to obtain this change, however other possible theories for this change in signature are also given. Shale material was sampled for rocks of the Gawler Craton where possible, as this rock type is well mixed, and thus would best represent an average of the source region (Allegre & Rousseau, 1984).

The continental (and oceanic) crust is ultimately derived from the Earths mantle. Fractionation processes involved in extraction of melts from this source tend to concentrate the more incompatible elements into the crust (Brown *et. al.*, 1992). Certain trace elements (Th, Sc, Y, Co, etc.), and all REE's have very short residence times (see section 4.1) in oceanic waters, and thus are almost exclusively transferred to the clastic sedimentary record (ie. as sands, clays, etc.), within basins developed on continental shelves, geosynclines, etc. (Taylor

& McClennan, 1985). Thus these elements, as well as other compatible and major elements are analysed to determine processes of geochemical evolution, involving also alteration and recycling processes affecting the sampled rocks.

CHAPTER 4.   GEOCHEMISTRY

4.1   Introduction

Sediments are the final products of weathering and erosion of the upper continental crust, representing (in part) the source rocks they were derived from. However chemical and mechanical processes acting during and after sedimentation may act to alter the geochemistry of some elements from their true value within the source region (Taylor & McClennan, 1985). One of the main problems in addressing clastic sediments as geochemical averages is that some elements have longer residence times in weathering fluids (ie. more soluble in oceanic waters), and thus are stored for longer periods of time within the fluids. Elements with longer residence times are likely to be deposited within chemical sediments (ie. carbonates, evaporites), whereas elements with short residence times are more likely to be transferred directly into the clastic sedimentary record (Taylor & McClennan, 1985).

Mobile elements during weathering processes are the more soluble alkali and alkaline earth elements, these elements are likely to be carried into the weathering fluids (ie. water), and deposited later. Immobile elements, those with high valence ions, eg. thorium (Th), niobium (Nb), REE's, yttrium (Y), scandium (Sc), etc., attach themselves to minerals readily, these minerals are then mechanically deposited into clastic sediments (Taylor & McClennan, 1985). Chemical alteration is believed to have less effect on these immobile elements as processes involved have to alter also the minerals they are attached to. Thus analyses of immobile elements would best represent unaltered information about provenance of the sediments analysed.

The Chemical Index of Alteration (CIA = $[Al_2O_3/(Al_2O_3+CaO+Na_2O+K_2O)]*100$) of Nesbitt and Young (1982), and the Chemical Index of Weathering (CIW = $[Al_2O_3/(Al_2O_3+CaO+Na_2O)]*100$) of Harnois (1988), are indices which are able to show effects of alteration and weathering upon the major elements of the analysed rocks, resulting from processes involved in sedimentation. The CIW index of Harnois is likely a better representation of this as it ignores potassium (K) which is largely mobile and thus readily affected by diagenesis and metamorphism (Condie, 1993).

4.2   Methodology

Samples for Proterozoic clastic sedimentary suites were collected from fresh diamond drill core, or selected hand specimens from located field samples [Appendix A - sample locations]. Sample preparation for analytical work is discussed in Appendic C.

Whole rock XRF analyses were carried out on a programmable Phillips PW 1480 X-ray spectrometer, major and selected trace element concentrations were determined and are presented in Appendix F. Results are similar to values obtained by Taylor & McClennan (1985) in estimating the bulk geochemistry for upper crustal averages. Trace element discrimination diagrams are normalised against these upper crustal average values (Taylor & McClennan, 1985; pp 46) and are presented in Fig 4.1a&b. Plots were also created depicting the changes of value in CIA and CIW over time (Fig 4.2a&b), reflecting effects of alteration in

Fig 4.1a

Trace element plot - Proterozoic suites
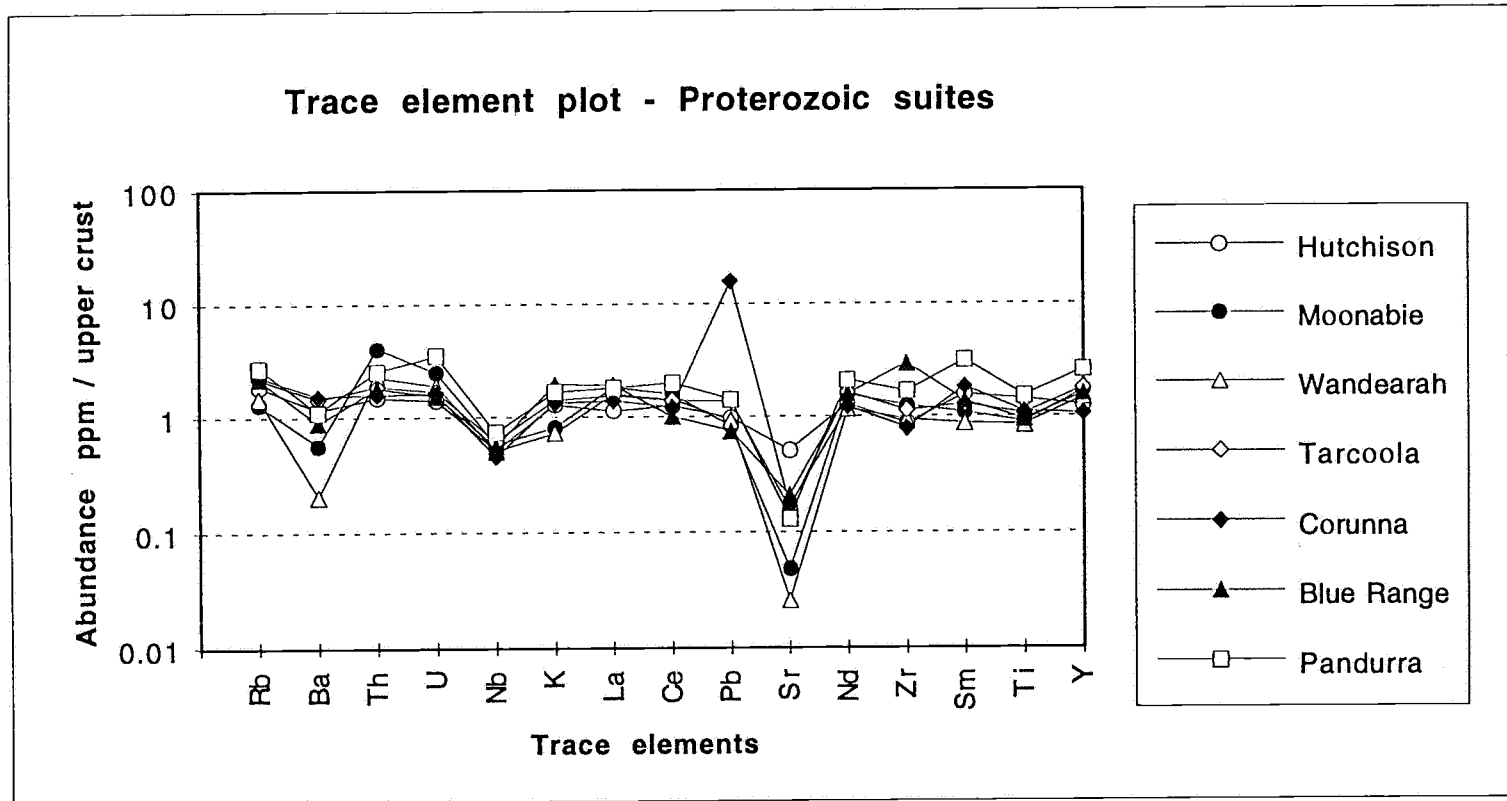
Data obtained and compiled by Author

Trace element discrimination diagram of seven analysed Proterozoic clastic sedimentary suites.
Normalisation factor is against average upper crustal bulk geochemical values of Taylor & McClennan, 1985.
Deviation away from normalised trend value (1) shows differences in Gawler Craton sampled crust to average bulk crust.

Fig 4.1b

Trace element plot - Cratonic suites

LEGEND

Envelope of compiled
Proterozoic trends

Average trends

Archaean

Lincoln

GRV

Adelaidean
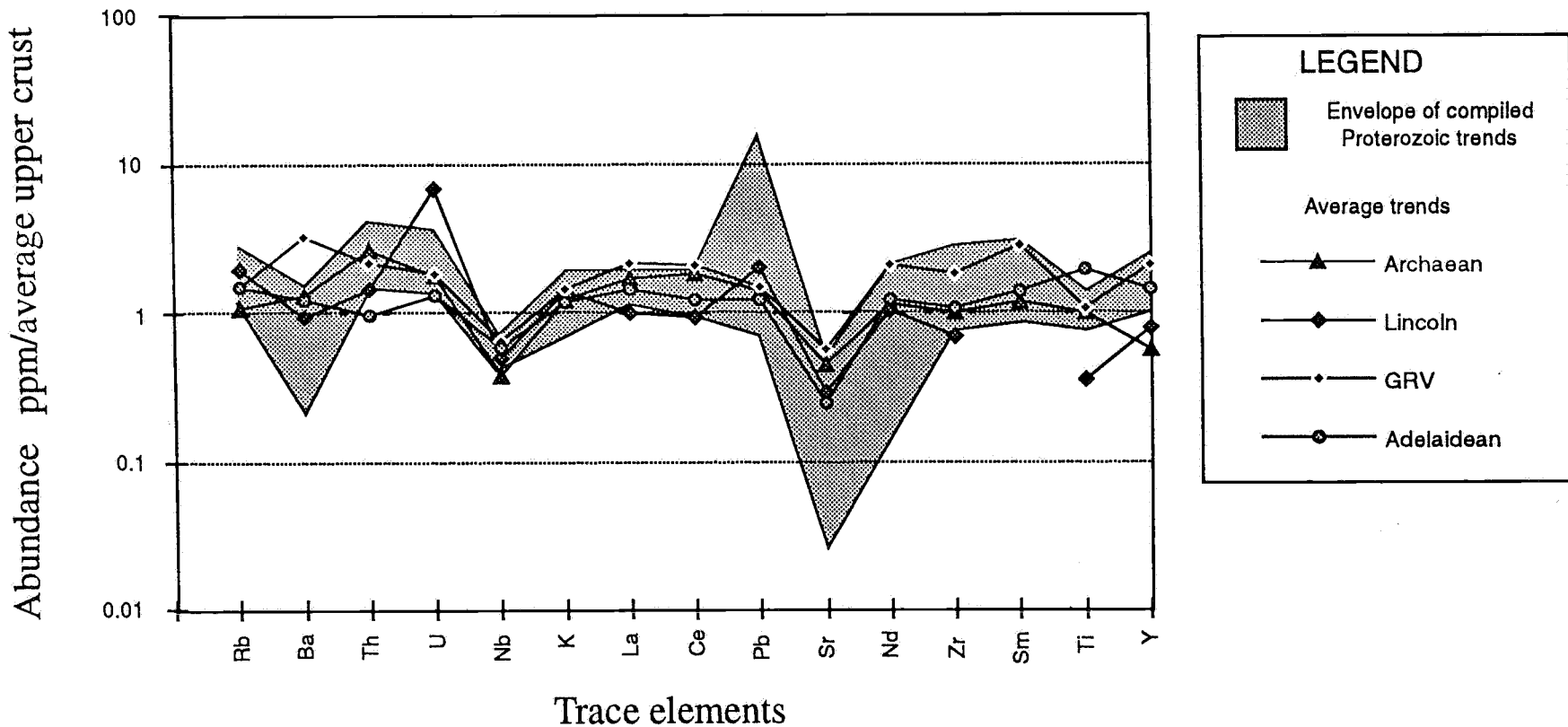
Compiled data - See Appendix F for references

Trace element trends are similar for analysed samples, and lie dominantly within the
envelope of Poterozoic sediments. Thus recycling of older signatures throughout the
Proterozoic is proposed

the major elements which comprise the rocks. Effects of fractionation, weathering and alteration influencing certain trace elements are determined via examination of the change in representative element ratios over time (Fig 4.3a&b).

4.3 Discussion of results

Fig 4.1a shows a comparison of averaged normalised trace element data from the seven analysed Proterozoic Gawler Craton clastic sedimentary suites. Most trace plots are reasonably similar (excluding Sr), possibly representing similar protolith sources for all of the Proterozoic sediments, ie. extensive recycling of older cratonic rocks throughout the Proterozoic. The lead (Pb) anomaly for the Corunna shale may be explained due to mineralisation, the samples having been taken from diamond drill core within areas targeted for economic mineralisation. Depletion in niobium (Nb) and strontium (Sr) is noted for all samples. Sr is a mobile alkali element, and thus may easily be transferred out of the clastic sedimentary record (to varying degrees), during sedimentation or metamorphism, thus accounting for different depletion proportions (reflecting different degrees of alteration during or after sedimentation) for different suites. Nb is considered an immobile element with a short residence time (Taylor & McClennan, 1985), and thus its depletion would be likely to represent a lack of enrichment in the source rocks. This is seen in Fig 4.2b where possible source rocks for Proterozoic sediments also show depletion in Nb. Thus it may be concluded that rocks of the Gawler Craton typically show this Nb depletion anomaly. Enrichment in the heat producing elements thorium (Th) and uranium (U) is noted, and would likely represent an influence from a granitic source with high contents of these elements (eg. Lincoln Complex, Archaean granitoids).

Fig 4.1b shows the envelope for Proterozic sediments, with possible source rock average traces also represented (Archaean gneisses, Lincoln Complex Granitoids, GRV). The plots show it is reasonable to conclude, that because of the similarity of trace element patterns, Proterozoic sediments are ultimately derived from local sources upon the Gawler Craton (source traces lie within Proterozoic envelope). The average trace for Adelaidean sediments is also displayed on this diagram, and shows a similar trace compared to Gawler Craton possible province sources, ie characteristic Nb, and Sr depletion. This may reflect recycling of Gawler into the Adelaide Fold Belt sediments, retaining the geochemical signatures. However, enrichment in the element titanium (Ti) may represent a different possible province input, supplying this extra concentration of Ti.

Fig 4.2a&b show CIA and CIW evolution of shales from Archaean to Adelaidean ages, with possible granitic sources also defined. The lower three Proterozoic sediments (black diamonds) are likely to contain substantial carbonate components, thus are not truly clastic sediments and can be ignored (J. Foden pers. comm.). Regarding this, all CIA values lie above the average upper crustal value, defined at 50 (Taylor & McClennan, 1985), but are within the range of average shale values (70 - 75). There appears to be a general trend from the Archaean to Proterozoic, with an increase in both CIA and CIW values, which would reflect an increase in weathering and alteration affecting these latter sediments. Possible Proterozoic source rocks (GRV, Lincoln Complex) show much lower values than sediments (expected as

Evolution of indices of alteration and weathering.

Fig 4.2a

Evolution of CIA - Archaean to Adelaidean

Legend:
- ■ Archaean gneisses
- □ GRV
- ◆ Proterozoic seds.
- ◇ Lincoln granites
- ▲ Adelaidean seds.

X-axis: Stratigraphic age (Ga)
Y-axis: CIA value

Fig 4.2b

Evolution of CIW - Archaean to Adelaidean

Legend:
- ■ Archaean gneisses
- □ GRV
- ◆ Proterozoic seds.
- ◇ Lincoln granites
- ▲ Adelaidean seds.

X-axis: Stratigraphic age (Ga)
Y-axis: CIW value
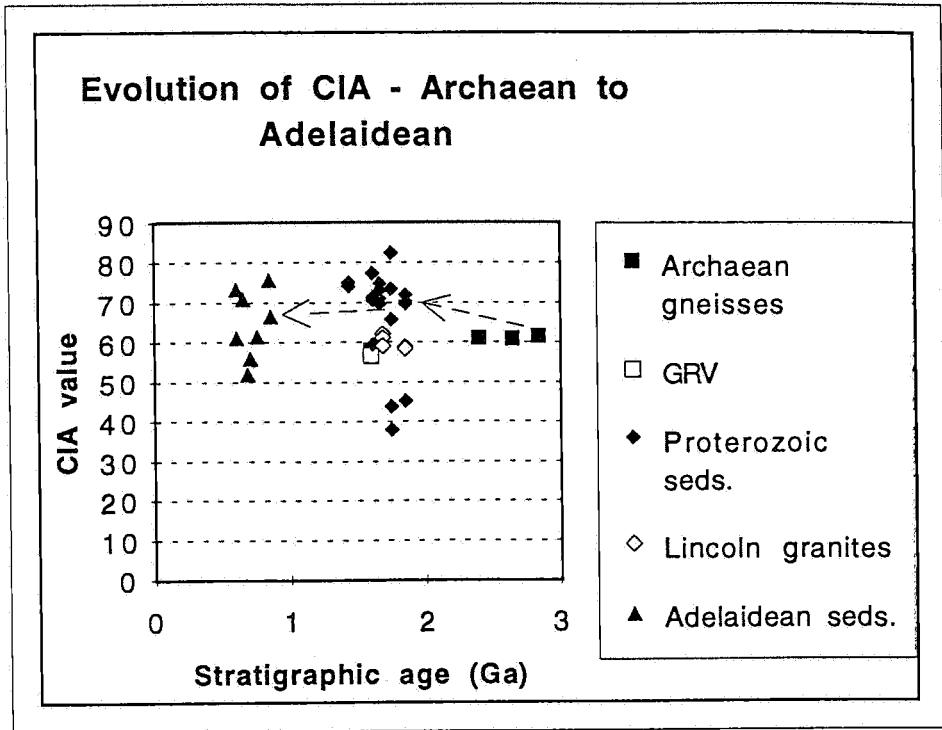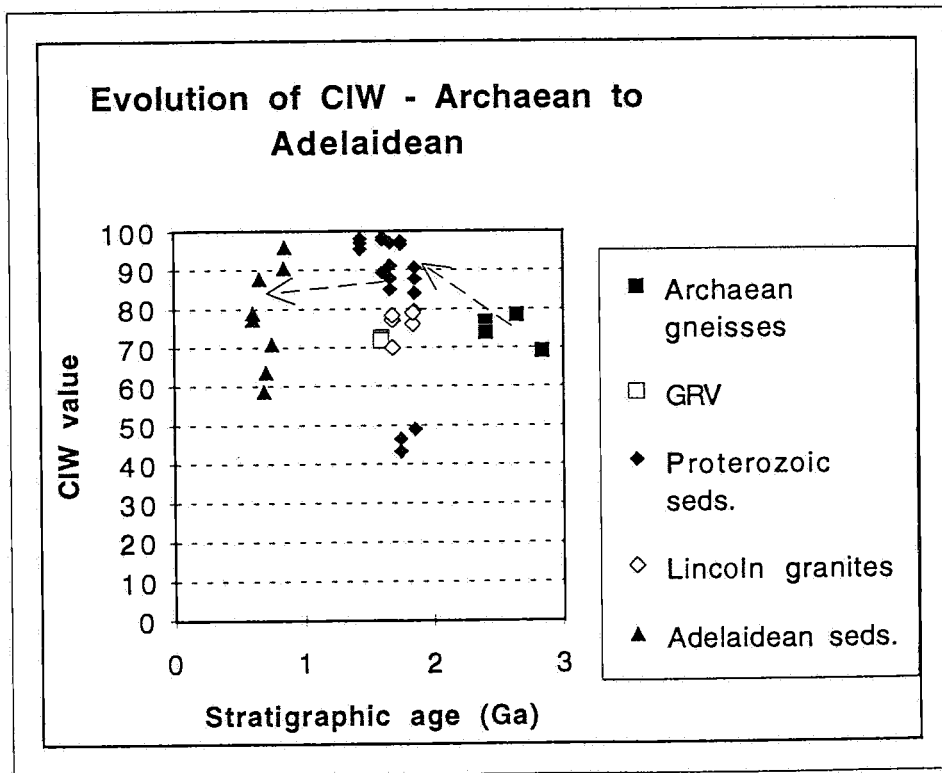
Compiled data - see Appendix F   for references
Evolutionion of indices of alteration and weathering through the
Archaean to Adelaidean geological time span.
Increase in values representing increase in effects of both processes.

Trace element evolution diagrams, Archaean to Adelaidean ages.

Fig 4.3 a

Evolution of La/Sc - Archaean to Adelaidean

Fig 4.3 b

Evolution of Th/Sc - Archaean to Adelaidean
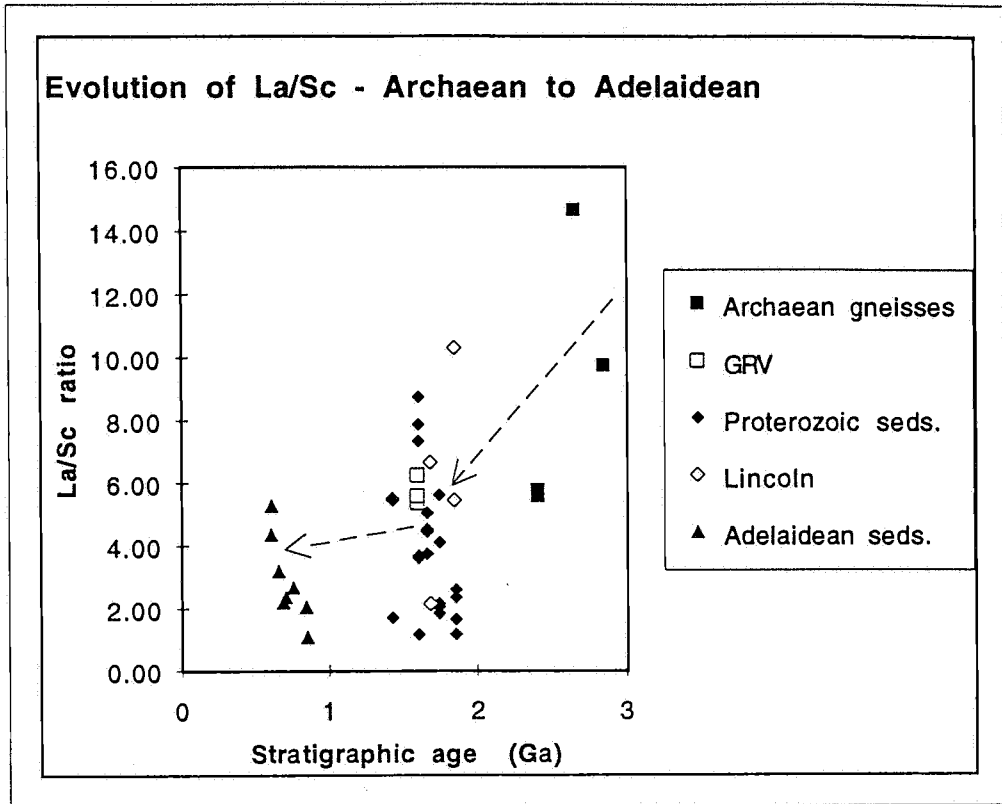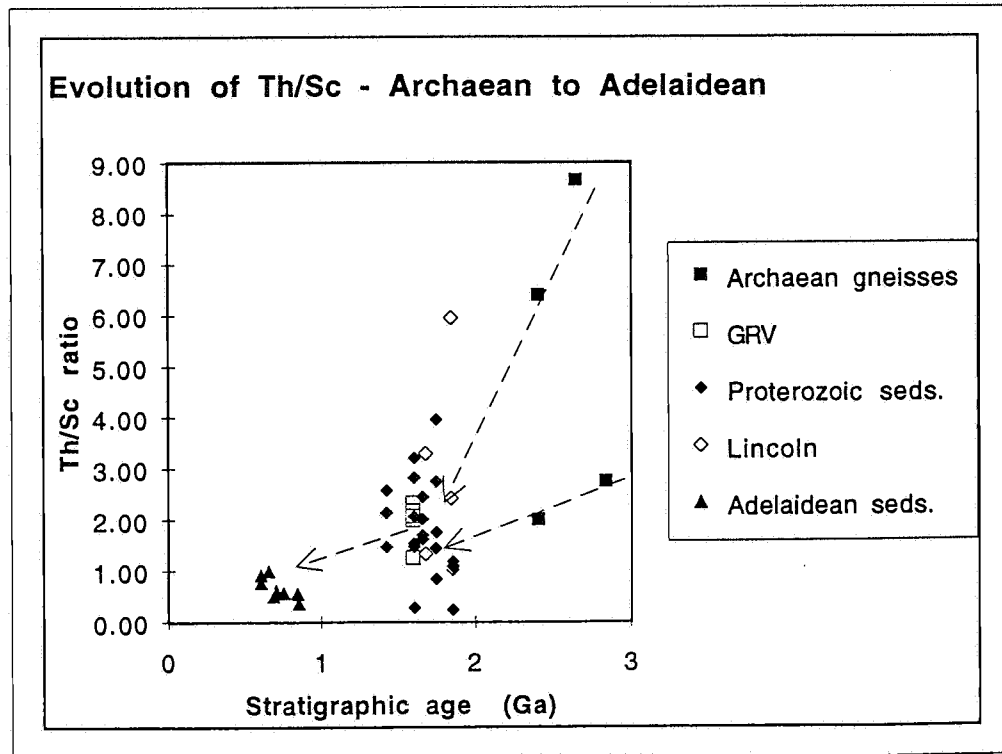
Compiled XRF data - see Appendix F for references
Differences are observed in ratios between Archaean, Proterozoic and Adelaidean samples.
Results indicate change in trace element geochemistry with age.

granites do not weather as easily as sediments), thus would not be responsibe for this change in signature. Therefore increased effects of alteration and weathering affecting sediments of the Gawler Craton can be postulated to be initiated during the Proterozoic, and reflected into the Adelaidean sediments.

Fig 4.3a&b show evolution of representative trace element ratios from Archaean to Adelaidean ages. These figures define a secular variation in geochemistry of the sedimentary suites from the Gawler Craton to the Adelaide Fold Belt. Thorium (Th) and lanthanum (La) are strongly incompatible elements, whereas scandium (Sc) is a strongly compatible element (Taylor & McClennan, 1985). However, the behavior of La, Th, & Sc during weathering and erosion is poorly understood (Condie, 1993), and should be used with caution. It is noted however (Appendix F - tabulated results), that Archaean samples have much lower Sc values than other analysed samples (~5.0 compared to ~10.0), therefore large Th/Sc and La/Sc values would result. Higher concentrations for Sc in Proterozoic and Adelaidean sediments must then be obtained from other sources (ie. GRV, Lincoln Complex), or possibly for the Adelaidean sediments from a much more distal source (addressed later). It is also possible that Sc being a more compatible element is deposited to a greater extent in post-Archaean shales due to changes in chemical weathering and erosion processes (Condie, 1993). Irrespective of the process there is however a definite chemical differentiation with age from Archaean samples to Adelaidean shales.

4.4   Summary

Geochemical data presented in this chapter, show evidence of extensive crustal recycling throughout the Proterozoic, retaining trace element signatures which are notably characteristic in Nb depletion (compared to upper crustal averages of Taylor & McClennan, 1985). Also the effects of weathering and alteration within the sedimentation process are addressed, and are believed to be responsible for some change in major and trace element ratios from Archaean to Adelaidean samples, ie lower Th/Sc and La/Sc ratios with age.

CHAPTER 5.   Sm-Nd ISOTOPES AS PROVENANCE INDICATORS

5.1   Introduction

Seven clastic sedimentary suites of the Gawler Craton, involving the Hutchison Group, Moonabie Formation, Wandearah Metasiltstone, Tarcoola Formation, Corunna Conglomerates, Blue Range beds, and Pandurra Formation (Fig 1.2), were isotopically analysed in order to determine upper crustal averages for the Gawler Craton at the time of deposition of the sediment. Provenance sources for these sediments are assumed to be dominantly local. The problem addressed within this chapter (previously addressed by Turner *et al.*, 1992), is that there is a change in isotopic signature from sampled rocks of the Gawler Craton, to sediments analysed within the Adelaide Fold Belt to the east (Fig 1.1).

5.2   Isotope systematics

The use of samarium (Sm) - neodymium (Nd) isotope tracers as indicators for models of crustal evolution and provenance sources was first applied by McCulloch & Wasserburg (1978), and since has been widely used by many authors (eg. McCulloch 1987, Allegre and Rousseau 1984, DePaolo 1991) for the same purposes. The systematics of the Sm-Nd isotopic system involves measuring the accumulation of a daughter product (^{143}Nd) decaying from a naturally radioactive unstable isotope (^{147}Sm), then by using the radioactive decay equation [Appendix D] one is able to estimate the age that the analysed rock has remained resident within the Earth's crust, ie. model age or residence age (DePaolo, 1988b). The model assumes extraction of melts from a depleted mantle [see Appendix D - isotope systematics] with evolution since formation to present measured values. Due to a lower charge/ionic-radius ratio of Nd compared to Sm, fractionation processes of partial melt magmas from a source will preferentially enrich Nd. Therefore extracted melts will have a lower Sm/Nd ratio than the source, and therefore will evolve away from the latter in the decay scheme (ie. lower accumulation of ^{143}Nd). The more 'mantle-like' the extracted melt, the higher the Sm/Nd ratio, eg. Sm/Nd ~0.19 for granites, and Sm/Nd ~0.32 for basalts (O'Halloran, 1992).

Fig 5.1   **Isotopic fractionation**
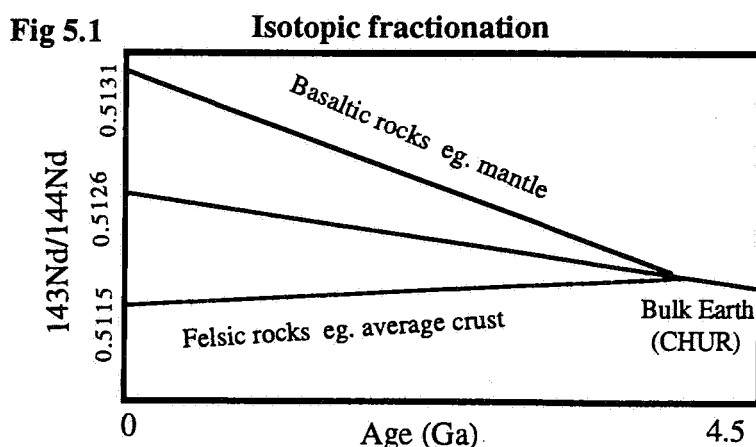
The isotopes are measured on modern mass spectrometers as a ratio to a reference non-radiogenic isotope (^{144}Nd), ie. $^{147}Sm/^{144}Nd$ and $^{143}Nd/^{144}Nd$ are measured. Differences between measured samples are in the order of the 4th decimal place (ie. 0.5115 ± 0.0005). Therefore a more convenient way of expressing differences between samples is the epsilon neodymium (ϵNd) notation, ϵNd being the parts per 10000 difference in $^{143}Nd/^{144}Nd$ between the sample and CHUR [See Appendix D]. ϵNd can also be calculated for any known time (t) in the past using modified variations of the radioactive decay equation [Appendix D], and therefore at any time (t) in the past, the ϵNd of a sample may be represented.

Due to crustal melts having a lower Sm/Nd ratio (more granite-like) than mantle sources, crustal rocks tend to more negative ϵNd values with age, whereas the mantle model (basaltic) tends to more positive ϵNd values (Fig's 5.2 and 5.3). The Sm/Nd isotopic system is believed to be 'robust' through the sedimentation cycle, ie. unaffected by diagenesis and metamorphism (McCulloch & Wasserburg, 1978). Therefore model ages (T_{DM}), Sm/Nd ratios and ϵNd signatures for sedimentary rocks will be represented by the weighted average of rocks which contribute to the sedimentary load (ie. contained within provenance region) (Allegre & Rousseau, 1984). For example a sedimentary rock with an old model age and very negative ϵNd (arrow a - Fig 5.2). can be assumed to contain a major component of older recycled material, whereas a rock with a larger (more positive) ϵNd value and much younger model age (arrow b - Fig 5.2), can be assumed to contain a larger component of more recently derived mantle material. Mixing models may be determined if signatures for proposed sources of the sediment is known, see Fig 5.2 below.

Fig 5.2   **Mixing models**

c is a weighted vector product of a + b
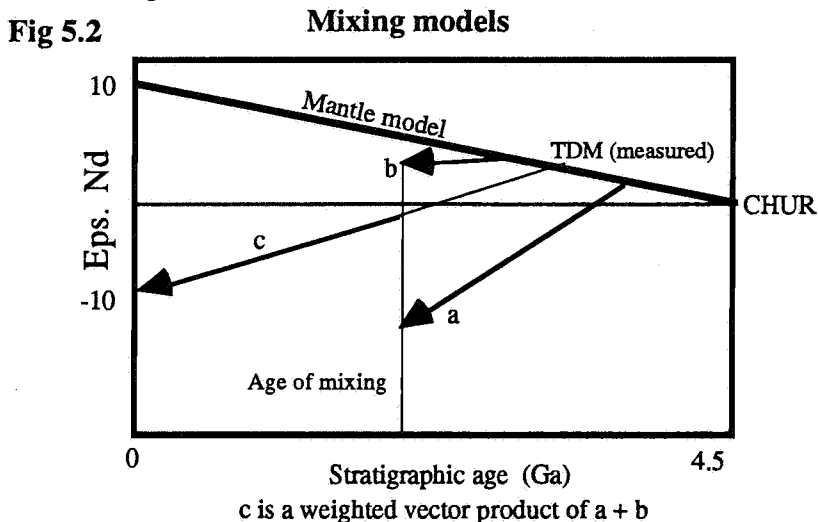
Analysis of a sequence of sedimentary rocks by this Sm-Nd method can then give information relating to any crustal additions and change in provenance sources that may occur, and therefore models for implications of crustal evolution may be determined, see Chapter 6.

5.3 Presentation of data

Shale material was sampled where possible as this rock type is well mixed and distal, and thus would best reflect crustal averages (Allegre & Rousseau, 1984). Locations for analysed suites are shown in Appendix A - drill hole logs. Samples were analysed for Nd, Sm, & Sr on a Finnagan MAT 261 thermal ionisation mass spectrometer, results are shown in Table 5.1.

For the seven analysed Proterozoic suites, average $^{143}Nd/^{144}Nd = 0.511560 \pm 0.000028$, with averages of Sm/Nd = 0.1839, ϵNd(0) [present] = -21.08, and T_{DM} = 2.30 Ga. these values are similar to typical shale values obtained by other authors upon rocks of similar ages throughout the world (eg. McCulloch 1987, DePaolo 1991). Compiled data for rocks of Archaean to Adelaidean (Neoproterozoic) age are tabulated in Appendix E.

Table 5.2 - average results for Gawler Craton and Adelaide Fold Belt sequences.

average Archaean gneisses	Sm/Nd = 0.17, T_{DM} = 2.79 Ga, ϵNd(0) = -31.85,
average Proterozoic sediments	Sm/Nd = 0.18, T_{DM} = 2.35 Ga, ϵNd(0) = -21.85,
average Proerozoic granitoids	Sm/Nd = 0.17, T_{DM} = 2.09 Ga, ϵNd(0) = -21.64,
average GRV + Hiltaba granitoids	Sm/Nd = 0.19, T_{DM} = 2.31 Ga, ϵNd(0) = -21.45,
average Adelaidean sediments	Sm/Nd = 0.19, T_{DM} = 2.01 Ga, ϵNd(0) = -16.20.

Average values for Proterozoic elements possibly involved in crustal evolution processes are shown above. Changes in values with age show some evolutionary trends.

5.4   Discussion of results

In Fig 5.3, Sm-Nd isotopic evolutionary paths are shown for sampled Proterozoic sedimentary suites, where it is noted that evolutionary trends are similar except for the Pandurra Formation. This change may be addressed by representation of a higher Sm/Nd ratio for this sediment (Fig 5.4a), which according to evolutionary calculations would result in its younger ϵNd(0) signature also observed (Fig 5.4b) [see isotope evolution equations - Appendix D]. The source for this higher ratio may be similar to changes observed for Adelaidean sediments (addressed later). Younger mantle model extraction ages are observed for some sedimentary suites (ie. Wandearah Metasiltstone, and Blue Range Beds) (Table 5.1, Fig 5.3), reflecting these samples have accessed 'new' crust in order to obtain younger isotopic signatures. Sources for new crustal additions would likely be from Proterozoic granitoids, or GRV sources, which exhibit possible mantle melt associations (section 2.2). The more positive ϵNd value for the Wandearah Metasiltstone at age of deposition (Fig 5.3) would suggest that an unrecognised (not observed in samples analysed) 'mantle-like' source has been accessed in order to obtain this signature.

Fig 5.5 shows isotopic evolution paths of Archaean and Proterozoic rock suites for the Gawler Craton. The problem of younger ϵNd values for the Adelaidean is indicated by their data points lying outside the envelopes of the former two at the deposition age. If the Gawler Craton was the sole provenance source region for Adelaide Fold Belt sediments, data points for the later would be expected to lie within the envelopes of the former. This is not so, and thus new 'younger' sources have been accessed in order to change this signature. The problem recognised within this thesis, and previously addressed by Turner *et. al.* (1992) is that a source for this younger signature is not recognised within the Gawler Craton. This is also seen in Fig 5.6, which shows that Adelaidean sediments have higher Sm/Nd ratios and younger ϵNd (initial) values, than possible sources shown by average values for Archaean and

Isotopic evolution paths for analysed Proterozoic clastic sedimentary suites.

Fig 5.3
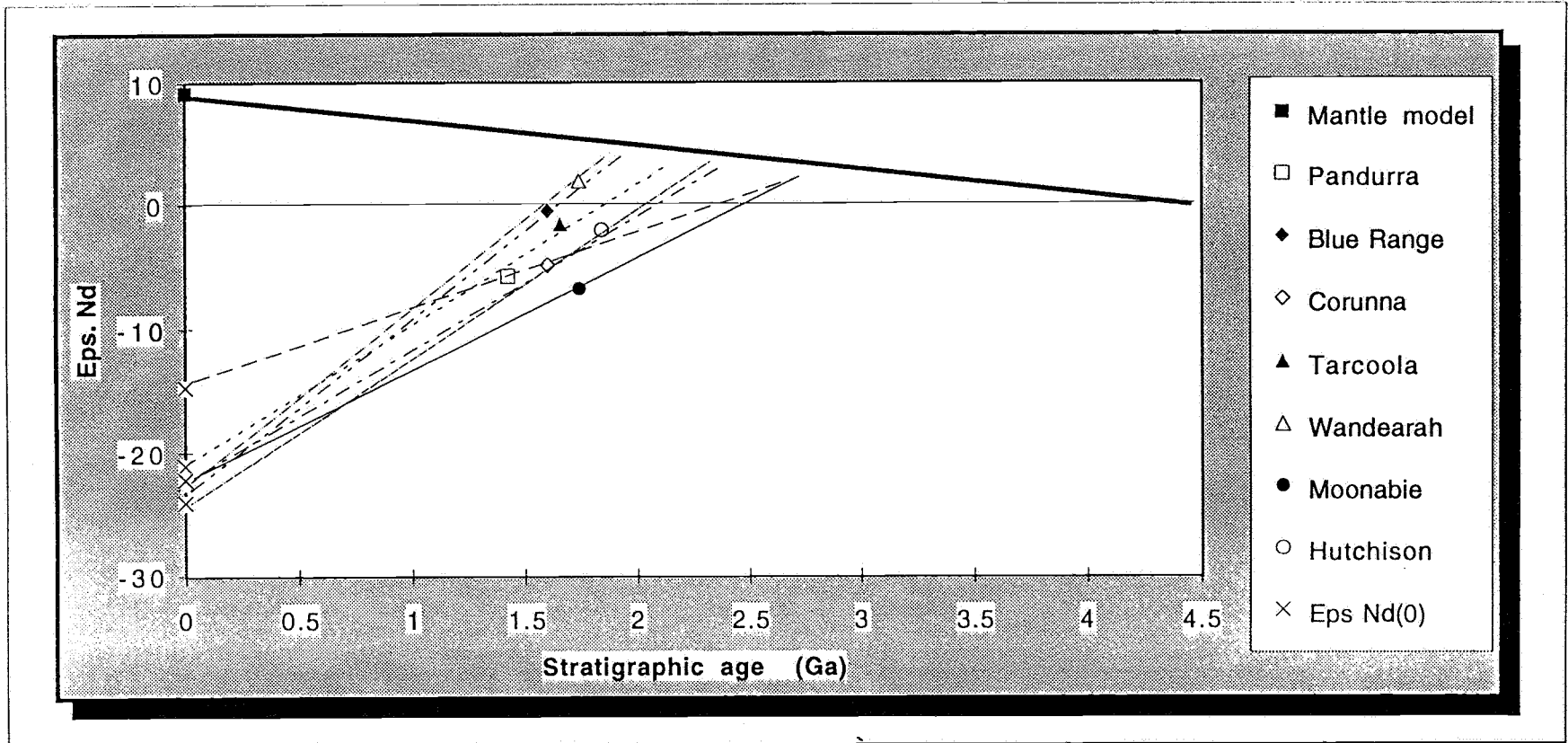
Data obtained and compiled by Author

Diagram showing epsilon neodymium evolution paths for sampled Proterozoic clastic sediments
The Pandurra formation is anomalous and may be explained by sampling an isotopically younger provenance source,
or geochemical alteration of the isotopic signature.

Proterozoic Gawler Craton samples - isotopic data

Fig 5.4a
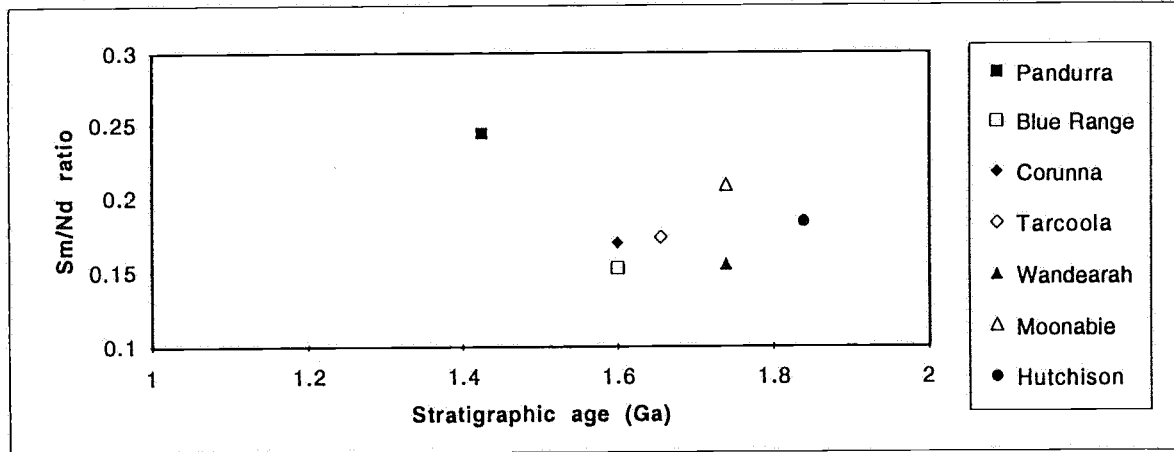
Fig 5.4b
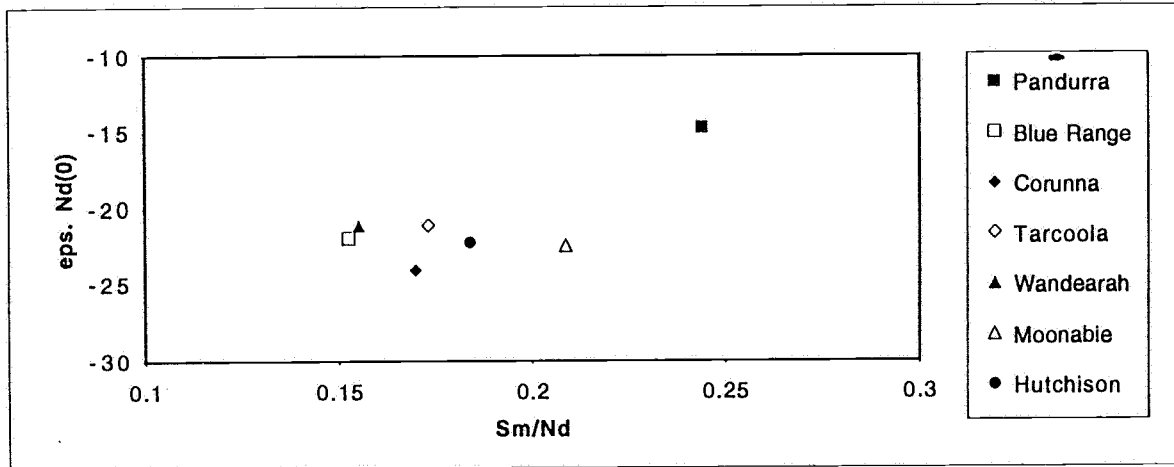
Data obtained and compiled by Author

Representation of changing isotopic signature of Pandurra Formation sample compared
to other Gawler Craton samples.

Fig 5.5 Evolution of Eps. Nd with stratigraphic age
Archaean, Proterozoic and Adelaidean samples
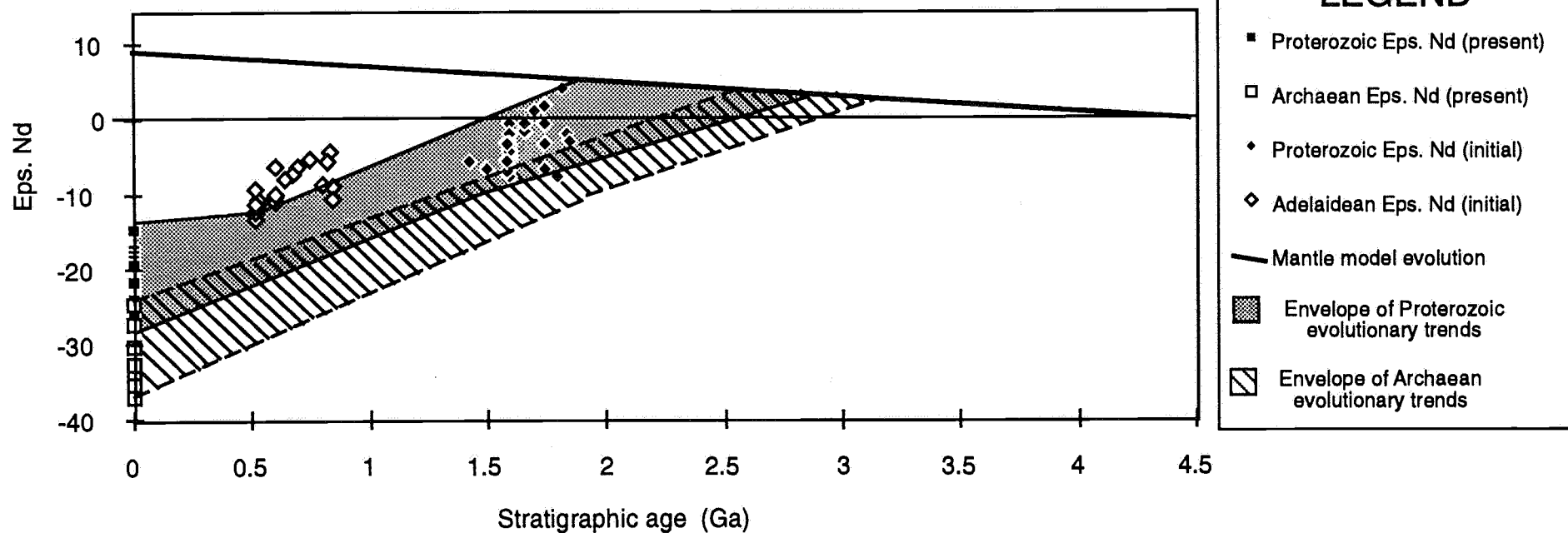
Diagram showing evolutionary trends for Archaean and Proterozoic compiled samples. Eps. Nd is presented for Proterozoic and Adelaidean samples at age of deposition. The problem is that the Adelaidean samples have younger Eps Nd values than these previous trends.

Fig 5.6

Change in isotopic signature from Gawler Craton rock suites to Adelaidean shales, addressing possible provenance sources for the later

Legend:
- ● Adelaidean seds.
- ◆ Proterozoic seds.
- △ GRV + Hiltaba
- ◇ Proterozoic granites
- □ Archaean gneisses
- + Average Willyama
- × Average Mt Painter
- ■ Pandurra Fm.

X-axis: Sm/Nd ratio (0.1, 0.15, 0.2, 0.25)
Y-axis: Eps. Nd at 700 Ma (0, -5, -10, -15, -20, -25, -30)
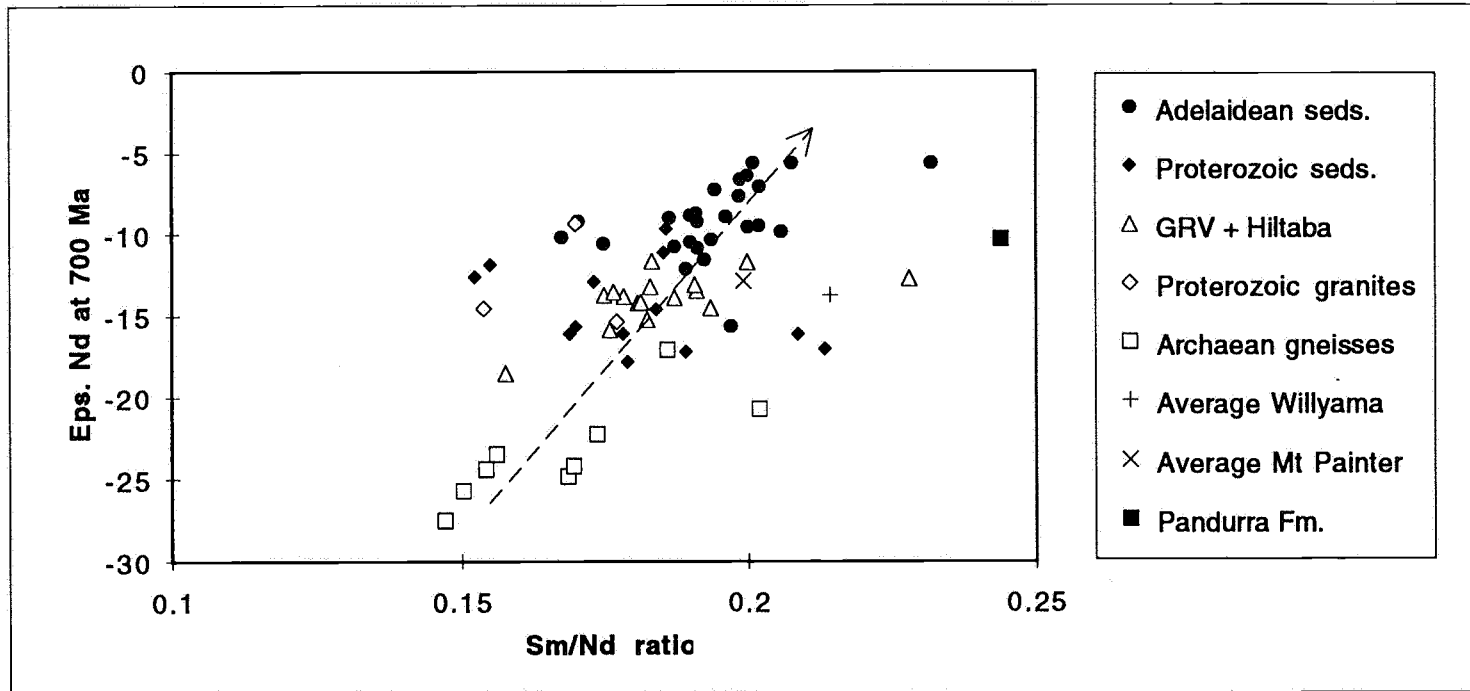
Compiled data - See Appendix E

Change in both epsilon neodymium signature (younger) and Sm/Nd ratio (higher) is observed for the average of Adelaidean sediments analysed. Implications for change in this signature are addressed in text.

Proterozoic provinces. The Sm/Nd ratio may be accounted for by selective sampling of those Proterozoic sources with higher Sm/Nd values equivalent with Adelaidean values. However, even possible sources indicated form the Mt Painter (Arkaroola - northern Flinders Ranges), and Willyama (Olary / Broken Hill region) inliers (both South Australian Proterozoic terrains), are unable to account for the higher (younger) εNd signature recognised at formation age for the Adelaidean sediments.

Other possible processes accounting for this change in signature may be from sampling a more distal Proterozoic terrain source such as from the Arunta and Musgrave blocks (north-western South Australia) which do show younger εNd signatures at this age (-12.84 & -7.45 respectively - see Appendix E), or possibly from the Grenville province of North America, which is postulated to have been adjacent to Eastern Australia during these Gondwana times (Moore, 1991). Data from this latter region was not collected (further work required). More local sources could be magmatics within the Adelaide Fold belt that are near-synchronous with sediment deposition, eg. Gairdner dykes, Wooltana volcanics, Truro volcanics, which show positive εNd values around formation ages (see Turner *et. al.*, 1992). Modelling calculations on these latter possible sources could be performed (further work), in order to estimate percentages of these sources needed to cause this change in signature, Gawler Craton material being basement to the Adelaide Fold Belt (section 2.2) is likely to constitute a large proportion of the sedimentary load, as it is the most local source.

Another possible source for this change in Adelaidean signature may be due to alteration in the Sm-Nd isotopic system during sedimentation processes (ie. diagenesis) [J. Foden pers. comm.]. The principle of this alteration is that isotopic exchange may occur with sea water during deposition, ie. sea water fluxing through the sedimentary pile essentially acts as a provenance source through isotopic exchange with the sedimentary load. This would account for both higher Sm/Nd and εNd values within the Adelaidean sediments, as oceanic waters are postulated to have a higher εNd value at the deposition age of these sediments (εNd ~ -5.0, Derry & Jacobsen, 1988). Estimates for sea water values are obtained via examination of Sm-Nd signatures within chemical sediments of varying ages (eg. phosphates, banded iron formations). This postulate contradicts earlier theories (McCulloch & Wasserburg 1978, Allegre & Rousseau 1984) in that the Sm-Nd isotopic system is not substantially disturbed during sedimentary processes. However, it is not out of the question for such a process to occur, as isotopic systematics in the use of geological applications is still a new and evolving science.

5.5   Conclusions

The problem addressed within this chapter is that the Adelaidean Fold Belt sediments show a younger εNd signature than compiled data for Gawler Craton samples, therefore rock suites of the Gawler Craton are concluded tnot to be the sole province source for sediments within the Adelaide Fold Belt. Possible other province sources for this signature change are proposed, with further work to confirm these being recommended. Within the Gawler Craton, the Pandurra Formation sediments exhibit a marked variation in isotopic signature compared to

other Archaean and Proterozoic samples. The trend is more towards the signature of Adelaide Fold Belt samples (younger $\varepsilon Nd(0)$ = -14.67, higher Sm/Nd = 0.2441) (Fig 5.6). Therefore processes which effect the change in signature for the Neoproterozoic Adelaide Fold Belt sediments are postulated to have began during late Mesoproterozoic times, thus effecting also the Pandurra Formation sediments upon the Stuart Shelf region.

CHAPTER 6.   PROTEROZOIC CRUSTAL GROWTH IN THE GAWLER CRATON

6.1   Introduction

It is now considered, through much earlier scientific debate, that the continents have grown through geological time by the process of additions from mantle sources (Allegre & Rousseau 1984, Taylor & McClennan 1985). Crustal growth involves the analysis of the rate these new mantle sources are added to the crust with age, also considering rates of crustal destruction due to subduction, or erosion into deep ocean basins. Two end-member models exist for theories relating to continental crustal evolution throughout the Earths geological history. (Fig 6.1 - Crustal growth). The steady-state model (eg. Armstrong, 1991) proposes early development of continental crust, which has remained at constant mass (no growth) due to balanced recycling and addition of any 'new' mass added to the crust. The second model (eg. Taylor & McClennan, 1985) suggests continued mass growth of the continents due to steady or episodic additions, with limited destruction of old mass.
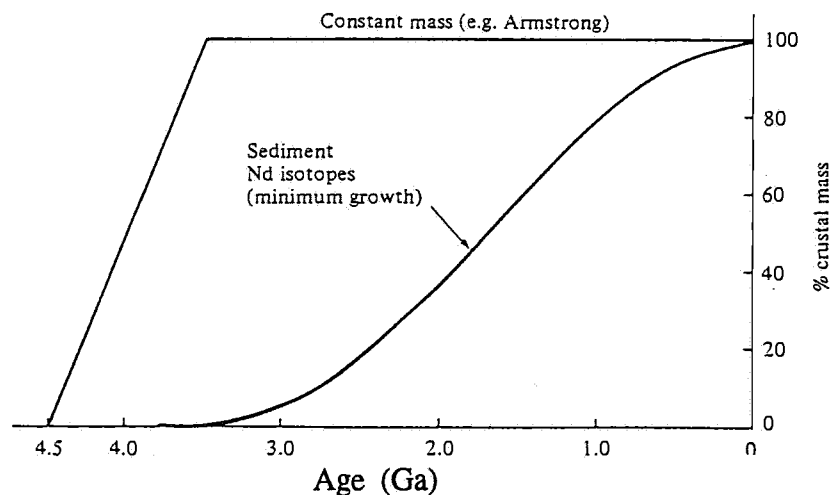
Fig 6.1 - Models of crustal growth. From Brown *et. al.* (1992).

The Sm-Nd isotopic system is a useful application for considering models of crustal growth, as analyses of this radioactive decay scheme are able to define ages that new mantle additions were added to the continental crust [section 5.1]. The age determined is a model age, that being the age at which a melt was extracted from the mantle [Appendix D]. The evolution of model ages to younger values with decreasing stratigraphic age would indicate new mantle additions have been accessed, supplying new isotopic signatures, throughout the time period analysed.

The analysis of shale material is a generally used application in order to show upper crustal isotopic averages at the time of sediment deposition (Allegre & Rousseau, 1984). The elements Sm & Nd are believed to be unfractionated during sedimentation processes (McCulloch & Wasserburg, 1978), and therefore retention of isotopic signatures into the sedimentary pile occurs. The source material for sediments, is the upper crustal rocks present at age of deposition contained within the provenance (sampling) region for the developed basin.

This provenance region would likely contain older crustal material (recycling of older crustal signatures) as well as any new crustal components that may have recently been added ie. volcanics, granites (younger signatures). Possible sites of new mantle additions to the continents, giving 'younger' isotopic signatures, are I-type granitoids within orogenic belts (Turner *et. al.*, 1992), where tectonism may cause significant rupturing of the crust to access the mantle beneath. Other possible sources of addition involve A-type granitoids at sites of mantle pluming (eg. GRV) where melts can be extracted into the upper crust, or mixed with crustal components. S-type granitoids recycle pre-existing crustal material, and as such would only represent any 'younger' signatures if new crustal material had been previously emplaced.

6.2   Discussion of results

Table 5.2 presents average isotopic results for crustal components of different age in the Gawler Craton; full isotopic data is presented in Appendix E. A trend for younging of mantle extraction age (T_{DM}) is observed and is also represented in Fig 6.2. Archaean samples have extraction ages similar to their stratigraphic ages, whereas younger samples deviate away from this (ie. deviate from concordia line), and so recycling of older crustal components retaining older extraction ages is postulated. There is however a trend toward younger extraction ages with stratigraphic age (Fig 6.2). Thus new crustal additions supplying new isotopic signatures must have been accessed. Possible sources for these signatures are also shown in Fig 6.2, the Proterozoic granitoids (Lincoln Complex,and McGregor Volcanics), and GRV + Hiltaba samples (Appendix E - tabulated results), showing younger model ages than Archaean samples, and therefore represent 'younger' isotopic signatures. Therefore it is proposed that these granitoids show evidence for new crustal additions into the Gawler platform, timing defined by mantle extraction ages (see Table 5.2, and Appendix E). This corresponds with crustal evolution models of Taylor & McClennan (1985), Allegre & Rousseau (1984), and many other authors, in that the continents have growth through geological time due to episodic mantle additions. Extraction ages represented for these samples may not be true ages of emplacement, as most of the granitoids exhibit a felsic component which may have been derived from re-melting older crust, thus mixing older signatures with new signatures (Fig 5.2).

Adelaidean samples show a much younger average age than other Proterozoic Gawler Craton samples. Therefore either selective sampling of crustal components with younger ages (Fig 6.2) occurred, or more likely a distal source was involved to supply these sediments with the younger signatures observed.

6.3   Summary

Crustal additions are recognised within the Proterozoic Gawler Craton, with the granitoids sampled representing younger extraction ages than previous Archaean samples, a trend is also observed for younger extraction ages with stratigraphic age within the sediments analysed. There is however a tendency for older extraction ages to be retained in some sediments (Fig 6.2). This would represent the provenance source for these samples involved a large proportion of older crustal material. There are only a few Proterozoic samples that show a

Evolution of model ages with stratigraphic age

Fig 6.2
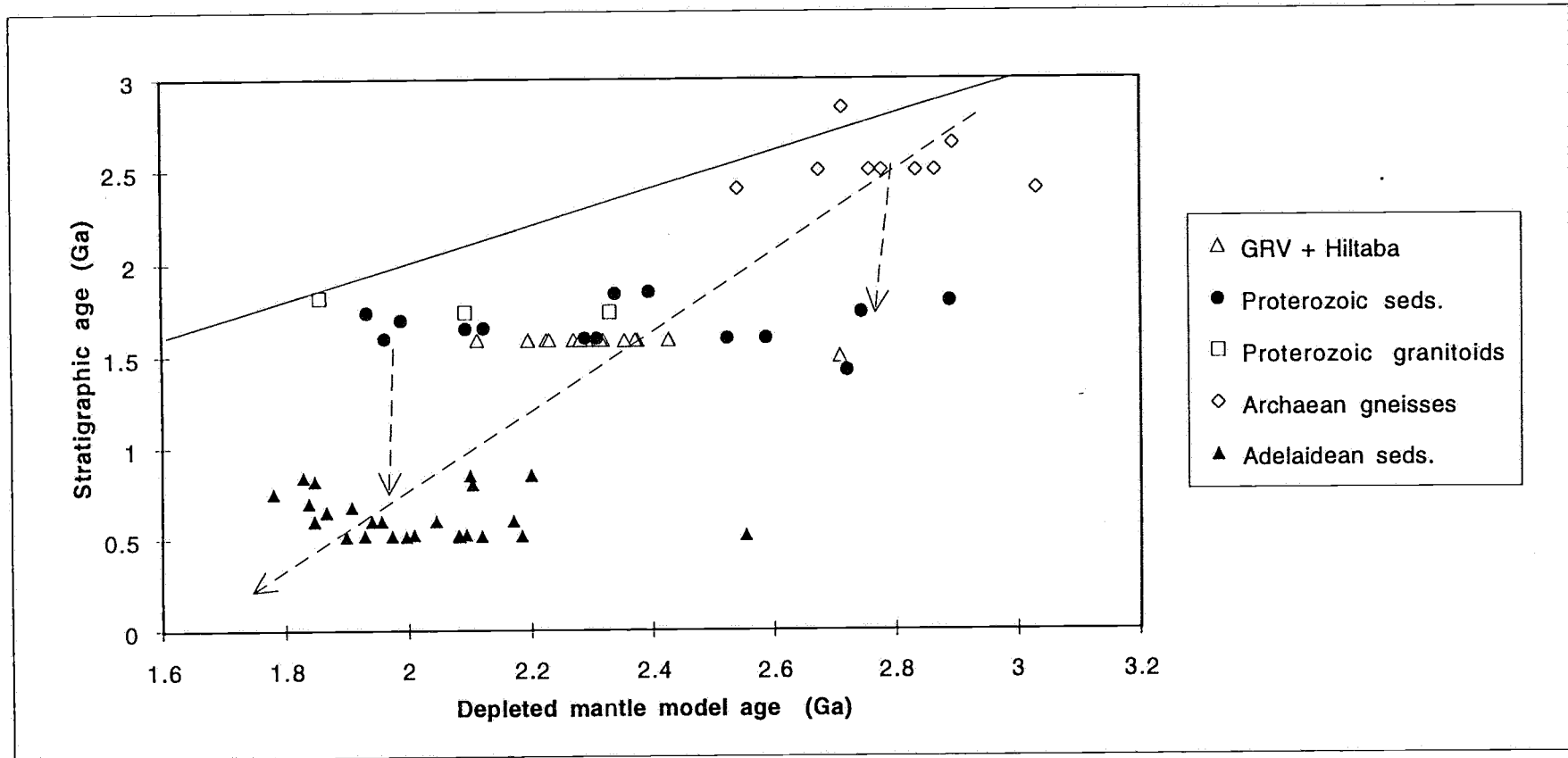
Compiled data - see Appendix E for references

Evolution of mantle extraction ages to younger values with stratigraphic age, for granitoids and sediments analysed.

Thus new crustal additions have been accessed in order for younger signatures to be obtained.

Recycling of some older signatures is observed by deviation away from concordia line (Black line, model age = strat. age)

young extraction age similar to Adelaidean samples, and therefore another source supplying a young signature for these latter sediments may be involved. This links with earlier hypotheses for a more distal source causing change in isotopic signature for sediments within the Adelaide Fold Belt (Chapter 5).

CHAPTER 7.   DISCUSSION AND CONCLUSIONS

Section A of this thesis is an outline of the regional geology, stratigraphy, and structural evolution of the Gawler Craton. A detailed analysis of these processes is described in Chapter 3, for the Tumby Bay region of eastern Eyre Peninsula (Cleve tectonic sub-domain). Processes acting within the Tumby Bay region are correlated to examples of similar processes in other domains of the Gawler Craton, therefore regional correlation is invoked. Late stage deformation of the Kimban Orogeny has caused extensive mylonitisation of the rock suites within the Tumby Bay region, obliterating much of the previous sedimentological and early structural history that these rocks would otherwise show. A new theory for development of two dominant lineation directions is given, this invokes two separate movement directions along the Kalinjala mylonite (shear) zone which is present within the Cleve tectonic sub-domain (map region).

Section B, presents new isotopic data for sediments of the Gawler Craton. Correlation of this with data obtained from other workers, enables development of models of continental crustal evolution for the Gawler Craton and Adelaide Fold Belt to be addressed. A change in isotopic signature is observed from samples of the Gawler Craton, compared to samples from the Adelaide Fold Belt (younger Eps. Nd signature and higher Sm/Nd ratio - Fig 5.5). Possible implications for this are: access to a 'new' unrecognised distal source (Musgraves, Grenville, etc.), OR a change in signature due to sea water fluxing through the sedimentary pile. True cause for this isotopic shift has not been resolved, possibly a combination of both the above processes may act. This isotopic shift is also observed for the Pandurra Formation of the Gawler Craton, thus processes acting to cause this isotopic shift are proposed to have begun during later Mesoproterozoic ages, effecting also the Pandurra Formation sediments of the Stuart Shelf region.

New crustal additions are proposed to have occurred within the Gawler Craton region, throughout the Proterozoic era. This is supported by a 'younging' of depleted mantle model ages with stratigraphic age, from the Archaean to the Adelaidean (Fig 6.2). Periods of addition are likely observed with emplacement of Proterozoic granitoids, and the GRV. Isotopic signatures for these granites do not show significantly young extraction ages (ie. lie away from concordia line), and are postulated to thus contain reworked components of older crustal material, retaining older signatures. This is also observed for the Proterozoic sediments, some of which show older isotopic signatures (province containing large component of older crustal material), whereas some represent younger signatures (sampling younger crustal inputs). Therefore there is proposed to be evidence for crustal additions in the Australian continent, supplying fresh isotopic signatures to the Gawler Craton upper crust, throughout the Proterozoic period.

ACKNOWLEDGMENTS:

I wish to thank my supervisor, John Foden, for his guidance and informative advice throughout the year. Also the Mines and Energy Department of South Australia (MESA), for their loan of a field vehicle, maps and photos, without which field work would have been a much more trying experience. Sue Daly is especially thanked in this regard for her friendly guidance and support with this.

Regards must be extended to Mr & Mrs Young of Lock, for the use of their holiday shack in Tumby Bay, this made field work bearable being able to use showers and cooking equipment (many fine meals were made in that kitchen). The locals of Tumby Bay, and property owners within the district whose land I trecked all over, made mapping an easier task through their friendly nature, hospitality, and keen interest in the projects we were working upon.

The technical staff of Adelaide University, in particular Sherry Proferes, David Bruce, John Stanley, Geoff Trevellyan, Keith Turnbull, and Rick Barrett, are greatly appreciated for their many hours of patient assistance in getting my samples analysed, and maps produced.

Final regards go to friends outside and within the University, for their constructive criticism, and support throughout the year, making this year bearable and at times even enjoyable. Thanks to all.

REFERENCE   LIST

Allegre C.J., Rousseau D.   1984,   The growth of the continent through geological time studied be Nd isotope analysis of shales.   Earth and Plan. Sci. Lett. 67: pp19 - 34

Armstrong R.L.   1991,   The persistant myth of crustal growth.   Aust. J of Earth Sci 38: pp 613 - 630

Bendall B.   1994,   Metamorphic and geochronological constraints on the Kimban Orogeny, Eyre Peninsula, South Australia.   Univ. of Adel. B.Sc (Hon) thesis (unpub.).

Benton R.   1994,   A Petrological, geochemical and isotopic investigation of granidoids from the Olary province of South Australia - implications for Proterozoic crustal growth.   Univ. of Adel. B.Sc (Hon) thesis (unpub.).

Brown G.C., Hawkesworth C.J., Wilson R.C.L.   1992,   Understanding the Earth, a new synthesis.   Cambridge University press.

Coin C.D.A.   1976,   A study of the Precambrian rocks in the vicinity of Tumby Bay, Southern Eyre Peninsula.   Univ. of Adel. Ph.D. thesis (unpub).

Condie K.C.   1993,   Chemical composition and evolution of the upper continental crust. Contrasting results from surface samples and shales.   Chem. Geol. 104: pp1 - 37.

Cooper J.A., Mortimer G.E., Rosier C.M, Uppill R.K.   1985,   Gawler Range magmatism - further isotopic data.   Aust. J. of Earth Sciences 32: pp115 - 123.

Cowley W.M.   1991,   The Pandurra formation.   SADME Report Bk. 91/7

Crawford A.R.   1964,   Cultana map sheet.   South Aust. geol. survey. Geological atlas 1:63 360 series.

Daly S.J.   1984a,   Wilgena 1 stratigraphic drill hole, Tarcoola.   S.A. geol survey. Qtly geol. notes 91: pp3 - 9

Daly S.J.   1984b,   Wilgena 1 well completion report.   SADME report book 84/13

Daly S.J.   1985,   Tarcoola map sheet, Geological atlas of South Australia, 1:250 000 series.   Geol. Surv. S. Aust. Adelaide.

Daly S.J., Webb A.W., Whitehead S.G.   1978,   Archaean to early Proterozoic banded iron formations in the Tarcoola region.   R. Soc. S. Aust. Trans. 102: pp 141 - 149.

Davi D.I. 1993, a structural interpretation of a detailed ground magnetic survey, Burrawing area, Tumby Bay, South Australia. Univ of Adel. B.Sc. (Hon.) thesis (unpub.).

DePaolo D.J. 1988a, Age dependance of the composition of the continental crust: evidence from Nd isotopic varioations in granitic rocks. Earth & Plan. Sci. Lett. 90: pp 263 - 271.

DePaolo D.J. 1988b, Neodymium isotope geochemistry, an introduction; In:- Minerals and Rocks. Springer - Verlag, Berlin.

DePaolo D.J. 1991, The continental crustal age sidtribution, methods of determining mantle separation ages from Sm-Nd isotopic data, and applications to the Southwestern United States. J. of Geophys. Res. vol. 96: pp 2071 - 2080.

Derry L.A., Jacobsen S.B. 1988, The Nd and Sr isotopic evolution of Proterozoic seawater. Geophys. Res. Lett. v15 no4: pp397 - 400.

DiaAline, Allegre C.J., Erlark A.J. 1990, The development of continental crust through geological time. Earth & Plan. Sci Lett. 98: pp 74 - 89.

Drexel J.F., Preiss W.V., Parker A.J. 1993, The geology of South Australia; V1 MESA Bul. 54

Fanning C. M. 1990, Single grain U-Pb zircon dating of two tuffaceous horizons from Wilgena 1. PRISE geochronology report 89-080 (unpub.).

Fanning C.M., Blissett A.H., Flint R.B., Ludwig K.R., Parker A.J. 1986a, A refined geological history for the southern Gawler Craton through U-Pb zircon dating of acid volcanics, and correlation with northern Australia. In:- 8th Aust. geol. convention Adelaide 1986, Geol Soc of Aust. Abstracts 15: pp67 - 68

Fanning C.M., Cooper J.A., Oliver R.L., Ludwig K.R. 1986b, Rb-Sr, and U-Pb geochronology of the Carnot gneisses: Complex isotopic systematics for the Late Archaean to early Proterozoic Sleaford complex, Southern Eyre Peninsula, South Australia. Geol. Soc of Aust. Abstracts 15: pp69 - 70

Fanning C.M., Flint R.B., Parker A.J., Ludwig K.R., Blissett A.H. 1988, Refined Proterozoic evolution of the Gawler Craton, South Australia, through U-Pb zircon geoghronology; Precambrian Res. 40/41: pp363 - 386

Fanning C.M., Flint R.B., Preiss W.V. 1983,   Geochronology of the Pandurra formation. South Aust. geol. survey. Qtly notes 88: pp 11 - 16.

Faure G. 1992,   Principles of isotope geology, 2nd Ed.

Flint R.B. 1988,   Newland 1 well completion report.   SADME report book 88/66

Flint R.B., Parker A.J. 1981,   The Blue range beds of central Eyre Peninsula.   S.A. geol. survey Qtly geol notes 80: pp12 - 15

Flint R.B., Preiss W.V. 1983,   Geochronology of the Pandurra formation.   S.A. geol. survey Qtly geol. notes 88: pp11 - 16

Flint R.B., Rankin C.R. 1991,   KIMBA, South Australia sheet SI53-7, S.A. geol survey 1:250 000 series - explanatory notes.

Giles C.W. 1980,   The origin of the Middle-Proterozoic Gawler RAnge Volcanics in the Lake Evverard area, South Australia.   In: A.J. Parker Symposium on the Gawler Craton. Geol. Soc. Aust. J. 27: pp 52.

Giles C.W., Goode A.D.T., Lemon N.M. 1980,   Middle-Proterozoic volcanism and sedimentation in the Moonabie area.   In: A.J. Parker Symposium on the Gawler Craton. Geol. Soc. Aust. J. 27: pp 53.

Goldstein S.J., Jacobsen S.B. 1988,   Nd & Sr isotopic systematics of river water suspended material, implications for crustal evolution. Earth & Plan. Sci Lett. 87: pp249 - 265.

Harnois L. 1988,   The CIW index: A new chemical index of weathering. Sediment. Geol. 55: pp 319 - 322.

Hobbs B.E., Means W.D., Williams P.F. 1976,   An outline of structural geology. John Wiley & Sons, Canada.

Huffadine S.J. 1993,   Environment, timing and petrogenesis of a mid-proterozoic volcanic suite: Pt. Victoria, South Australia.   Univ. of Adel. B.Sc (Hon.) thesis (unpub.).

Jacobsen S.B. 1988,   Isotopic constraints of crustal growth and recycling. Earth & Plan. Sci. Lett. 90: pp 315 - 329.

McClennan S.M., McCulloch M.T., Taylor S.R., Maynard J.B. 1989,   Effects of sedimentary sorting on Nd isotopes in deep-sea turbidites.   Nature 337: pp 547 - 549.

McCulloch M. T. 1987, Sm - Nd isotopic constraints on the evolution of Pre-Cambrian crust in the Australian continent; Proterozoic Lith. evol.. Am Geophys. Union Geodyn. ser. 17: pp115 - 130.

McCulloch M. T., Wasserburg 1978, Sm-Nd and Rb-Sr chronology of continental crust formation; Science 200: pp1003 - 1011.

Miller R.G., O'Nions R.K., Hamilton P.J., Welin E. 1986, Crustal residence ages of clastic sediments, orogeny and continental evolution. Chem. Geol. 57: pp 87 - 99.

Moores E.M. 1991, Southwest U.S. - East Antartica (SWEAT) connection: A hypothesis. Geology V19: pp 425 - 428.

Mortimer G. 1985, Early to Middle Proterozoic granitoids, basaltic dykes, and associated layered rocks of S.E. Eyre Peninsula, South Australia. Univ. of Adel. Ph.D. thesis (unpub.).

Mortimer G.E., Cooper J. A., Oliver R. L. 1988, The geochemical evolution of Proterozoic granitoids near Pt. Lincoln in the Gawler Orogenic domain of South Australia. Precambrian Res. 40/41: pp 387 - 406.

Nesbitt H.W., Young G.M. 1982, Early Proterozoic climates and plate motions inferred from the major element chemistry of lutites. Nature 299: pp 715 - 717.

O'Halloran G. 1992, The sedimentology and Nd isotopic geochemistry of some early Adelaidean rocks from the Northern Flinders Ranges. S.A. Univ of Adel. B.Sc.(Hon.) thesis (unpub.).

Oussa S.A. 1993, Description of a granulite facies shear zone (Kalinjala mylonite zone), and inferred cooling ratios of following granulite facies metamorphism. Univ of Melbourne B.Sc.(Hon.) thesis (unpub.).

Parker A.J. 1978, Structural, stratigraphic, and metamorphic geology of Lower Proterozoic rocks in the Cowell / Cleve district, Eastern Eyre Peninsula. Univ. of Adel. Ph.D. thesis (unpub.).

Parker A.J. 1979, Symposium on the Gawler Craton, 11 December 1979. Geol. Soc. of Aust. Journal 27: pp45 - 53

Parker A.J. 1980, The Kalinjala mylonite zone of eastern Eyre Peninsula. South Aust. Geol. Survey. Qtly geol. notes 75: pp 6 - 11.

Parker A.J.   1990,   Gawler Craton and Stuart Shelf - regional geology and mineralisation.
In:- Hughes F.C. (Ed.) Geology of the mineral deposits of Australia and Papua New
Guinea.   Australasian institute of mining and metallurgy.   Monograph series 14:
pp999 - 1008

Parker A.J., Daly S.J.   1982,   Symposium on the Gawler Craton - drill hole logs.
SADME report book 82/91.

Parker A.J., Fanning C.M., Flint R.B., Martin A.R., Rankin L.R.   1988,   Archaean -
Early Proterozoic granitoids, metasediments, and mylonites of southern Eyre
Peninsula, South Australia;   Spec. grp. in Tect. and Struct. geol. field guide 2.

Parker A.J., Lemon N.M.   1982,   Reconstruction of the early Proterozoic stratigraphy of
the Gawler Craton. S.A.   Geol. Soc. of Aust. Journal 29: pp221 - 238

Rankin L.R., Flint R.B.   1987,   Broadveiw 1 well completion report.   SADME
report book 87.92

Rankin L.R., Flint R.B., Fanning C.M.   1988,   The Bosanquet formation of the Gawler
Craton.   S.A. geol. survey Qtly geol. notes 105: pp12 - 18

Rankin L.R., Flint R.B., Fanning C.M.   1990,   Palaeoproterozoic Nuyts volcanics of
the western Gawler Craton.   SADME report book 90/60.

Robertson B.D.   1989,   The geology, petrology and geochemistry of the volcanics in the
Kokathu region, Gawler Ranges, South Australia;   Univ. of Adel. B.Sc. (Hon.)
thesis (unpub.).

Schaefer B. F.   1993,   Isotopic and geochemical constraints on Proterozoic crustal growth
from the Mt Painter inlier.   Univ. of Adel. B.Sc.(Hon.) thesis (unpub.)

Stewart K.P.   1992,   High temperature felsic volcanism and the role of mantle magmas in
Proterozoic crustal growth: The Gawler RAnge volcanic province.   Univ. of Adel.
Ph.D. (unpub.).

Taylor S.R., McLennan S.M.   1985,   The Continental crust: Its composition and
evolution.   Blackwell.

Tessalar J.M.   1994,   A Geophysical investigation of the Lake Harris komatiite, South
Australia.   Univ. of Adel. B.Sc (Hon) thesis (unpub.).

Thomson B.P. (compiler) 1980, Geological map of South Australia. South Aust. geol. survey. Maps of South Australia series 1:1 000 000.

Turner S., Foden J., Sandiford M. , Bruce D. 1992, Sm - Nd isotopic eidence for the provenance of sediments from the Adelaide fold belt and South East Ausralia, with implications for episodic crustal addition; Geochimica et. Cosmochima Acta V57: pp1837 - 1856.

Wawryk C.M. 1989, Strontium ore rare earth element geochemistry of barite - flourite mineralisation at Olympic Dam, South Australia. Univ. of Adel. B.Sc (Hon.) thesis (unpub.).

Webb A.B., Thompson B.P., Blissett A.H., Daly S., Flint R.B., Parker A.J. 1986, Geochronology of the Gawler Craton, South Australia. Aust. J. of Earth Sci. 33: pp119 - 143.

Whitehead S.G. 1978, A comparism of some Archaean and Proterozoic iron formations in South Australia. SADME open file env. 3200 (unpub.).

Wurst A. 1994, An analysis of late stage Mesoproterozoic syn and post tectonic magmatic events in the Moonta sub-domain, - implications for Cu-Au mineralisation in the Copper triangel of South Australia. Univ. of Adel. B.Sc (Hon.) thesis (unpub.).

Zhao J.X., McCulloch M.T., Bennett V.C. 1992, Sm-Nd and U-Pb zircon isotopic constraints on the provenance of sediments from the Adadeous Basin, central Australia: Evidence for REE fractionation. Geochem. et. Cosmin Acta V56: pp 921 - 940.

APPENDIX A

Sample locations &
Drill hole logs

SAMPLE LOCATIONS AND DESCRIPTIONS

Sample numbers: analytical	map	Lithology	Location		Description	Work done: T.S.	XRF	Isotope
1031/								
001	bS4	PPhw	Tumby hills		mylonite orientated quartzite ?	Y		
003	bS6	PPhw	Tumby hills		mylonite orientated gneiss	Y		
005	cS12	PPhc	Tumby hills		gt amphibolite schist	Y		
006	cS19	PPlmy	Tumby hills		leucocratic pegmatite c oxides, tourm.	Y	Y	
004	cS22	PPhb	Tumby hills		slaty amphibolite	Y		
002	cS24	PPhb	Tumby hills		green-grey banded amphibolite	Y	Y	
030	cS41	PPhc	Tumby hills		gt schist		Y	
007	dS44	PPhw	Tumby hills		grey quartzite/granite	Y		
008	dS74	PPld	Tumby hills		highly foliated black gneiss	Y	Y	
031	EP4	PPhc	Cleve		Garnet schist		Y	
032	EP5	PPhy	Cleve		Yadnarie schist	Y	Y	Y
012	C1	PMcc	CC1	80.5 - 80.7m	Banded siltsone / sandstone		Y	
011	C2	PMcc	CC2	168.2 - 168.4m	black shale	Y	Y	
013	C3	PPh	CC2	255.5 - 255.7m	green gneiss		Y	
014	C4	PPmm	SOC1	129.4 - 129.6m	med. grained volc. sandstone	Y	Y	Y
010	C5	PPmw	SOC7	80.8 - 81.0m	Fe-stained clastic siltsone breccia	Y	Y	
009	C6	PPmw	SOC8	153.3 - 153.5m	banded metasiltstone	Y	Y	
015	C7	PPmm	SOC8	181.5 - 181.8m	coarse volcaniclastic grit		Y	
016	C8	PMcc	Roop6	70.2 - 70.4m	grey-black shale, some banding		Y	Y
017	C9	PPmw	Roop6	251.4 - 251.6m	Chloritised siltstone	Y	Y	Y
018	C10	PPt	Wilg1	311.7 - 311.9m	shale, small qtz veining		Y	
019	C11	PPt	Wilg1	640.8 - 641.0m	banded shale, near adjacent U-Pb	Y	Y	Y
020	C12	PPt	Wilg1	779.6 - 779.8m	homogeneous carbonaceous shale		Y	
021	C13	PPt	Wilg1	889.1 - 889.3m	Black shale, some banding		Y	
022	C14	PPbo	Broa1	350.9 - 351.1m	Fine grained calcsilicate gneiss		Y	
023	C15	PPhms	Broa1	400.5 - 400.6m	Fine grained black schist		Y	
024	C16	PMbr	Newl1	424.5 - 424.7m	Red siltsone, white alteration patches	Y	Y	Y
025	C17	PMbr	Newl1	442.5 - 442.7m	Red siltsone, white alteration patches		Y	
026	C18	PMbr	Newl1	460.8 - 460.9m	Red siltsone, white alteration patches		Y	
027	C19	PMp	EC21	419.6 - 419.7m	Red shale, little alteration	Y	Y	Y
028	C20	PMp	PY1	593.0 0 593.2m	Red shale, green alteration patches		Y	
029	C21	PMp	PY4	482.0 - 482.2m	Red, finely banded shale		Y	

SOUTH AUSTRALIA - LOCATION MAP

133° E   135°   137°   139°

30° S

Tarcoola ■ ⊗ Wilgena 1

⊗⊗ CSR EC 21,
PY 1, & PY 4

32°

■ Ceduna

N

Corunna CC1 & CC2
⊗⊗

■ Pt. Augusta

SAMEDAN SOC 1, ⊗⊗
SOC 7, & SOC 8 ⊗⊗ Roopena 6

Whyalla ■

⊗ Broadveiw 1

34°

KEY

⊗ Sampled diamond
   drill hole locations

■ Location of City
   or township

Tumby Bay area
For more detail
see Appendix: G

ADELAIDE ■

■ **Pt Lincoln**

0   100   200

km

36°
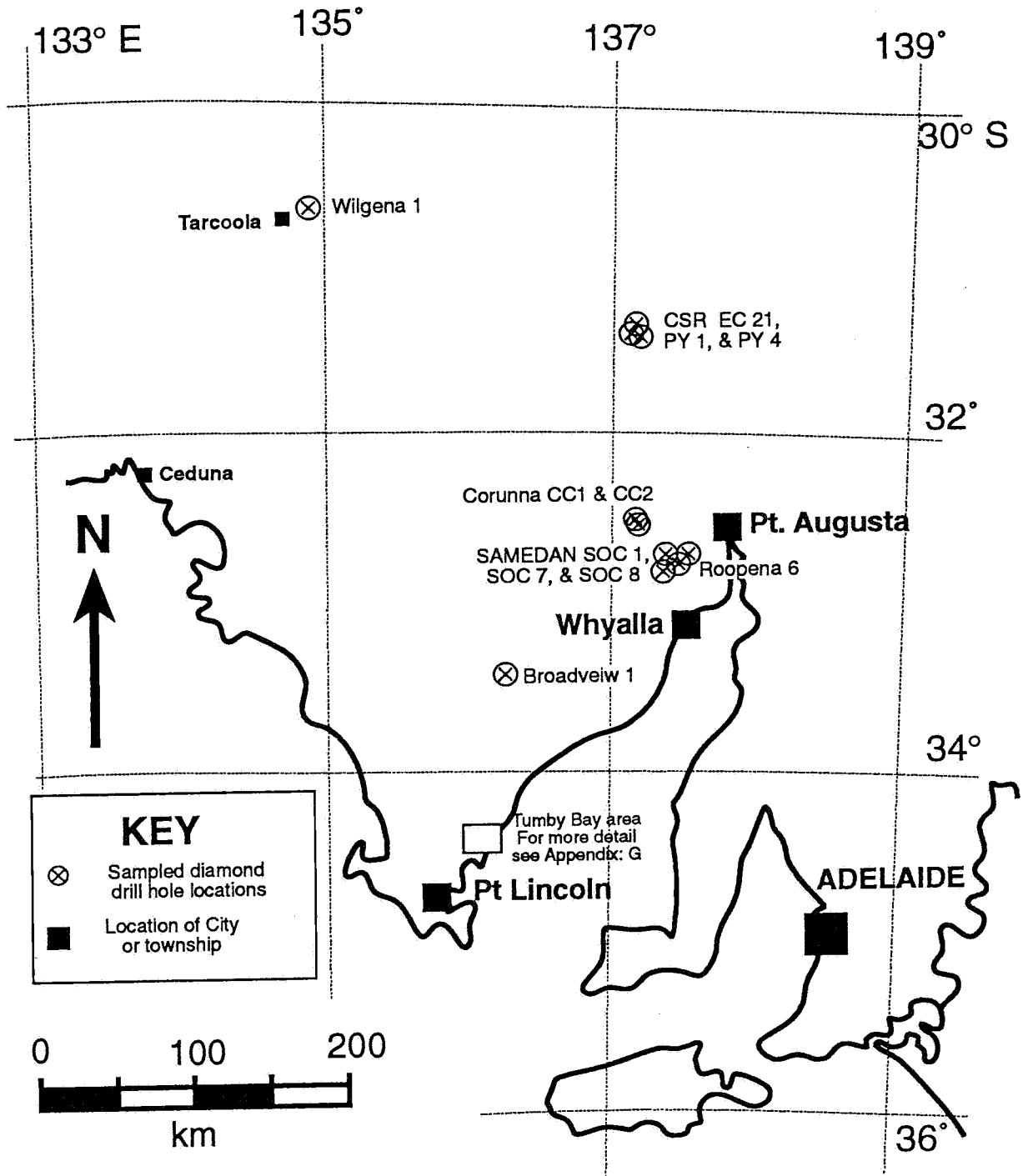
DRILL HOLE SUMMARY LOGS

LEGEND:

PMp	Mesoproterozoic;	Pandurra Formation sediments
PMbg	Mesoproterozoic;	Gairdner dykes
PMar	Mesoproterozoic;	Roopena volcanics
PMa	Mesoproterozoic;	Gawler Range volcanics
PMcc	Mesoproterozoic;	Corunna conglomerate
PMbr	Mesoproterozoic;	Blue Range beds
PPt	Palaeoproterozoic;	Tarcoola Formation
PPmm	Palaeoproterozoic;	Moonabie Formation
PPmg	Palaeoproterozoic;	McGregor volcanics
PPmw	Palaeoproterozoic;	Wandearah metasiltstone
PPbo	Palaeoproterozoic;	Bosanquet Formation
PPhms	Palaeoproterozoic;	HutchisonGroup, Mt.Shannan Iron formation
PPh	Palaeoproterozoic;	Hutchison Group metasediments

DME Corunna CC1

From	To	Strat. symbol	Rock type	Sampled	Sample No.	Description
0.00	79.60	PMcc	Conglomerate		1031/	
79.60	80.10	PMbg	Dolerite			
80.10	91.00	PMcc	Siltstone	80.48 - 80.63	C1 012	banded siltstone and clastic sandstone
91.00	91.50	PMbg	Dolerite			
91.50	119.60	PMcc	Siltstone			
119.60	127.80	PMa	Feldspar porphry			
127.80	135.50	PMcc	Siltstone			
135.50	150.30	PMa	Feldspar porphry			
	EOH 150.36 m		6386956mN	692745mE		50 deg. inclin.

DME Corunna CC2

From	To	Strat. symbol	Rock type	Sampled	Sample No.		Description
					1031/		
0.00	166.65	PMcc	Dolomite / conglom.				
166.65	188.50	PMcc	Shale / siltstone	168.20 - 168.35	C2	011	black shale
188.50	259.00	PPh	Gneiss / Schist	255.54 - 255.74	C3	013	green gneiss
	EOH 259.10 m		6388784mN	692441mE			90 deg. inclin.

SAMEDAN SOC1

From	To	Strat. symbol	Rock type	Sampled	Sample No.		Description
					1031/		
0.00	80.30	PMar	Basalt				
80.30	81.10	PMcc	Conglomerate				
81.10	124.20	PPmg	Rhyolite				
124.20	132.50	PPmm	Quartzite	129.40 - 129.60	C4	014	med. grained volc. sandstone some alteration patches.
	EOH 133.00 m		6375022mN	723214mE			90 deg. inclin.

SAMEDAN SOC7

From	To	Strat. symbol	Rock type	Sampled	Sample No.		Description
					1031/		
0.00	50.00	PMar	Siltstone / sandstone				
50.00	106.70	PPmw	Meta-siltstone	80.80 - 80.95	C5	010	Fe-stained clastic siltsone breccia
106.70	184.50	PPmm	Quartzite				
	EOH 184.50 m		6374029mN	722796mE			77 deg. inclin.

SAMEDAN SOC8

From	To	Strat. symbol	Rock type	Sampled	Sample No.	Description
0.00	46.70	PMar	Basalt / Siltstone		1031/	
46.70	47.80	PMcc	Conglomerate			
47.80	176.70	PPmw	Siltstone / sandstone	153.30 - 153.45	C6 009	banded metasiltstone
176.70	203.00	PPmm	Quartzite	181.50 - 181.75	C7 015	coarse volcaniclastic grit
	EOH 203.00 m		6373984mN	722738mE		77 deg. inclin.

DDH Roopena 6

From	To	Strat. symbol	Rock type	Sampled	Sample No.	Description
0.00	20.00	PMar	Amygdaloidal basalt		1031/	
20.00	55.00	PMcc	Sandsone / siltstone			
55.00	60.00	PMcc	Tuffaceous sandstone			
60.00	90.00	PMcc	Sandstone / siltstone	70.20 - 70.40	C8 016	grey-black shale, some banding
90.00	95.00	PMcc	Laminated tuff			
95.00	105.00	PMcc	Sandy siltstone			
105.00	115.00	PMar	Amygdaloidal basalt			
115.00	127.00	PMcc ?	Conglomerate			
127.00	153.00	PMcc ?	Sandstone (purple)			
153.00	158.00	PMcc ?	Conglomerate / sandstone			
158.00	245.00	PPmw	Silicified siltstone breccia			
245.00	256.68	PPmw	Chloritised siltstone	251.40 - 251.55	C9 017	Chloritised siltstone
	EOH 256.68					

DDH Wilgena 1

From	To	Strat. symbol	Rock type	Sampled	Sample No.		Description
0.00	9.00	Q	Sands		1031/		
9.00	15.00	PPt	Silcreted sands				
15.00	65.00	PPt	Claystone / siltstone				
65.00	221.70	PPt	Carbonaceous siltstone				
221.70	234.06	PPt	Rhyolite				
234.06	336.30	PPt	Quartzite / siltstone	311.72 - 311.90	C10	018	shale, small qtz veining
336.30	448.00	PPt	Qtz veined siltstone				
448.00	562.70	PPt	Qtzite / sitlstone / tuff				
562.70	618.99	PPt	Carbonaceous siltstone				
618.99	677.50	PPt	Qtzite / siltstone / tuff	640.85 - 641.00	C11	019	banded shale, near adjacent U-Pb
677.50	759.64	PPt	Quartzite				
759.64	832.85	PPt	Carbonaceous siltstone	779.60 - 779.80	C12	020	homogeneous carbonaceous shale
832.85	854.00	PPt	Quartzite				
854.00	892.35	PPt	Carbonaceous siltstone	889.15 - 889.35	C13	021	black shale, some banding
892.35	973.00	PPt	Quartzite c styolites				
	EOH 973 m		location 7 km East of Tarcoola				90 deg. inclin.

DDH Broadveiw 1

From	To	Strat. symbol	Rock type	Sampled	Sample No.		Description
0.00	26.20	Cain.	Clay / sands / conglom.		1031/		
26.20	112.30	PPbo	Rhyodacite				
112.30	127.60	PPbo	Calcsilicate gneiss				
127.60	187.25	PPbo	Rhyodacite c diopside				
187.25	189.15	PPbo	Calcsil. gneiss c diopside				
189.15	302.20	PPbo	Rhyodacite				
302.20	305.50	PPbo	Calcsil. gneiss c diopside				
305.50	346.00	PPbo	Rhyodacite				
346.00	351.25	PPbo	Calcsilicate gneiss	350.90 - 351.05	C14	022	fine grained calcsilicate gneiss
351.25	400.33	PPbo	Rhyodacite				
400.33	401.00	PPhms	Schist	400.50 - 400.64	C15	023	fine grained black schist
401.00	407.80	PPbo	Rhyodacite				
407.80	414.98	PPhms	Iron formation				
414.98	450.20	PPbo	Calcsilicate gneiss				
450.20	578.60	PPbo / PPhms	Interbanded calcsil gneiss, and banded schist				
	EOH 578.60 m		33 deg. 25 min Lat. 136 deg. 19 min Long.				60 deg. inclin.

DDH Newland 1

From	To	Strat. symbol	Rock type	Sampled	Sample No.		Description
0.00	373.00		NOT LOGGED		1031/		
373.00	388.95	PMbr	Conglomerate				
388.95	389.40	PMbr	Sandstone / conglomerate				
389.40	423.40	PMbr	Conglomerate				
423.40	428.60	PMbr	Sandstone / red siltstone	424.53 - 424.68	C16	024	Red siltsone, white alteration patc
428.60	429.50	PMbr	Sandstone				
429.50	431.04	PMbr	Sandy conglomerate				
431.04	432.00	PMbr	Sandstone / red siltstone				
432.00	442.05	PMbr	Conglomerate / sandstone				
442.05	442.83	PMbr	Sandstone / siltstone	442.55 - 442.70	C17	025	Red siltsone, white alteration patc
442.83	450.24	PMbr	Conglomerate / sandstone				
450.24	450.70	PMbr	Siltstone / sandstone				
450.70	455.43	PMbr	Conglomerate				
455.43	463.70	PMbr	Sandstone / siltstone	460.85 - 460.92	C18	026	Red siltsone, white alteration patc
463.70	465.95	PMbr	Clastic sandstone				
	EOH 465.95M		NOTE: top of hole not logged				

CSR DDH EC21

From	To	Strat. symbol	Rock type	Sampled	Sample No.	Description
0.00	144.00	PMp	Sandstone / quartzite		1031/	
144.00	216.00	PMp	Sandstone			
216.00	314.00	PMp	Heavy mineral sandstone			
314.00	376.00	PMp	Quartzite / sandstone			
376.00	415.54	PMp	Sandstone / shale			
415.54	442.59	PMp	Red / green shales	419.57 - 419.70	C19 027	Red shale, little alteration
442.59	467.74	PMp	Sandstone			
467.74	521.19	PMp	Grit			
521.19	545.50	PMar ?	Volcanic breccia			
545.50	835.50	PMar ?	Altered volcanics / tuffs			
835.50	992.25	PPmm ?	Folded metasediments			
992.25	1002.00	Hiltiba ?	Granite breccia			
	EOH 1002 m		6652650 mN	709400 mE		90 deg. inclin.

CSR   DDH PY1

From	To	Strat. symbol	Rock type	Sampled	Sample No.		Description
0.00	3.90	Cainozoic ?	Sands		1031/		
3.90	39.80	Tapley Hill	Dolomite				
39.80	432.25	PMp	Sandstone				
432.25	590.00	PMp	Sandstone / shale				
590.00	608.40	PMp	Red shale	593.00 - 593.15	C20	028	Red shale, green alteration patches
608.40	631.01	PMp	Sandstone				
631.01	679.65	PMp	Conglomerate				
679.65	825.56	PMar ?	Acid volcanics				
825.56	851.72	PMar ?	Volcanic conglomerates				
851.72	993.92	PMar ?	Altered volcanics				
993.92	1163.08	PMar ?	Acid volcanics				
1163.08	1293.30	PMar ?	Altered volcanics				
	EOH 1293.3 m		6516000 mN	709000 mE			90 deg. inclin.

CSR DDH PY4

From	To	Strat. symbol	Rock type	Sampled	Sample No.		Description
0.00	1.00	Q	Lake mud		1031/		
1.00	34.45	Tregolana	Shale				
34.45	37.02	Whyalla	Sandstone				
37.02	46.50	Brighton	Limestone				
46.50	283.50	PMp	Sandstone / conglomerate				
283.50	464.70	PMp	Sandstone / shale				
464.70	494.70	PMp	Red / green shale	482.00 - 482.15	C21	029	Red, finely banded shale
494.70	562.58	PMp	Conglomerate / sandstone				
562.58	622.86	PMar ?	Basic volcanic				
622.86	646.57	PMar ?	Intermediate volcanic				
646.57	663.00	PMar ?	Altered volcanic breccia				
663.00	790.25	PMar ?	Trachyandisite				
790.25	820.52	PMar ?	Volcaniclastic conglomerate				
820.52	831.13	PMar ?	Altered basalt				
831.13	906.78	PMar ?	Acid pyroclastics				
906.78	932.00	PMar ?	Volcanic breccia				
932.00	960.80	PMar ?	Basalt				
960.80	1015.00	PMar ?	Trachy - andesite				
	EOH 1015.0 m		6518000 mN	712000 mE			90 deg. inclin.

APPENDIX B

Selected sample descriptions & Photographs

Selected Thin section descriptions

(for locations see locations map Appendix H)

1031-001 Mylonitised quartzite Photo A & B

Quartz	80%	Feldspars	18%
Biotite	2%	Muscovite	5%
Tourmaline	5%		

Metasediment: Composite and undulose quartz grains indicating high stresses exerted upon rock, muscovite and biotite show orientation of strain fabric, tourmaline of various sizes, mostly as fragmented grains.

1031-002 Banded amphibolite no photo

Quartz	15%	Feldspars	15%
Hornblende	35%	Pyroxenes	35%

Metasediment / Metavolcanic ?: Banding due to mineral compositions, dark - hornblende rich, light - plagioclase feldspar, and pyroxene rich. Pyroxenes observed as both orthopyroxene and clinopyroxene. Feldspars dominantly observed as plagioclase.

1031-003 Mylonitised gneiss Photo F

Quartz	20%	Feldspars	30%
Muscovite	30%	Biotite	10%
Hornblende	10%		

Metasediment ?: Quartz as composite undulose grains, metamorphic fabric defined by muscovite, biotite and fine-grained hornblende. Feldpars observed dominantly as microcline, both as porphyroblasts, and smaller grains within fabric. Fabric is observed wrapping around porphyroblasts.

1031-005 Garnet schist Photo G & H

Quartz	45%	Feldspars	25%
Biotite	20%	Garnet	6%
Muscovite	2%	Silliminite	1%
Opaques	1%		

Metasediment: Quartz undulose and composite grains, due to accumulation of stresses. Feldspars perthitic, microcline and plagioclase, angular and interconnected, possibly due to melting ie migmatisation. Biotite expresses strain fabric, also wrapped around porphyroblasts. Garnets observed are generally well rounded, late stage growth in tectonic history ?.

1031-006   Leucogranite   Photo E

        Quartz   20%   Feldspars   70%

        Muscovite   18%   Oxides   2%

meta-igneous: Feldspars observed as both microcline and plagioclase in almost equal proportions. Quartz is undulose representing has been strained, muscovite where observed represents a fabric within the rock (metamorphic fabric).

1031-008   Highly foliated gneiss   Photo C & D

        Quartz   20%   Feldspars   60%

        Hornblende   10%   Muscovite   6%

        Biotite   4%

Meta-igneous: Highly deformed gneiss, re-melting of quartz into fabric, undulose extinctions observed. Rock dominantly composed of feldspars (plagioclase and microcline), with fabric minerals (muscovite, biotite) wrapping around these larger porphyroblasts. Hornblende occurrs as porphyroblasts and fragmented grains within the slide.

1031-032   Crenulated schist   no photo

        Quartz   85%   muscovite   10%

        Opaques   5%

Metasedimentary: Fine grained composite quartz bulk mineralogy of the rock. Muscovite defines crenulated metamorphic fabric. Opaques disseminated with sub-angular nature (detrital).

Selected Photograph descriptions

(for locations see locations map Appendix H)

Photo 1.   Boulder conglomerate within the Corunna conglomerate suite, Tassie Creek reservoir, near Corunna homestead (north of Iron Knob). Clasts are rounded to sub-rounded indicating relatively large transport distance and times, and are observed to be of many different origins (eg. GRV, Hutchison Group metasediments).

Photo 2.   Location eS12, western rgion of Tumby Bay map (locations - Appendix H). Amphibolite xenoliths observed within Leucogranitic material defining an intrusive reltion for the latter. A minor fault is observed off-setting xenoliths, likely representing late stage tectonism (eg Wartakan event).

Photo 3.   Location bS6 (locations - Appendix H). Typical mylonite within map region, elongate feldspar porphyroblasts due to mylonitisation. Matrix composed dominantly of metamorphic minerals (muscovite, biotite) giving dark colour.

Photo 4.   Location aS16 (locations - Appendix H), within Tumby Bay map area. Sheared contact of granite and metasediment, strain gradient accross boundary also observed, with less observed strain within granite thus late tectonic.

Photo A.   sample 1031-001   Rock photo
Mylonitied quartzite belonging to the Warrow quartzite unit, located within mylonite zone of Tumby Bay map region (locations - Appendix H). Lineations are observed (pen mark on top) measured in the field to be dipping 20° N, foliations are seen to be horizontal in the specimen.

Photo B.   sample 1031-001   Thin section photo
Mylonitised quartzite showing orientation of metamorphic fabric (foliation) being vertical in photo and defined by metamorphic minerals. The tourmaline (bottom right) within photo is commonly found as fractured grains within this rock type.

Photo C.   sample 1031-008   Rock photo
Mylonitised Donington Suite granitoid (black gneiss), foliation is observed vertical in specimen
with lineations, defined by elongation of feldspars, horizontal. This sample is located in large
'kink band' in southern region of the map (appendix H), and is observed to be highly deformed
due to the accumulation of stresses within this region.

Photo D.   sample 1031-008   Thin section photo
Highly deformed granite, feldspar rich. Porphyroblasts of Hornblende (top of photo) show
stretching of tails due to intense deformation. The fabric, as defined by deformed quartz,
muscovite and biotite minerals, wraps around these porphyroblasts.

Photo E.   sample 1031-006   Rock photo
Deformed Moody Suite leucogranite (Yunta Well) showing lower strain fabric than Donington
Suite granitoid, ie influenced less by tectonism. Oxides are observed in left region of the
photo, possibly relict garnets ?.

Photo F.   sample 1031-003   Thin section photo
Mylonitised gneiss, matrix of feldspar and quartz, feldspar porphyroblasts show deformation
from stresses. Metamorphic minerals (muscovite, biotite) show orientation of mylonite fabric
(horizontal).

Photo G.   sample 1031-005   Rock photo
Garnet schist, large and smaller feldspars are observed as porphyroblasts formed possibly due
to migmatisation (re-melting) under deformation of these rocks. Foliation is defined by biotite
minerals (horizointal). Rounded Garnets are readily observable in hand specimen (do not show
well in photo). This rock type is commonly found within map area, but garnets are only
observed within distinct bands (compositional layering) which are rare. These bands traverse
the region, parallel to mylonitic fabric (parallel to compositional layering).

Photo H.   sample 1031-005   Thin section photo
Schist showing high component of biotite in fabric, rounded garnets are observed within this
fabric. Large grouping of feldpar crystals in top-left corner represent a feldspar porphyroblast.

Selected Field Photographs

Photo 1.

Photo 2.

Photo 3.
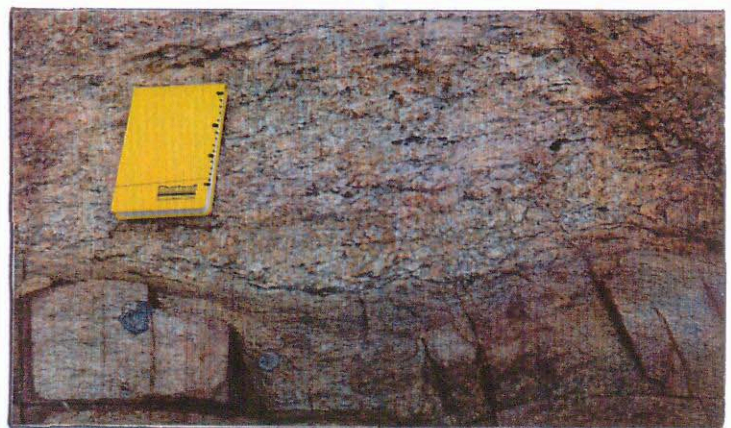
Photo 4.

Selected Rock & Thin section Photographs
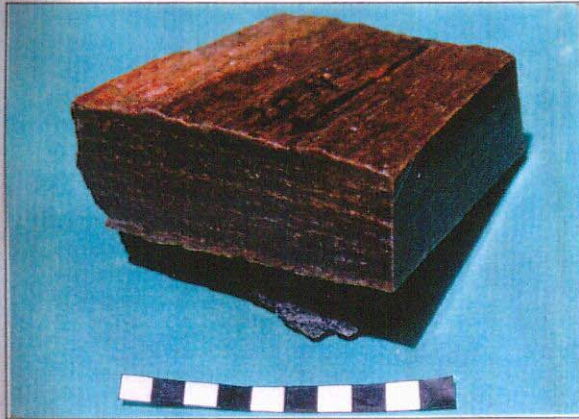
APPENDIX C
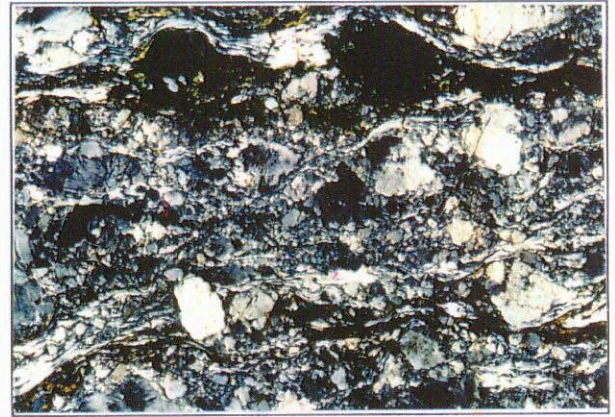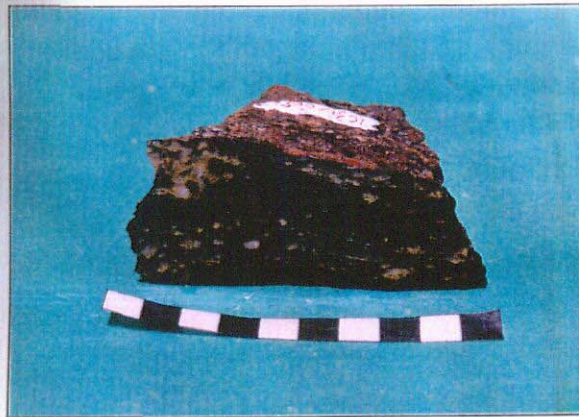
Analytical Procedures

Appendix C: Analytical Procedures.

Sample preparation:
Samples were collected from located diamond drill holes ($^1/_4$ Hq, Nq, & Bq core), or from field rock-grab samples, which were subsequently cut by a diamond saw to remove weathered surfaces. Selected 'fresh' samples were then crushed in a jaw crusher and milled in a tungsten carbide mill to produce a fine workable powder.

Isotope analysis:
Seven selected milled samples were isotopically analysed to obtain data for discussion within this thesis. Sample dissolution was carried out in teflon 'bombs' encased in spring loaded metal jackets, in order to pressurise samples under high temperatures, enabling dissolution of highly resistant accessory minerals, eg. zircons.

Acids used to dissolve samples were Hydrofluoric acid (HF), and HF - HNO_3 (Nitric acid). Samples were then converted to chlorides using dissolution in HCl (Hydrochloric acid), then solutions were split, and approximately $^1/_3$ spiked with 2 drops of ^{150}Nd - ^{147}Sm solution for isotope dilution. Both spiked and un-spiked solutions were processes to extract Sr, Sm, & Nd fractions for analysis. Sr was separated using cation exchange columns, residues were collected and processed through a second set of columns (teflon + EDEHP (complexing agent)), to collect Sm & Nd.

Sr samples were loaded onto single tantalum filaments, whereas Sm & Nd were loaded onto double tantalum - rhenium filaments. A Finnigan MAT 261 solid source mass spectrometer was used to measure isotopic ratios of analysed elements, with data blocks of 11 scans repetitively run until results were satisfactory within experimental error.

XRF analysis:
Milled samples were analysed by X-ray fluorescence in order to obtain geochemical data on selected rock types for discussion within this thesis. Pressed pellets for trace elements, and fused discs for whole rock analyses were prepared.

Pellets were made by mixing ~5 grams of sample powder with a binding PVA solution, and compressing to produce a smooth flat surface. Fused discs were produced by igniting ~4 grams of sample powder at 960°C overnight, then reweighed to determine percentage loss of volatiles. 1 gram of sample was then mixed with 4 grams of flux, and fused on a Norrish Prometheus fusion apparatus.

Both pressed pellets and fused discs were analysed by X-ray fluorescence on a programmable Phillips PW 1480 X-ray spectrometer.

APPENDIX D

Isotope Systematics

Appendix D: Isotope Systematics:

Isotope geology uses the principle of natural radioactive decay of an unstable isotope of a particular element (^{147}Sm), to a daughter stable isotope of another element (^{143}Nd). Half lives for time of decay for this process vary for different elements (eg. seconds to billions of years). In the geological application of isotopically dating rocks, very long half lives are desirable, but the elements used must be of significant concentration in the rocks analysed to be able to be measured.

Radioactive decay is an application used in a variety of different scientific problems. The equation describing radioactive decay as a function of time is:

$$N = N_0 \exp(-Lt) \tag{1}$$

Where: N = number of radioactive parent atoms left at time t.

N_0 = initial number of radioactive parent atoms.

L = decay constant for that parent atom

The half life of a particular isotope is the time taken for half the initial number of parent atoms to decay to daughter products. Half life for Sm dacay is around 106 Ga, which is some 23 times greater than the age of the Earth.

$$t\,^{1}/_2 = \ln 2\,/\,L \tag{2}$$

The number of new daughter atoms D* produced from destruction of parent atoms N at time t is given by:

$$D^* = N_0\,(1 - \exp(-Lt)) \tag{3}$$

But in most all applications there is already some initial daughter element present in the rock, this must be considered, thus total (measured) isotopic concentration of daughter product in the rock is:

$$D = D_0 + N_0\,(1 - \exp(-Lt))$$
$$= D_0 + N\,(\exp(-Lt) - 1)\quad\text{[from equation (1)]}\tag{4}$$

From equation (4) we may now observe that by measuring the amount of daughter D, and radioactive N at present time, with L an experimentally determined constant, we may solve for t which will give us the age of the rock. Assumptions must be made about D_0, as this is a value that cannot be measured from a single sample. ie. we cannot measure the concentration of D at formation age (eg. 1600 Ma) which would give us the D_0 value.

$$t = {^{1}/_L}\,(\,\ln\,((D - D_0)\,/\,N) - 1))\quad\text{[from equation (4)]}\tag{5}$$

In practical application it is easier (and more accurate) to measure isotopic ratios on modern mass spectrometers than absolute values of D & N by other methods (eg. XRF). In this way relative abundances these isotopes are measured as a ratio to a reference non-radiogenic isotope.

In the Sm-Nd isotopic system, $D = {}^{143}Nd$, $N = {}^{147}Sm$, and both are measured against ${}^{144}Nd$. Thus equation (4) becomes:

$$\left[\frac{{}^{143}Nd}{{}^{144}Nd}\right]_t = \left[\frac{{}^{143}Nd}{{}^{144}Nd}\right]_i + \left[\frac{{}^{147}Sm}{{}^{144}Nd}\right]_t (exp(-Lt) - 1) \qquad - (6)$$

$({}^{143}Nd / {}^{144}Nd)_0$ and $({}^{147}Sm / {}^{144}Nd)_0$ are measured on the mass spectrometer and $L = 6.54 * 10^{12}$ is the value for the decay constant for ${}^{147}Sm$ decaying to ${}^{143}Nd$. Thus t can be calculated if $({}^{143}Nd / {}^{144}Nd)i$ (initial) is known.

For the Sm-Nd isotopic system model ages are determined relative to a presumed source of the material. (eg. the mantle), thus $({}^{143}Nd / {}^{144}Nd)i$ is obtained by assuming a value for this from a created model of mantle evolution. Thus the time t calculated will give us the age that the rock under analysis was extracted from this source, ie. a model age.

Two models are considered, a uniform evolving mantle (CHUR), and a depleted mantle that has experienced a single major depletion event early in the period of Earth formation. From substituting into equation (5):

$$t_{model} = \frac{1}{L}\left(\ln\left(\left(\frac{({}^{143}Nd / {}^{144}Nd)_0 - ({}^{143}Nd / {}^{144}Nd)i}{({}^{147}Sm / {}^{144}Nd)_0}\right) - 1\right)\right) \qquad - (7)$$

Thus $({}^{143}Nd / {}^{144}Nd)i$ is taken from one of two model values;

CHUR model: ${}^{143}Nd / {}^{144}Nd = 0.512638$

Depleted mantle model: ${}^{143}Nd / {}^{144}Nd = 0.513108$

Model ages (t_{mod}) obtained from these values give ages of extraction from bulk Chondritic Earth and Depleted mantle respectively.

A more convenient way of expressing Nd values, as measured and calculated values commonly vary around 0.5115 ± 0.0002, is the Epsilon (ε) notation. That is the parts per 10000 difference between the sample and CHUR:

$$\varepsilon Nd_t = \left(\left(\frac{({}^{143}Nd / {}^{144}Nd)_t\ sample}{({}^{143}Nd / {}^{144}Nd)_t\ CHUR}\right) - 1\right) * 10\ 000 \qquad - (8)$$

Thus for any given time (t), εNd for the sample can be calculated using a linear evolution model, from εNd measured at present ($\varepsilon Nd(0)$), and εNd at time of extraction

$(\varepsilon Nd(T_{mod:dep})$. Comparison of εNd values and model ages are powerful tools in understanding the timing of crustal additions from the mantle and evolution of a terrain over time. See diagram below.

Extraction of melts from mantle source
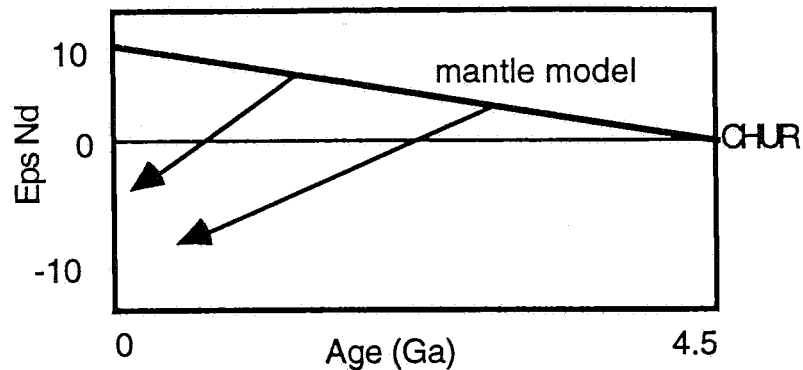
During magmatic fractionation processes of melts from a source, Nd is preferentially enriched over Sm due to a lower charge/ionic radius of Nd. Thus extracted melts will have lower Sm/Nd ratios than sources, and the rate of ^{143}Nd accumulation will then be less. Therefore the trend for dominantly felsic crustal rocks to trend to more negative εNd values with age. (ie. accumulation of ($^{143}Nd/^{144}Nd$) sample < accumulation of ($^{143}Nd/^{144}Nd$) CHUR - from equation (8)), is observed.

These models of isotopic age calculation and evolution are made on assumptions of non-alteration of isotopic ratios due to metamorphism or diagenetic processes (during sedimentation). In the Sm-Nd isotopic system this is believed to be the case, the Rare Earth Elements (REE's) Sm & Nd having short residence times (less than oceanic mixing times) in oceanic waters, and thus are almost exclusively transferred into the sedimentary record, associated with many common rock forming minerals.

As these REE's are incompatible, and of similar ionic radius, they are believed to be 'robust' during sedimentation and metamorphic processes. Thus fractionation processes observed to occur in other isotopic systems (eg. Rb-Sr), causing resetting of isotopic signatures (eg. change in $^{147}Sm/^{144}Nd$ ratio), are assumed not to occur in the Sm-Nd isotopic system. If fractionation does occur by any method, change in isotopic ratios (Sm/Nd) will alter evolutionary paths, and the measured isotopic values today will not be representative of true sources.

APPENDIX E

Compiled Isotopic data

rock	Pandurra fm.	Blue Range Beds	ISOTOPIC DATA		Moonabie fm.	Yadnarie schist
			Sampled Proterozoic clastic sedimentary suites			
			Corunna conglom.	Tarcoola fm.	Wandearah meta.	Moonabie fm.	Yadnarie schist
sample no.	1031-027	1031-024	1031-016	1031-019	1031-017	1031-014	1031-032
Nd ppm	58.05	40.26	48.29	33.28	25.30	23.38	38.28
Sm ppm	14.17	6.13	8.20	5.76	3.92	4.88	7.04
143/144 Nd	0.511886	0.511513	0.511404	0.511556	0.511557	0.511488	0.511498
2 sigma	0.000059	0.000041	0.000036	0.000049	0.000052	0.000042	0.000057
Sm/Nd	0.2441	0.1524	0.1699	0.1731	0.1551	0.2087	0.1839
147Sm/144Nd	0.1476	0.0922	0.1028	0.1047	0.0938	0.1262	0.1112
143/144Nd ch	0.512638	0.512638	0.512638	0.512638	0.512638	0.512638	0.512638
143/144Nd dep	0.513108	0.513108	0.513108	0.513108	0.513108	0.513108	0.513108
T mod:chur	2.33	1.64	2.00	1.79	1.60	2.48	2.03
T mod:dep	2.72	1.96	2.29	2.12	1.93	2.74	2.34
eps Nd (0)	-14.67	-21.95	-24.07	-21.11	-21.09	-22.43	-22.24
age (T)	1.424	1.6	1.6	1.656	1.74	1.74	1.84
143/144(T)	0.510505	0.510543	0.510323	0.510416	0.510484	0.510043	0.510151
143/144ch T	0.510798	0.510569	0.510569	0.510496	0.510387	0.510387	0.510257
eps Nd (T)	-5.73	-0.50	-4.81	-1.57	1.90	-6.73	-2.07
eps Nd/500	-11.55	-15.29	-18.09	-15.25	-14.53	-17.95	-16.80
eps Nd/700	-10.30	-12.61	-15.69	-12.89	-11.90	-16.16	-14.61
eps Nd/1000	-8.41	-8.59	-12.08	-9.35	-7.94	-13.45	-11.33
eps Nd/1500	-5.25	-1.85	-6.03	-3.42	-1.30	-8.92	-5.83
eps Nd/2000	-2.08	4.93	0.06	2.54	5.37	-4.36	-0.29
eps Nd/2500	1.12	11.74	6.18	8.54	12.08	0.22	5.28
eps Nd (Tdep)	2.53	4.40	3.60	4.01	4.47	2.47	3.48

	Archaean:			Compiled data					
rock	Paragneiss [1]	Paragneiss [1]	Augen gneiss [1]	Leucogneiss [1]	Gneiss [2]	Gneiss [2]	[2]	[2]	[2]
sample no.	Kimba	Wadikee rocks	Cape Carnot	Cape Carnot	Cape Carnot	Cape Carnot	Tarcoola	Tarcoola	Tarcoola
Nd ppm	32.62	29.37	40.24	17.12	28.90	91.60	28.60	43.20	36.00
Sm ppm	6.59	5.46	6.78	2.64	4.90	14.30	4.30	7.50	5.30
143/144 Nd	0.511235	0.511377	0.510933	0.510916	0.510967	0.510967	0.510837	0.511078	0.510737
2 sigma									
Sm/Nd	0.2020	0.1859	0.1685	0.1542	0.1696	0.1561	0.1503	0.1736	0.1472
147Sm/144Nd	0.1222	0.1125	0.1019	0.0933	0.1026	0.0944	0.0909	0.1050	0.0891
143/144Nd ch	0.512638	0.512638	0.512638	0.512638	0.512638	0.512638	0.512638	0.512638	0.512638
143/144Nd dep	0.513108	0.513108	0.513108	0.513108	0.513108	0.513108	0.513108	0.513108	0.513108
T mod:chur	2.85	2.27	2.73	2.52	2.69	2.48	2.58	2.58	2.68
T mod:dep	3.03	2.54	2.90	2.71	2.87	2.68	2.76	2.78	2.84
eps Nd (0)	-27.37	-24.60	-33.26	-33.59	-32.59	-32.59	-35.13	-30.43	-37.08
age (T)	2.4	2.4	2.643	2.837	2.5	2.5	2.5	2.5	2.5
143/144(T)	0.509302	0.509598	0.509156	0.509169	0.509277	0.509411	0.509338	0.509347	0.509269
143/144ch T	0.509526	0.509526	0.509208	0.508954	0.509396	0.509396	0.509396	0.509396	0.509396
eps Nd (T)	-4.41	1.41	-1.03	4.22	-2.33	0.30	-1.13	-0.96	-2.48
eps Nd/500	-22.64	-19.24	-27.24	-27.02	-26.61	-26.09	-28.41	-24.60	-30.24
eps Nd/700	-20.74	-17.09	-24.82	-24.38	-24.20	-23.48	-25.71	-22.26	-27.50
eps Nd/1000	-17.88	-13.85	-21.18	-20.41	-20.59	-19.55	-21.65	-18.74	-23.36
eps Nd/1500	-13.09	-8.43	-15.09	-13.75	-14.54	-12.97	-14.85	-12.85	-16.44
eps Nd/2000	-8.28	-2.98	-8.96	-7.07	-8.45	-6.36	-8.01	-6.92	-9.48
eps Nd/2500	-3.43	2.51	-2.80	-0.34	-2.33	0.30	-1.13	-0.96	-2.48
eps Nd (Tdep)	1.76	2.97	2.10	2.55	2.17	2.64	2.44	2.39	2.25
[1] - Turner et.al., (1992), [2] - corrected McCulloch, (1987), [3] - Robertson, (1989), [4] - Huffadine, (1993), [5] - Stewart, (1992).									

2

rock	Proterozoic: Cook gap schist [1]	Donnington [1]	Broadveiw schist [1]	McGregor volc. [1]	McGregor volc. [1]	Doora schist [4]
sample no.	Lincoln	Granite	Lincoln	Corunna	Corunna	Yorke Peninsula
Nd ppm	37.48	33.80	14.29	33.46	55.53	29.60
Sm ppm	6.68	5.74	3.05	5.15	9.83	5.60
143/144 Nd	0.511405	0.511728	0.511456	0.511418	0.511440	0.511380
2 sigma						
Sm/Nd	0.1782	0.1698	0.2134	0.1539	0.1770	0.1892
147Sm/144Nd	0.1078	0.1027	0.1291	0.0931	0.1071	0.1144
143/144Nd ch	0.512638	0.512638	0.512638	0.512638	0.512638	0.512638
143/144Nd dep	0.513108	0.513108	0.513108	0.513108	0.513108	0.513108
T mod:chur	2.11	1.47	2.65	1.79	2.03	2.32
T mod:dep	2.39	1.86	2.89	2.09	2.33	2.59
eps Nd (0)	-24.05	-17.75	-23.06	-23.80	-23.37	-24.54
age (T)	1.85	1.82	1.8	1.74	1.74	1.6
143/144(T)	0.510093	0.510498	0.509927	0.510352	0.510215	0.510176
143/144ch T	0.510244	0.510283	0.510309	0.510387	0.510387	0.510569
eps Nd (T)	-2.96	4.22	-7.48	-0.67	-3.38	-7.69
eps Nd/500	-18.40	-11.76	-18.76	-17.20	-17.67	-19.31
eps Nd/700	-16.12	-9.36	-17.04	-14.55	-15.37	-17.21
eps Nd/1000	-12.71	-5.74	-14.44	-10.57	-11.93	-14.05
eps Nd/1500	-6.98	0.32	-10.10	-3.89	-6.16	-8.75
eps Nd/2000	-1.23	6.42	-5.73	2.82	-0.35	-3.43
eps Nd/2500	4.56	12.55	-1.33	9.57	5.48	1.92
eps Nd (Tdep)	3.34	4.66	2.11	4.08	3.50	2.86

rock	Doora schist [4]	Doora schist [4]	Tarcoola Fm. [1]	Corunna congl. [1]	Yardea dacite [1]	Volcanic [2]	Volcanic [3]
sample no.	Yorke Peninsula	Yorke Peninsula	Wilgena-1	Corunna	Gawler Ranges	Gawler Ranges	Gawler Ranges
Nd ppm	25.70	42.05	26.67	37.00	68.52	174.90	51.11
Sm ppm	4.60	7.10	4.94	6.87	13.07	39.90	8.06
143/144 Nd	0.511320	0.511380	0.511679	0.511755	0.511593	0.511719	0.511224
2 sigma							
Sm/Nd	0.1790	0.1688	0.1852	0.1857	0.1907	0.2281	0.1577
147Sm/144Nd	0.1083	0.1021	0.1120	0.1123	0.1154	0.1380	0.0954
143/144Nd ch	0.512638	0.512638	0.512638	0.512638	0.512638	0.512638	0.512638
143/144Nd dep	0.513108	0.513108	0.513108	0.513108	0.513108	0.513108	0.513108
T mod:chur	2.26	2.02	1.72	1.59	1.95	2.38	2.12
T mod:dep	2.52	2.31	2.09	1.99	2.29	2.71	2.38
eps Nd (0)	-25.71	-24.54	-18.71	-17.22	-20.38	-17.93	-27.58
age (T)	1.6	1.6	1.654	1.7	1.592	1.5	1.59
143/144(T)	0.510181	0.510306	0.510460	0.510499	0.510385	0.510359	0.510227
143/144ch T	0.510569	0.510569	0.510499	0.510439	0.510579	0.510699	0.510582
eps Nd (T)	-7.60	-5.16	-0.75	1.18	-3.80	-6.66	-6.95
eps Nd/500	-20.09	-18.52	-13.32	-11.85	-15.21	-14.19	-21.14
eps Nd/700	-17.83	-16.10	-11.15	-9.69	-13.13	-12.69	-18.55
eps Nd/1000	-14.43	-12.47	-7.89	-6.44	-10.00	-10.44	-14.65
eps Nd/1500	-8.74	-6.38	-2.44	-1.00	-4.77	-6.66	-8.13
eps Nd/2000	-3.01	-0.25	3.05	4.47	0.50	-2.86	-1.57
eps Nd/2500	2.74	5.91	8.57	9.97	5.80	0.96	5.03
eps Nd (Tdep)	3.02	3.55	4.08	4.34	3.59	2.56	3.38

rock	Volcanic [3]	Volcanic [3]	Volcanic [5]	Volcanic [5]	Volcanic [5]	Volcanic [5]	Volcanic [5]	Volcanic [5]
sample no.	Gawler Ranges	Gawler Ranges	Gawler Ranges	Gawler Ranges	Gawler Ranges	Gawler Ranges	Gawler Ranges	Gawler Ranges
Nd ppm	33.60	49.78	60.52	68.52	58.42	60.19	71.27	78.90
Sm ppm	6.13	9.95	11.56	13.07	10.70	11.01	12.46	14.26
143/144 Nd	0.511461	0.511690	0.511577	0.511593	0.511648	0.511567	0.511517	0.511509
2 sigma								
Sm/Nd	0.1824	0.1999	0.1910	0.1907	0.1832	0.1829	0.1748	0.1807
147Sm/144Nd	0.1104	0.1209	0.1155	0.1154	0.1108	0.1106	0.1058	0.1093
143/144Nd ch	0.512638	0.512638	0.512638	0.512638	0.512638	0.512638	0.512638	0.512638
143/144Nd dep	0.513108	0.513108	0.513108	0.513108	0.513108	0.513108	0.513108	0.513108
T mod:chur	2.07	1.90	1.99	1.95	1.75	1.89	1.87	1.96
T mod:dep	2.37	2.27	2.32	2.29	2.11	2.23	2.20	2.28
eps Nd (0)	-22.96	-18.49	-20.70	-20.38	-19.31	-20.89	-21.87	-22.02
age (T)	1.59	1.59	1.592	1.592	1.592	1.592	1.592	1.592
143/144(T)	0.510307	0.510426	0.510368	0.510385	0.510488	0.510409	0.510410	0.510365
143/144ch T	0.510582	0.510582	0.510579	0.510579	0.510579	0.510579	0.510579	0.510579
eps Nd (T)	-5.38	-3.05	-4.14	-3.80	-1.78	-3.34	-3.31	-4.20
eps Nd/500	-17.47	-13.67	-15.53	-15.21	-13.84	-15.41	-16.08	-16.46
eps Nd/700	-15.26	-11.73	-13.46	-13.13	-11.64	-13.21	-13.75	-14.23
eps Nd/1000	-11.94	-8.81	-10.34	-10.00	-8.34	-9.90	-10.25	-10.87
eps Nd/1500	-6.38	-3.93	-5.11	-4.77	-2.80	-4.36	-4.39	-5.24
eps Nd/2000	-0.79	0.98	0.15	0.50	2.77	1.21	1.50	0.42
eps Nd/2500	4.83	5.92	5.43	5.80	8.37	6.82	7.42	6.11
eps Nd (Tdep)	3.39	3.64	3.52	3.59	4.03	3.75	3.83	3.62

rock	Volcanic [5]	Volcanic [5]	Volcanic [5]	Volcanic [5]	Hiltaba granite	Hiltaba granite	Adelaidean [1] Callana beds	Callana beds
sample no.	Gawler Ranges	Gawler Ranges	Gawler Ranges	Gawler Ranges	Olympic Dam	Olympic Dam	Blinman	Arkaroola
Nd ppm	71.08	70.82	78.17	89.78	182.00	68.00	16.89	8.62
Sm ppm	13.30	13.70	13.94	16.28	32.00	12.00	3.27	1.63
143/144 Nd	0.511544	0.511529	0.511523	0.511514	0.511411	0.511532	0.511744	0.511639
2 sigma								
Sm/Nd	0.1871	0.1934	0.1783	0.1813	0.1758	0.1765	0.1936	0.1891
147Sm/144Nd	0.1132	0.1170	0.1079	0.1097	0.1064	0.1067	0.1171	0.1144
143/144Nd ch	0.512638	0.512638	0.512638	0.512638	0.512638	0.512638	0.512638	0.512638
143/144Nd dep	0.513108	0.513108	0.513108	0.513108	0.513108	0.513108	0.513108	0.513108
T mod:chur	1.99	2.11	1.91	1.96	2.06	1.87	1.71	1.84
T mod:dep	2.32	2.43	2.23	2.28	2.35	2.20	2.10	2.20
eps Nd (0)	-21.34	-21.63	-21.75	-21.93	-23.94	-21.57	-17.44	-19.49
age (T)	1.592	1.592	1.592	1.592	1.588	1.588	0.85	0.85
143/144(T)	0.510359	0.510304	0.510394	0.510366	0.510301	0.510418	0.511091	0.511001
143/144ch T	0.510579	0.510579	0.510579	0.510579	0.510585	0.510585	0.511541	0.511541
eps Nd (T)	-4.31	-5.39	-3.63	-4.18	-5.56	-3.27	-8.80	-10.56
eps Nd/500	-16.02	-16.56	-16.10	-16.39	-18.19	-15.85	-12.37	-14.25
eps Nd/700	-13.89	-14.53	-13.82	-14.16	-15.88	-13.55	-10.33	-12.14
eps Nd/1000	-10.68	-11.46	-10.41	-10.82	-12.40	-10.09	-7.27	-8.97
eps Nd/1500	-5.30	-6.33	-4.69	-5.21	-6.59	-4.29	-2.14	-3.67
eps Nd/2000	0.11	-1.17	1.07	0.42	-0.74	1.54	3.02	1.66
eps Nd/2500	5.55	4.02	6.86	6.09	5.15	7.40	8.20	7.03
eps Nd (Tdep)	3.53	3.26	3.74	3.62	3.44	3.83	4.06	3.82

rock	Burra group	Belair sub-group	Appila tillite	Tapley hill fm	Umberatana shale	Umberatana shale	Wilpena shale	Brachina fm.
sample no.	Clarendon	Belair	Sturt gorge	Tapley hill	Flinders Ranges	Flinders Ranges	Flinders Ranges	Flinders Ranges
Nd ppm	29.62	39.57	26.11	32.66	29.76	29.11	48.61	29.93
Sm ppm	6.15	7.86	5.27	6.56	5.95	5.88	9.44	6.94
143/144 Nd	0.512024	0.511947	0.511811	0.512005	0.511962	0.511934	0.511902	0.512092
2 sigma								
Sm/Nd	0.2076	0.1986	0.2018	0.2009	0.1999	0.2020	0.1942	0.2319
147Sm/144Nd	0.1256	0.1202	0.1221	0.1215	0.1209	0.1222	0.1175	0.1403
143/144Nd ch	0.512638	0.512638	0.512638	0.512638	0.512638	0.512638	0.512638	0.512638
143/144Nd dep	0.513108	0.513108	0.513108	0.513108	0.513108	0.513108	0.513108	0.513108
T mod:chur	1.31	1.37	1.69	1.28	1.36	1.44	1.41	1.47
T mod:dep	1.83	1.85	2.10	1.78	1.84	1.91	1.87	2.05
eps Nd (0)	-11.98	-13.48	-16.13	-12.35	-13.19	-13.73	-14.36	-10.65
age (T)	0.84	0.82	0.8	0.75	0.7	0.68	0.65	0.6
143/144(T)	0.511332	0.511301	0.511171	0.511408	0.511407	0.511389	0.511402	0.511541
143/144ch T	0.511554	0.511580	0.511606	0.511671	0.511735	0.511761	0.511800	0.511865
eps Nd (T)	-4.35	-5.46	-8.51	-5.14	-6.42	-7.27	-7.79	-6.33
eps Nd/500	-7.44	-8.60	-11.38	-7.55	-8.36	-8.98	-9.31	-7.05
eps Nd/700	-5.62	-6.64	-9.47	-5.63	-6.42	-7.08	-7.28	-5.61
eps Nd/1000	-2.88	-3.69	-6.60	-2.73	-3.50	-4.21	-4.23	-3.44
eps Nd/1500	1.70	1.25	-1.79	2.12	1.39	0.60	0.88	0.20
eps Nd/2000	6.32	6.21	3.04	7.00	6.30	5.43	6.02	3.86
eps Nd/2500	10.96	11.21	7.91	11.91	11.25	10.29	11.19	7.55
eps Nd (Tdep)	4.73	4.69	4.05	4.85	4.71	4.54	4.64	4.20

rock	Brachina fm.	Bunyeroo fm.	Bunyeroo fm.	Bunyeroo fm.	Bunyeroo fm.	Normanville: [1] Sellicks hill shale	Heatherdale shale	Kanmantoo: [1] Carrickalinga shale
sample no.	Echunga	Officer basin	Pichi Richi	L. Torrens	Merna Merna	Sellicks Hill	Carrickalinga	Carrickalinga
Nd ppm	44.34	38.27	54.67	35.67	36.25	38.40	17.34	32.39
Sm ppm	7.55	7.27	11.25	6.81	6.75	7.68	3.40	6.38
143/144 Nd	0.511738	0.511810	0.511803	0.511818	0.511792	0.511802	0.511824	0.511482
2 sigma								
Sm/Nd	0.1703	0.1900	0.2058	0.1909	0.1862	0.2000	0.1961	0.1970
147Sm/144Nd	0.1030	0.1149	0.1245	0.1155	0.1126	0.1210	0.1186	0.1191
143/144Nd ch	0.512638	0.512638	0.512638	0.512638	0.512638	0.512638	0.512638	0.512638
143/144Nd dep	0.513108	0.513108	0.513108	0.513108	0.513108	0.513108	0.513108	0.513108
T mod:chur	1.46	1.54	1.76	1.54	1.53	1.68	1.59	2.26
T mod:dep	1.85	1.96	2.17	1.96	1.94	2.09	2.01	2.55
eps Nd (0)	-17.56	-16.15	-16.29	-16.00	-16.50	-16.31	-15.88	-22.55
age (T)	0.6	0.6	0.6	0.6	0.6	0.526	0.525	0.523
143/144(T)	0.511333	0.511358	0.511314	0.511364	0.511349	0.511385	0.511416	0.511074
143/144ch T	0.511865	0.511865	0.511865	0.511865	0.511865	0.511960	0.511961	0.511964
eps Nd (T)	-10.39	-9.89	-10.77	-9.78	-10.07	-11.23	-10.65	-17.39
eps Nd/500	-11.58	-10.94	-11.69	-10.82	-11.15	-11.48	-10.90	-17.62
eps Nd/700	-9.19	-8.85	-9.84	-8.74	-8.99	-9.55	-8.90	-15.64
eps Nd/1000	-5.58	-5.70	-7.06	-5.61	-5.76	-6.63	-5.90	-12.66
eps Nd/1500	0.46	-0.42	-2.41	-0.38	-0.34	-1.75	-0.86	-7.67
eps Nd/2000	6.54	4.88	2.27	4.89	5.11	3.16	4.20	-2.65
eps Nd/2500	12.65	10.21	6.98	10.18	10.60	8.09	9.29	2.40
eps Nd (Tdep)	4.68	4.42	3.89	4.42	4.46	4.08	4.29	2.95

rock	Carrickalinga shale	Backstairs Pass. shale	Tapanappa shale	Tunkalilla shale	Balquhidder shale	Petrel Cove shale
sample no.	Carrickalinga	Monarto	Kangaroo Is.	Victor Harbour	Torrens Vale	Port Elliot
Nd ppm	29.28	39.42	35.42	37.95	38.15	31.01
Sm ppm	5.81	7.38	6.77	6.63	7.34	5.89
143/144 Nd	0.511894	0.511704	0.511711	0.511679	0.511678	0.511725
2 sigma						
Sm/Nd	0.1984	0.1872	0.1911	0.1747	0.1924	0.1899
147Sm/144Nd	0.1200	0.1132	0.1156	0.1057	0.1164	0.1149
143/144Nd ch	0.512638	0.512638	0.512638	0.512638	0.512638	0.512638
143/144Nd dep	0.513108	0.513108	0.513108	0.513108	0.513108	0.513108
T mod:chur	1.48	1.70	1.74	1.60	1.82	1.70
T mod:dep	1.93	2.08	2.12	1.97	2.19	2.08
eps Nd (0)	-14.51	-18.22	-18.08	-18.71	-18.73	-17.81
age (T)	0.522	0.521	0.52	0.519	0.518	0.517
143/144(T)	0.511484	0.511317	0.511317	0.511320	0.511283	0.511336
143/144ch T	0.511965	0.511967	0.511968	0.511969	0.511971	0.511972
eps Nd (T)	-9.41	-12.68	-12.71	-12.69	-13.43	-12.42
eps Nd/500	-9.63	-12.90	-12.92	-12.91	-13.61	-12.60
eps Nd/700	-7.66	-10.77	-10.84	-10.58	-11.56	-10.51
eps Nd/1000	-4.71	-7.56	-7.72	-7.07	-8.47	-7.36
eps Nd/1500	0.23	-2.18	-2.50	-1.21	-3.29	-2.09
eps Nd/2000	5.20	3.23	2.76	4.69	1.91	3.22
eps Nd/2500	10.21	8.67	8.04	10.63	7.15	8.55
eps Nd (Tdep)	4.49	4.11	4.02	4.38	3.85	4.11

rock	Boxing Bay shale	Boxing Bay shale	Average [6]	Average [7]	Average [8]	Average [8]
sample no.	Kangaroo Is.	Kangaroo Is.	Willyama inlier	Mt Painter inlier	Arunta block	Musgrave block
Nd ppm	34.40	27.42	60.07	49.89		
Sm ppm	5.76	5.24	12.83	9.71		
143/144 Nd	0.511679	0.511793	0.511627	0.511630	0.511602	0.511896
2 sigma						
Sm/Nd	0.1674	0.1911	0.2143	0.1992		
147Sm/144Nd	0.1013	0.1156	0.1297	0.1205	0.1141	0.1181
143/144Nd ch	0.512638	0.512638	0.512638	0.512638	0.512638	0.512638
143/144Nd dep	0.513108	0.513108	0.513108	0.513108	0.513108	0.513108
T mod:chur	1.53	1.58	2.33	2.05	1.91	1.44
T mod:dep	1.90	2.00	2.64	2.39	2.25	1.89
eps Nd (0)	-18.71	-16.48	-19.73	-19.67	-20.21	-14.47
age (T)	0.516	0.516	1.6	1.6	1.6	1.6
143/144(T)	0.511337	0.511402				
143/144ch T	0.511973	0.511973				
eps Nd (T)	-12.43	-11.15				
eps Nd/500	-12.63	-11.32				
eps Nd/700	-10.18	-9.24	-13.75	-12.87	-12.84	-7.45
eps Nd/1000	-6.51	-6.12				
eps Nd/1500	-0.36	-0.89				
eps Nd/2000	5.83	4.37				
eps Nd/2500	12.05	9.66				
eps Nd (Tdep)	4.56	4.32				
	[6] - Benton, (1994), [7] - Schaefer, (1993), [8] - Zhao et.al., (1992).					

APPENDIX F

Compiled XRF data

WRA XRF DATA

ELEMENTS	SAMPLE NO. 1031-			Bolingbroke	Yunta Well	Moody Tank													
	002	006	008	SEP-026 [1]	SEP-062 [1]	SEP-063 [1]	013	023	030	031	032	022	014	015	009	010	017	018	019
LITHOLOGY	amphibolite	Yunta well	PPld	S1 granite	leucogranite	adamellite	PPh	PPhms	PPhc	PPhc	PPhy	PPbo	PPmm	PPmm	PPmw	PPmw	PPmw	PPt	PPt
MAJOR ELEMENTS (%)		Map area					Drill holes												
SiO2	50.06	74.73	71.14	76.49	73.88	71.93	48.88	59.08	63.99	57.78	66.92	69.68	78.06	55.48	79.16	64.05	61.38	65.59	67.61
Al2O3	14.06	14.94	12.96	13.12	14.39	14.22	11.10	13.30	15.93	19.74	15.03	11.40	9.42	6.34	10.09	5.22	12.78	18.28	15.19
Fc2O3	10.71	0.27	4.60	0.26	0.87	1.97	10.27	10.22	8.30	8.56	6.17	6.02	4.98	9.35	4.07	5.52	12.14	4.14	3.47
MnO	0.18	0.03	0.06	0.00	0.03	0.02	0.18	0.15	0.20	0.10	0.03	0.06	0.04	0.99	0.01	1.82	0.08	0.04	0.03
MgO	5.59	0.13	0.60	0.11	0.19	0.44	12.59	4.84	2.33	2.75	2.32	3.04	0.65	6.65	0.72	3.34	5.91	1.67	1.44
CaO	14.85	1.75	1.45	1.20	0.48	1.14	9.16	3.00	0.76	0.83	0.97	2.63	0.17	7.22	0.18	6.75	0.40	0.21	0.55
Na2O	2.92	4.68	2.65	2.31	3.82	2.84	2.41	0.42	1.48	1.22	1.90	0.22	0.08	0.10	0.09	0.09	0.06	1.57	2.14
K2O	0.43	2.66	4.92	5.80	4.84	5.85	1.84	6.01	4.53	5.67	3.67	4.40	4.68	0.81	3.39	1.71	2.26	4.43	3.92
TiO2	1.16	0.02	0.46	0.06	0.05	0.29	0.74	0.63	0.71	0.71	0.77	0.60	0.45	0.44	0.39	0.31	0.58	0.51	0.54
P2O5	0.13	0.07	0.12	0.01	0.25	0.10	0.23	0.15	0.16	0.15	0.16	0.08	0.04	0.17	0.09	0.54	0.04	0.08	0.07
SO3	0.03	0.00	0.01	0.00	0.00	0.00	0.09	0.05	0.01	0.01	0.01	0.12	0.07	0.20	0.01	0.18	0.07	0.06	0.07
L.O.I.	0.34	0.23	0.35	0.28	0.56	0.47	1.28	2.10	1.56	2.36	1.77	1.47	1.35	12.10	1.62	10.00	4.39	3.21	4.64
Totals	100.45	99.50	99.32	99.64	99.36	99.27	98.76	99.95	99.96	99.86	99.71	99.70	100.00	99.84	99.81	99.54	100.10	99.80	99.67
C.I.A.	43.58	62.17	58.96	58.49	61.16	59.13	45.29	58.51	70.18	71.89	69.68	61.13	65.64	43.81	73.38	37.91	82.45	74.64	69.68
C.I.W.	44.17	69.91	75.97	78.89	76.99	78.13	48.96	79.55	87.67	90.59	83.97	80.00	97.41	46.41	97.39	43.28	96.53	91.13	84.96
TRACE (ppm)																			
Rb	8.2	63.0	118.4	256.5	393.6	278.5	70.5	252.1	261.1	275.3	184.4	152.7	232.4	59.4	234.4	109.2	152.5	225.2	188.8
Ba	187.0	215.0	1137.0	667.0	66.0	490.0	742.0	441.0	485.0	633.0	899.0	420.0	607.0	23.0	136.0	86.0	117.0	689.0	731.0
Th	0.8	1.6	15.2	13.1	4.6	42.3	6.9	13.8	16.3	23.3	19.0	7.5	17.5	70.3	22.1	31.1	19.4	24.6	18.1
U	2.1	3.4	2.4	3.9	8.7	78.4	1.9	3.8	5.7	6.1	2.1	2.5	3.3	10.6	4.1	5.1	6.7	4.1	5.6
Nb	3.6	0.8	17.0	3.7	17.2	23.0	3.9	12.9	17.9	16.5	13.8	10.9	10.0	19.1	11.9	11.4	15.1	15.9	14.9
K	3570	22082	40843	48149	40179	48564	15275	49892	37606	47069	30466	36527	38851	6724	28142	14196	18761	36776	32542
La	3.0	8.0	65.0	12.0	3.0	65.0	35.0	32.0	25.0	33.0	45.0	31.0	36.0	74.0	12.0	76.0	55.0	45.0	40.0
Cc	11.0	16.0	138.0	27.0	3.0	122.0	75.0	66.0	58.0	113.0	89.0	55.0	65.0	138.0	25.0	143.0	107.0	91.0	74.0
Pb	2.0	45.2	29.4	41.7	26.6	59.3	13.5	24.3	20.2	29.8	10.6	14.3	8.2	24.9	11.8	43.6	0.7	45.8	26.5
Sr	143.5	108.0	132.7	129.4	27.8	104.5	597.1	62.3	84.2	60.1	89.4	81.2	22.4	11.5	9.9	10.6	6.9	54.6	83.8
P	567	305	524	44	1091	436	1004	655	698	655	698	349	175	742	393	2357	175	349	305
Nd	8.0	10.0	57.0	15.0	3.0	52.0	39.0	28.0	23.0	34.0	43.0	22.0	26.0	55.0	12.0	49.0	30.0	44.0	35.0
Zr	66.1	20.2	264.6	157.2	30.1	196.9	80.9	122.9	221.5	147.0	258.5	95.5	211.7	265.6	210.9	137.1	190.9	195.5	187.8
Sm												7.04		4.88				3.92	5.76
Ti	6954	120	2758	360	300	1739	4436	3777	4256	4256	4616	3597	2698	2638	2338	1858	3477	3057	3237
Y	30.9	4.3	42.3	7.4	12.4	22.2	16.9	31.7	28.9	30.1	30.9	30.4	26.4	47.6	21.1	43.1	31.9	37.7	33.1
Sc	41.4	1.2	6.3	2.2	1.4	2.4	30.0	13.6	15.2	19.7	17.4	13.2	6.4	40.2	5.6	37.1	13.4	10.1	10.7
Cr	91	10	9	3	2	4	1123	110	124	109	185	74	53	95	18	94	109	38	68
V	351.9	4.0	6.4	9.1	3.7	13.6	233.9	97.5	101.5	109.1	110.4	88.1	43.1	186.2	39.7	236.3	82.9	59.1	69.8
Co	61.1	71.3	39.7	54.3	55.2	41.8	53.4	25.9	45.0	27.2	30.5	36.9	34.2	126.9	33.5	60.8	45.6	8.8	14.0
Ga	15.4	11.7	23.1	15.7	19.0	21.2	16.2	17.4	21.4	27.8	18.9	17.9	9.8	12.0	12.2	9.8	21.6	22.2	19.6
Cu	100	3	7	0	7	4	294	1	15	135	47	1	3	3	7	73	nb	19	45
Zn	100	4	84	6	29	43	140	103	91	141	72	71	43	331	41	38	63	71	87
Ni	74	4	2	1	0	1	241	40	41	44	44	24	10	99	7	42	26	18	29

[1] - Data from B.F. Schaefer (1994); in prep.

ELEMENTS	020	021	011	012	016	024	025	026	027	028	029	Proterozoic Gawler Ranges					Archaean samples		
												58	79	80	49	Yardea Dacite	Gneiss	Gneiss	Paragneiss
LITHOLOGY	PPt	PPt	PMcc	PMcc	PMcc	PMbr	PMbr	PMbr	PMp	PMp	PMp	GRV [2]	GRV [2]	GRV [2]	GRV [2]	GRV [3]	Carnot [3]	Carnot [3]	W Eyre pen [3]
MAJOR ELEMENTS (%)												Compiled data							
SiO2	65.12	63.10	14.57	63.15	61.62	66.90	72.96	71.91	63.74	64.49	61.09	69.52	69.46	69.33	72.32	68.02	76.75	70.08	73.24
Al2O3	17.36	17.76	1.09	14.99	18.42	18.60	15.50	15.83	17.24	18.06	18.86	13.61	14.38	14.43	12.79	13.68	12.87	14.97	14.3
Fe2O3	3.71	4.51	6.42	5.35	6.15	3.06	2.53	2.51	7.56	6.41	7.94	4.07	3.31	3.16	3.06	5.1	1.77	3.59	2.45
MnO	0.07	0.04	0.34	0.06	0.17	0.03	0.02	0.02	0.13	0.11	0.10	0.11	0.14	0.09	0.09	0.14	0.02	0.04	0.02
MgO	1.07	1.43	13.81	2.31	0.98	0.62	0.34	0.46	1.15	1.23	1.23	0.9	0.45	0.49	0.62	0.57	0.4	2.08	0.69
CaO	0.51	0.36	24.42	1.01	0.29	0.02	0.02	0.02	0.50	0.12	0.33	1.71	1.2	1.15	0.99	2.03	2.02	1.32	1.16
Na2O	1.92	0.21	0.19	0.79	0.15	0.28	0.24	0.23	0.31	0.25	0.27	3.64	4.26	4.58	3.84	3.29	3.75	2.79	3.24
K2O	4.67	5.97	0.27	8.38	4.94	7.48	5.96	6.19	5.25	5.64	6.04	4.61	5.14	4.79	4.71	5.19	2.31	5.5	4.62
TiO2	0.53	0.55	0.07	0.66	0.91	0.56	0.36	0.50	0.63	0.64	1.02	0.57	0.46	0.47	0.5	0.67	0.25	0.64	0.27
P2O5	0.10	0.10	0.00	0.17	0.10	0.03	0.03	0.03	0.37	0.07	0.20	0.15	0.07	0.08	0.09	0.17	0.03	0.09	0.09
SO3	0.18	0.34	0.59	0.10	0.05	0.01	0.01	0.01	0.01	0.01	0.01								
L.O.I.	4.52	5.29	37.56	2.10	5.71	2.20	1.84	1.93	2.88	2.94	2.93					0.95	0.33	0.15	0.27
Totals	99.77	99.67	99.33	99.09	99.50	99.78	99.81	99.64	99.77	99.96	100.01	99.76	99.32	99.02	99.47	99.81	100.5	101.25	100.35
C.I.A.	70.97	73.09	4.20	59.56	77.39	70.51	71.36	71.08	73.99	75.03	73.96	57.74	57.57	57.84	57.28	56.55	61.43	60.90	61.32
C.I.W.	87.72	96.89	4.24	89.28	97.67	98.41	98.35	98.45	95.51	97.99	96.92	71.78	72.48	71.58	72.59	72.00	69.05	78.46	76.47
TRACE (ppm)																			
Rb	214.9	355.6	15.6	488.4	266.9	297.7	203.5	229.7	304.3	332.9	296.1	162.0	171.0	147.0	143.0	208.4	43.0	126.0	177.1
Ba	794.0	983.0	19.0	2391.0	146.0	660.0	401.0	419.0	546.0	634.0	660.0	1306.0	2338.0	2412.0	1679.0	1410.0	503.0	664.0	415.0
Th	18.0	19.8	1.2	19.6	30.0	18.5	17.9	21.1	30.5	26.6	25.2	23.0	26.0	25.0	10.0	31.0	11.0	52.0	32.0
U	4.3	4.9	2.2	2.7	8.8	5.2	3.4	4.3	11.7	7.1	10.5	4.8	4.5	6.2	2.0	8.5	0.2	2.3	14.4
Nb	14.6	16.6	2.1	14.0	18.0	14.9	11.7	15.5	18.3	18.4	18.6	13.8	17.3	18.2	10.9	21.0	6.0	7.0	12.0
K	38768	49560	2241	69566	41009	62095	49477	51386	43583	46820	50141	38270	42670	39764	39100	43085	19176	45658	38353
La	50.0	50.0	5.0	48.0	72.0	66.0	49.0	59.0	65.0	69.0	29.0	62.0	75.0	69.0	43.0	84.0	39.0	88.0	28.0
Ce	99.0	93.0	14.0	88.0	133.0	72.0	65.0	57.0	155.0	127.0	104.0	117.0	153.0	147.0	79.0	178.0	70.0	215.0	61.0
Pb	15.7	21.6	191.9	48.7	711.9	19.6	13.0	12.4	30.4	23.3	31.9	28.0	38.0	30.0	28.0	26.0	14.9	40.0	31.0
Sr	53.3	31.4	40.3	84.9	52.8	94.3	61.2	63.4	45.0	56.1	36.0	206.0	210.0	211.0	191.0	165.6	135.0	140.0	59.6
P	436	436	0	742	436	131	131	131	1615	305	873	655	305	349	393	742	131	393	393
Nd	47.0	46.0	0.0	40.0	55.0	44.0	38.0	41.0	63.0	56.0	45.0	48.0	66.0	60.0	31.0	68.5	17.1	40.2	29.4
Zr	257.0	217.4	13.3	183.8	254.5	446.7	529.1	696.1	288.1	244.2	422.3	340.0	360.0	365.0	231.0	432.0	171.0	275.0	135.0
Sm					8.20	6.13			14.17							13.07	2.64	6.78	5.46
Ti	3177	3297	420	3957	5455	3357	2158	2997	3777	3837	6115	3417	2758	2818	2997	4017	1499	3837	1619
Y	40.8	44.7	6.0	20.8	43.4	35.1	32.3	36.4	67.1	49.7	54.1	39.0	52.0	49.0	25.0	66.0	10.0	16.0	12.0
Sc	11.1	9.9	4.3	13.3	19.6	9.0	5.6	7.5	11.9	12.5	17.1	9.9	12.0	12.6	8.0	15.0	4.0	6.0	5.0
Cr	25	69	9	81	240	32	6	11	45	50	57	1	1	1	1	5	398	434	240
V	48.7	55.5	77.0	68.1	210.9	27.7	19.7	22.3	70.5	77.8	73.0	31.0	3.0	4.0	20.0	20.0	17.0	60.0	27.0
Co	11.2	9.9	5.1	28.4	53.7	23.0	29.3	21.8	22.2	21.9	23.1								
Ga	22.4	22.8	2.8	18.7	23.4	20.5	15.7	17.3	23.2	22.9	18.0	19.0	20.0	18.0		21.0	13.0	19.0	17.6
Cu	21	25	nb	2	113	7	7	10	41	43	14	1	5	2	5				
Zn	61	318	289	602	54	29	8	16	133	147	121	74	87	87	65				
Ni	10	19	11	34	40	13	4	7	29	30	32	4	3	2	5	3	11	21	12

[2] - selected GRV samples - Robertson, 1989

ELEMENTS	Adelaidean samples								
	Paragneiss	Arkaroola	Clarendon	Tapley hill	Etina fm	Enorama	Flinders Ra	Flinders Ra	Echunga
LITHOLOGY	Kimba [3]	Callana beds [3]	Burra group [3]	Tapley hill fm [3]	Umberatana [3]	Umberatana [3]	Wilpena [3]	Brachina fm [3]	Brachina fm [3]
MAJOR ELEMENTS (%)									
SiO2	65.16	49.96	64.94	55.64	56.37	55.95	60.16	68.42	59.51
Al2O3	16.06	18.98	14.84	13.26	13.35	12.42	18.25	13.11	15.55
Fe2O3	5.4	4.67	7.61	6.33	6.14	5.85	7.41	6.95	6.93
MnO	0.05	0.02	0.01	0.06	0.08	0.11	0.03	0.05	0.16
MgO	1.75	12.2	3.55	6.71	3.93	4.15	2.64	2.22	5.14
CaO	2.41	0.12	0.36	3.82	6.03	7.02	0.25	0.43	2.86
Na2O	3.32	0.68	1.16	1.61	1.54	1.62	2.28	3.05	1.68
K2O	4.46	8.77	3.21	2.85	2.93	2.72	4.88	1.23	5.3
TiO2	0.84	0.92	0.84	0.9	0.78	0.81	1.53	1.24	0.76
P2O5	0.22	0.07	0.18	8.33	8.51	0.16	0.18	0.24	0.19
SO3									
L.O.I.	0.48	2.11	4.12	8.33	8.51	8.91	3.98	2.63	1.02
Totals	100.15	98.5	100.82	99.7	99.82	99.72	101.59	99.57	99.1
C.I.A.	61.18	66.48	75.83	61.56	55.97	52.23	71.12	73.57	61.24
C.I.W.	73.70	95.96	90.71	70.95	63.81	58.97	87.82	79.02	77.40
TRACE (ppm)									
Rb	138.0	336.4	145.8	114.4	122.4	114.6	221.1	56.4	241.2
Ba	1331.0	1020.0	651.0	481.0	384.0	498.0	410.0	236.0	1786.0
Th	18.0	8.0	8.0	8.8	10.0	7.8	19.0	8.6	13.0
U	0.0	2.0	3.3	4.4	3.0	4.3	6.7	3.1	2.3
Nb	13.0	17.0	12.0	13.0	13.0	13.0	23.0	15.0	13.0
K	37025	72804	26648	23659	24323	22580	40511	10211	43998
La	52.0	23.0	29.0	40.0	38.0	33.0	61.0	48.0	74.0
Ce	130.0	42.0	62.0	73.0	76.0	65.0	115.0	90.0	109.0
Pb	27.0	0.0	31.0	29.0	20.0	19.0	27.0	48.0	5.4
Sr	302.7	43.3	36.3	179.6	105.7	113.8	39.3	55.0	118.4
P	960	305	786	36354	37139	698	786	1047	829
Nd	32.6	8.6	29.6	32.7	29.8	29.1	48.6	29.9	44.3
Zr	196.0	161.0	151.0	173.0	181.0	195.0	273.0	305.0	176.0
Sm	6.59	1.63	6.15	6.56	5.95	5.88	9.44	6.94	7.55
Ti	5036	5515	5036	5395	4676	4856	9172	7434	4556
Y	12.0	32.0	31.0	29.0	30.0	29.0	47.0	36.0	20.0
Sc	9.0	21.0	14.0	15.0	16.0	15.0	19.0	11.0	14.0
Cr	209	136	121	97	99	96	149	57	292
V	106.0	168.0	215.0	186.0	137.0	128.0	197.0	110.0	113.0
Co									
Ga	21.0	23.0	18.0	16.0	16.0	15.0	24.0	14.0	18.0
Cu									
Zn									
Ni	29	48	63	44	35	36	39	31	49

[3] - selected Archaean and Adelaidean from Turner et.al., 1992

APPENDIX G

Mapping methodology & measurements

Appendix G:

Mapping methodology:

Mapping of a chosen area on the Lincoln 1:250,000, Tumby Bay 1:100,000 geology sheets, was performed in order to fulfil a field geology component towards the completion of an Honours degree at Adelaide University 1994. The area was selected, being an area of near-substantial mappable outcrop, which contained deformed suites of Proterozoic rocks, of which are analysed within this thesis

Mapping was achieved via 'foot' and a 4WD Subaru wagon, supplied by the Mines and Energy Department of South Australia (MESA). Most of the study was undertaken on foot with the vehicle used to transport to and from the map area, and around any access roads. A total area af approx 50 Km^2 was traversed.

Readings and samples were taken at many sites, which were located onto one of six, 1:20,000 aerial photographs a,b,c,d,e,f, corresponding to different photo sections over the total map area.
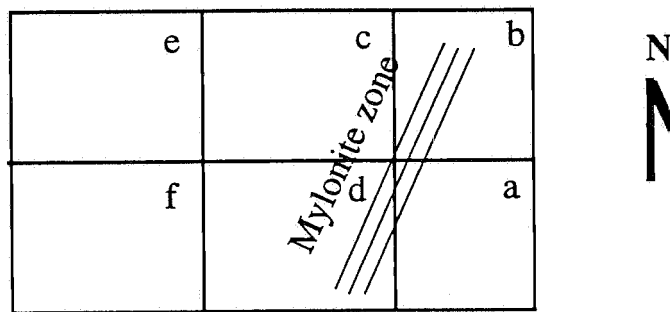
Sample sites were marked in ascending numbers for each site of interest, this would not necessarily mean that a sample or a measurement was taken.

Samples were taken when in interest of comparism to other hand specimens or with the idea of thin sections being made to better understand the mineralogy. In this way a selection of 8 mappable units has been selected, corresponding to geochemically distinct lithologies, however adjacent to the defined mylonite zone, the lithologies are more highly sheared, and deformed, and thus make it much more difficult to define between lithologies in hand specimen.

Samples are breifly described as hand specimens in Appendix A, with any samples used for analytical work having a corresponding accession number, as well as its sample number. Results for field measurements of lineation and foliation directions throughout the map region are presented within this appendix.

MAPPING MEASUREMENTS

LOCATION	STRIKE	Pole:	DIP	LINEATION
aS 1	046	136	85 E	20 N
aS 2	038	128	80 E	20 N
aS 3	040	310	85 W	20 N
aS 4	050	320	85 W	40 N
aS 5	048	138	90	30 N
aS 6	054	324	80 W	30 N
aS 7	070	340	80 W	30 N
aS 8	070	160	90	
aS 9	060	330	85 W	20 N
aS 10	040	130	85 E	10 N
aS 11	100	190	90	
aS 12	030	120	90	0 N
aS 13	038	128	90	10 N
aS 14	042	132	90	0 N
aS 15	050	140	80 E	20 N
aS 16	030	120	85 E	15 N
aS 18	040	310	85 W	10 N
aS 19	040	130	90	
aS 21	050	320	80 W	20 N
aS 22	050	320	85 W	20 N
aS 23	050	140	90	10 N
aS 24	044	134	70 E	0
aS 25	026	116	70 E	0
aS 26	044	134	70 E	
aS 27	044	134	80 E	0
aS 29	046	136	90	10 S
aS 30	030	120	90	20 N
aS 31	020	110	70 E	50 N
bS 1	038	128	90	
bS 2	040	310	85 W	10 N
bS 3	030	120	85 E	10 N
bS 4	024	114	45 E	20 N
bS 5	034	124	90	20 N
bS 6	038	308	85 W	5 N
bS 7	040	130	90	10 N
bS 8	044	314	85 W	20 N
bS 9	044	314	85 W	20 N
bS 10	030	300	85 W	20 N
bS 11	038	128	85 E	10 N
bS 13	034	124	70 E	15 N
bS 14	032	122	85 E	
bS 15	032	122	80 E	10 N
bS 16	032	122	75 E	10 N
bS 17	046	136	80 E	0
bS 18	030	300	80 W	20 N
bS 19	026	296	80 W	
bS 20	030	120	80 E	20 N
bS 21	030	300	80 W	
bS 22	034	124	80 E	15 N
bS 23	042	132	80 E	0
bS 24	040	310	80 W	5 N
bS 25	040	310	80 W	
bS 26	050	140	85 E	0
bS 27	040	310	85 W	

MAPPING MEASUREMENTS

LOCATION	STRIKE	Pole:	DIP	LINEATION
bS 28	046	136	90	
bS 29	048	138	90	
bS 31	030	120	80 E	20 N
bS 32	026	116	70 E	20 N
bS 33	048	138	90	60 N
bS 34	046	136	90	
bS 35	040	130	80 E	5 N
bS 36	040	130	90	
bS 37	032	302	85 W	
bS 38	030	120	90	
bS 39	030	300	80 W	
bS 40	032	122	90	
bS 41	036	126	80 E	
bS 42	038	308	80 W	
bS 43	050	140	80 E	
bS 44	044	314	80 W	
cS 1	005	095	70 E	20 N
cS 2	010	100	85 E	15 N
cS 3	010	100	90	
cS 5	040	130	90	
cS 8	030	120	90	
cS 9	040	130	080 E	
cS 10	040	130	90	
cS 11	050	140	85 E	
cS 12	050	140	80 E	60 S
cS 13	050	140	80 E	60 S
cS 14	040	130	80 E	70 S
cS 15	050	140	85 E	90
cS 16	050	140	90	
cS 17	060	150	80 E	
cS 18	030	120	75 E	70 S
cS 19	050	140	80 E	
cS 21	040	130	90	
cS 22	044	134	90	
cS 23	070	160	70 E	
cS 24	060	150	80 E	
cS 25	060	150	80 E	
cS 26	060	150	80 E	
cS 27	060	150	70 E	
cS 28	090	180	80 S	
cS 29	050	140	80 E	
cS 30	054	144	85 E	
cS 31	054	144	85 E	85 S
cS 32	030	120	85 E	85 S
cS 33	040	130	80 E	80 S
cS 34	040	130	90	
cS 35	050	140	90	
cS 36	020	290	80 W	
cS 37	020	290	80 W	
cS 38	040	310	80 W	
cS 39	030	120	90	75 S
cS 40	030	120	90	
cS 41	030	120	80 E	
cS 42	040	130	80 E	

MAPPING MEASUREMENTS

LOCATION	STRIKE	Pole:	DIP	LINEATION
cS 43	040	130	80 E	
cS 44	040	130	85 E	
cS 46	040	130	90	
cS 47	030	120	80 E	80 S
cS 48	040	130	80 E	
cS 49	040	130	80 E	
cS 50	045	135	80 E	
cS 51	040	130	90	70 S
cS 52	036	126	90	75 S
cS 53	044	134	90	
cS 54	038	128	90	
cS 55	030	120	85 E	70 S
cS 57	034	124	80 E	
cS 58	036	126	80 E	
cS 59	016	106	80 E	
cS 61	020	110	70 E	20 N
cS 62	030	120	90	
cS 64	044	134	75 E	
cS 67	038	128	70 E	
cS 68	030	120	80 E	
cS 69	036	126	80 E	
cS 70	024	114	85 E	
cS 71	024	114	80 E	
cS 76	060	150	60 E	
cS 85	040	130	50 E	
cS 87	050	140	60 E	
cS 88	040	130	60 E	
cS 92	040	130	60 E	
cS 94	030	120	60 E	
cS 97	044	134	60 E	
cS 98	060	150	80 E	
cS 100	060	150	85 E	
cS 101	054	144	85 E	
cS 102	054	144	85 E	
cS 105	050	140	50 E	
cS 111	050	140	60 E	
cS 113	044	134	70 E	
cS 114	040	130	90	
cS 115	038	128	85 E	40 S
cS 116	050	140	80 E	
dS 1	030	120	90	
dS 2	030	120	90	
dS 3	030	120	90	
dS 4	020	110	70 E	54 N
dS 5	050	140	90	15 N
dS 6	040	130	80 E	
dS 7	020	290	85 W	15 N
dS 8	030	120	80 E	40 N
dS 9	024	114	80 E	
dS 10	030	120	80 E	30 N
dS 11	038	128	70 E	40 N
dS 12	000	270	70 W	70 N
dS 13	040	130	90	70 N
dS 14	006	096	70 E	60 N

MAPPING MEASUREMENTS

LOCATION	STRIKE	Pole:	DIP	LINEATION
dS 15	020	110	80 E	70 N
dS 16	030	120	90	
dS 18	020	110	60 E	70 N
dS 21	030	120	85 E	
dS 22	012	102	80 E	
dS 23	048	138	80 E	50 S
dS 24	050	140	80 E	70 S
dS 25	044	134	85 E	
dS 26	060	150	90	
dS 27	040	130	80 E	
dS 32	054	144	70 E	80 S
dS 33	044	134	85 E	
dS 34	030	120	60 E	
dS 35	040	130	70 E	
dS 36	036	126	80 E	
dS 37	052	142	80 E	
dS 38	040	130	70 E	
dS 39	038	308	85 W	70 N
dS 40	038	128	80 E	60 N
dS 41	030	300	80 W	50 N
dS 42	040	130	70 E	50 N
dS 43	066	156	80 E	
dS 44	030	120	80 E	
dS 45	010	100	90	
dS 46	076	166	85 S	
dS 47	092	182	85 S	
dS 48	084	174	80 S	90
dS 50	150	060	70 W	
dS 51	052	142	70 E	
dS 52	030	300	80 W	
dS 54	040	130	90	
dS 56	030	300	80 W	
dS 57	050	140	90	
dS 58	052	142	90	
dS 60	030	300	80 W	
dS 63	050	140	85 E	50 N
dS 64	070	340	80 N	50 E
dS 65	090	180	80 S	
dS 67	040	130	80 E	
dS 68	048	318	85 W	
dS 69	050	320	80 W	
dS 70	046	136	70 E	
dS 71	040	130	70 E	90
dS 72	050	320	60 W	70 N
dS 73	070	160	80 S	
dS 75	026	116	80 E	
dS 77	072	162	80 S	
dS 78	080	170	80 S	
dS 79	060	150	85 E	
dS 80	120	210	80 S	60 E
dS 81	100	190	80 S	70 E
dS 82	050	140	90	
dS 83	060	150	90	
dS 85	130	040	80 N	50 E
dS 86	100	190	90	

MAPPING MEASUREMENTS

LOCATION	STRIKE	Pole:	DIP	LINEATION
dS 87	100	190	85 S	
dS 88	050	140	90	
dS 89	020	110	80 E	
dS 90	030	120	85 E ·	
dS 91	036	126	90	
dS 92	056	146	80 E	
dS 94	044	134	80 E	
dS 95	050	140	80 E	
dS 98	150	240	90	
dS 99	100	190	85 S	
dS 101	030	300	80 W	
dS 102	130	220	90	
dS 103	140	230	80 S	
dS 104	010	280	80 W	
dS 106	024	114	90	
dS 108	010	280	80 W	80 N
eS 12	020	110	60 E	
eS 21	056	146	80 E	
eS 23	060	150	85 E	30 N
eS 31	060	150	60 E	
fS 1	058	148	80 E	
fS 2	050	140	80 E	
fS 3	044	134	80 E	
fS 4	034	124	80 E	
fS 6	056	146	90	
fS 7	046	136	85 E	
fS 9	090	180	80 S	60 E
fS 11	040	130	90	
fS 12	080	170	80 S	
fS 13	060	150	90	
fS 17	030	120	50 E	
fS 18	030	120	60 E	
fS 19	040	130	70 E	
fS 20	050	140	80 E	
fS 21	040	130	70 E	
fS 22	044	134	85 E	
fS 23	060	150	90	
fS 24	044	134	80 E	
fS 25	050	140	80 E	
fS 26	050	140	80 E	
fS 27	050	140	85 E	
fS 28	060	150	90	
fS 29	044	134	80 E	
fS 30	044	134	80 E	
fS 31	044	134	80 E	
fS 32	040	310	80 W	
fS 33	050	140	80 E	
fS 35	050	140	90	
fS 41	038	128	80 E	
fS 43	030	120	60 E	
fS 44	044	134	70 E	
fS 47	050	140	80 E	

APPENDIX H

Tumby Bay Structural &
Geological maps

Tumby Bay - Cross sections

A Geology (from observation of outcrop) **B**

Structure (from observation of changing dip)

C Geology (from observation of outcrop) **D**

Structure (from observation of changing dip)

LEGEND

- Carpa granite
- Leucogranite
- Amphibolite
- B.I.F.
- Dolomite
- Schist
- Quartzite
- Lincoln granite

KEY

- Lithological boundary
- Structural trends
- Mylonite zone trend

SCALE 1:40 000

m 0 200 400 600 800 1000

NW —— SE
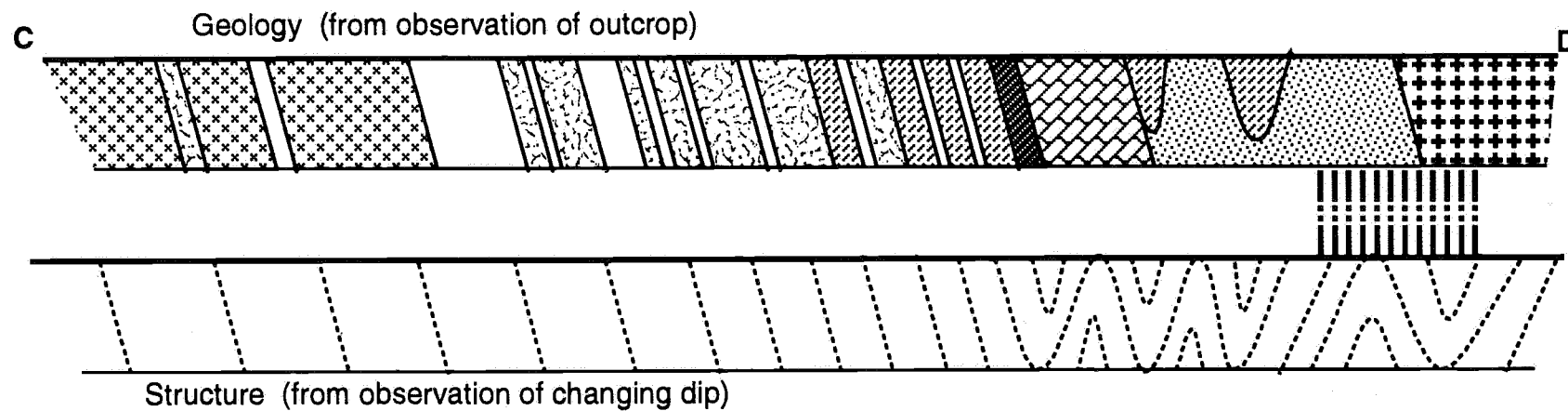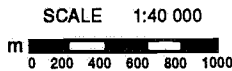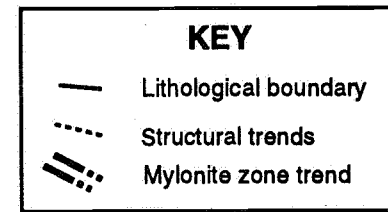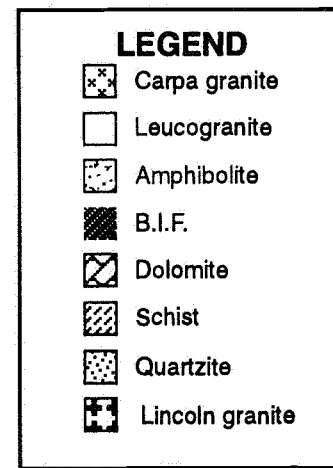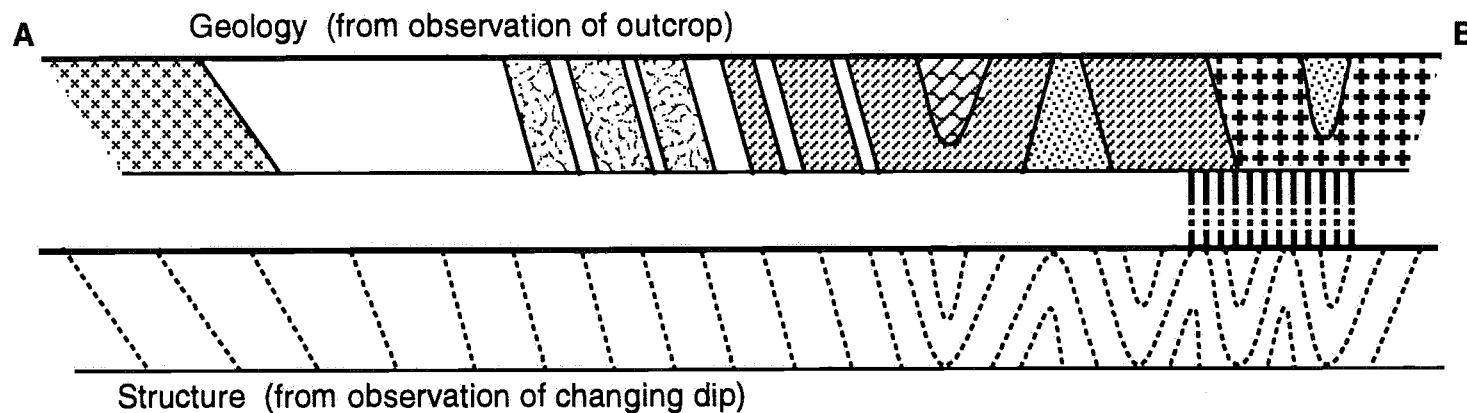
TUMBY BAY STRUCTURAL MAP & MEASUREMENTS

KEY
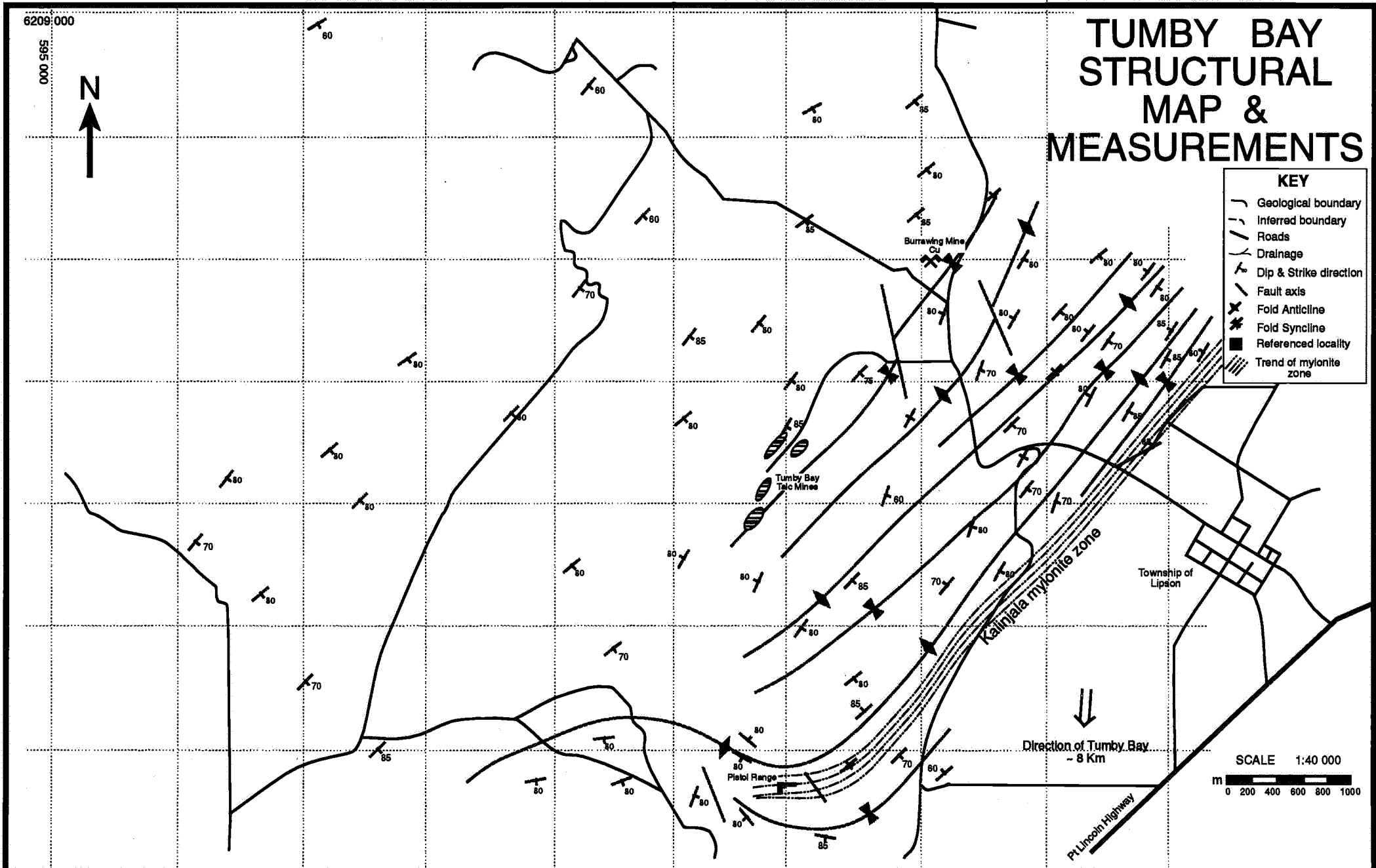
⌒	Geological boundary
⌒	Inferred boundary
	Roads
	Drainage
⊢	Dip & Strike direction
	Fault axis
	Fold Anticline
	Fold Syncline
■	Referenced locality
	Trend of mylonite zone

6209 000

595 000

N

Burrawing Mine
Cu

Tumby Bay
Talc Mines

Kalinjala mylonite zone

Township of
Lipson

Pistol Range

Direction of Tumby Bay
~ 8 Km

Pt Lincoln Highway

SCALE   1:40 000

m   0 200 400 600 800 1000

TUMBY BAY LOCATIONS MAP

6209 000
595 000

N

A'
X-Section

C
X-Section

Photo E
Photo G & H

Area (a) - Steep
south lineations

Burrawing Mine
Cu

Photo 2

Photo 3 & F

Photo A & B

Photo 4

B

Tumby Bay
Talc Mines

Area (b) - Shallow
north lineations

Township of
Lipson

Photo C & D
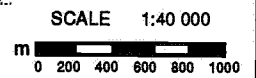
Pistol Range

D

Direction of Tumby Bay
~ 8 Km

Pt Lincoln Highway

KEY

Symbol	Description
	Geological boundary
	Inferred boundary
	Roads
	Drainage
	Dip & Strike direction
	Fault axis
	Fold Anticline
	Fold Syncline
	Referenced locality
	Trend of mylonite zone

SCALE   1:40 000

m   0 200 400 600 800 1000

TUMBY BAY GEOLOGICAL MAP

6209 000

595 000

N

KEY

⌐	Geological boundary
⌐	Inferred boundary
	Roads
	Drainage
	Dip & Strike direction
	Fault axis
✕	Fold Anticline
✹	Fold Syncline
■	Referenced locality
▥	Trend of mylonite zone

Burrawing Mine
Cu

Tumby Bay
Talc Mines

Township of
Lipson

Direction of Tumby Bay
~ 8 Km

Pistol Range

Pt Lincoln Highway

SCALE   1:40 000

m
0 200 400 600 800 1000

LEGEND

▨	Carpa granite
☐	Leucogranite
▦	Amphibolite
▰	B.I.F.
▧	Dolomite
▨	Schist
▒	Quartzite
✛	Lincoln granite